New Proposal for the Detection of Concealed Weapons: Electromagnetic Weapon Detection for Open Areas

ALAN AGURTO GOYA

A thesis submitted to the University of Huddersfield in partial fulfillment of the requirements for The degree of Master of Philosophy

School of Computing and Engineering

University of Huddersfield

July 2009

COPYRIGHT

ABSTRACT

Terrorist groups, hijackers, and people hiding guns and knifes are a constant and increasing threat. Concealed weapon detection (CWD) has turned into one of the greatest challenges facing the law enforcement community today. Current screening procedures for detecting concealed weapons such as handguns and knives are common in controlled access settings such as airports, entrances to sensitive buildings and public events. Unfortunately screening people in this way prior to entering controlled areas is ineffective in preventing some weapons from getting through and also produces bottle-necks in crowded environments. Also the screening technologies employed have a high rate of false alarms due to poor discrimination capability. A reliable CWD that is able to work in open areas and a robust method capable to discriminate between ferromagnetic weapons are necessary.

This thesis reviews recent developments in the area of CWD using largely electromagnetic methods. The advantages and disadvantages of these approaches are discussed and a new research direction in CWD is presented. This thesis proposes a cost-effective weapon detection system based on pulse induction technology which is able to work in open areas without invading individual privacy. This approach employs a uniform magnetic field generator to transmit pulses that cause eddy currents to flow in any metal object carried by people. The induced eddy currents decay exponentially following sudden changes in the exciting magnetic field with a characteristic decay time (time constant) that depends on the size, shape, and material composition of the object. The decay currents generate a secondary magnetic field and the rate-of-change of the field is detected by the sensors. This thesis introduces models based on finite element analysis (FEA) to study the potential use of the time constant as a signature for weapon discrimination. Experimental work is also presented that confirms the theoretical predictions obtained from FEA. It is shown that further work on signature extraction and signal processing needs to be done to build the weapon signature database necessary for classification.

ACKNOWLEDGEMENTS

I would like to express my sincere gratitude to Dr Martin Sibley for his advice, guidance and encouragement throughout this work.

The author is especially thankful to his wife and daughter for being his biggest motivation on this work.

.

TABLE OF CONTENTS

LIST OF FIGURES

LIST OF TABLES

LIST OF ABBREVIATIONS

AMMW	Active Millimetre Wave
AMR	Anisotropic Magnetoresistive
AWG	American Wire Gauge
CCTV	Closed Circuit Television
CW	Continuous Wave
CWD	Concealed Weapon Detection
DC	Direct Current
EM	Electromagnetic
EMF	Electromotive Force
EMW	Electromagnetic Wave
FEA	Finite Element Analysis
GMR	Giant Magnetoresistance
HMF	Horizontal Magnetic Field
INL	Idaho National Laboratory
IR	Infrared
MMW	Millimetre Wave
NAC	Nonlinear Acoustic
PI	Pulse Inductive
PML	Perfectly Matched Layers
PMMW	Passive Millimetre Wave
RCS	Radar Cross Section
RF	Radio Frequency
SQUID	Superconducting Quantum Interference Devices
THz	Terahertz
UMFG	Uniform Magnetic Field Generator
WAMD	Wide Area Magnetic Detection
3DSMF	3D steerable Magnetic Filed Sensor

Chapter 1: INTRODUCTION

From year 2000 there has been an increased security threat in public areas. Today, terrorist groups, hijackers and people hiding weapons are a constant and increasing threat. There is an immediate requirement for law enforcement and homeland security to identify concealed weapons, which may present a threat to official personnel and the general public. This involves suicide bomb vests, handguns, knife blades and other threatening weapons. Concealed weapons detection is one of the greatest challenges facing the law enforcement community today [1].

Current security-detection systems, which include portals and hand-held devices for detecting concealed weapons such as handguns, knives and explosives, are common in controlled access settings like airports, entrances to sensitive buildings, and public events. The presence of a portal weapon detection system and hand held devices in a security check point warn in advance those individuals trying to hide threatening weapons. Current security detection systems also need to be near an individual to work. They generally provide sufficient warning when it comes to detecting a knife, but they cannot detect weapons that can kill beyond arm's reach. For instance by the time a handgun or a bomb vest is detected, it generally is too close to be dealt with safely. It is clear that screening people in this way using current security detection systems prior to entering secured areas is ineffective in preventing some weapons from getting through. It is an almost impossible task to achieve 100% success given the equipment screeners have available today. To detect concealed weapons requires not only simple metal detectors in controlled environments as used today, but detectors from a standoff distance on streets and any safety critical environments. It is vital for law enforcement agencies to be able to detect and respond to weapons at a sufficient distance to allow officers to make decisions and take actions that deal safely with the situation.

There must be reliable ways to detect and identify not only metal but also non-metallic weapons or other threatening objects that may be concealed under clothing or vehicles.

Many approaches have been attempted since terrorist attack to different targets in USA of 11th September 2001. The Department of Homeland Security established Homeland Security Advanced Research Projects Agency (HSARPA) (http://www.dhs.gov/xres/grants/#1) to promote revolutionary technologies that would address homeland security vulnerabilities. It is an important component of the US response to terrorist attacks of all kinds. In the meantime, the UK in common with other European countries has initiated several research programs on crime prevention including gun detection. It is a technological challenge that requires innovative solutions in sensor technologies and image processing.

This thesis has reviewed the recent progress of research and development of the CWD technologies. As a part of the collaboration project partners (Manchester University, Manchester Metropolitan University, Newcastle University and Queen Mary London University) in the weapon detection research, this investigation is focused on providing a cost effective and reliable solution employing technologies with working radiation frequency within 0 and 1GHz. As a result of the research a new weapon detection system based on pulse induction technology able to work in open areas without invading individual privacy has been proposed. The eventual outcome of this work and other approaches at several non-overlapping wavelengths could result in a reliable integrated multimodal sensing system.

The thesis is organised as follows. Chapter 2 will review and discuss individual methods at different frequencies within the wide electromagnetic spectrum. Chapter 3 presents Finite Element (FE) based models for guns and knives characterisation using Passive (Earth field distortion) and Active (EM wave illumination) weapon detector technologies. Chapter 4 presents the theory for the proposed CWD, system description, FE model simulations and preliminary practical work. In the last chapter the conclusions and future work are presented.

Chapter 2: LITERATURE SURVEY

This chapter reviews recent developments in the area of CWD. These methods largely use electromagnetic means including metal detection, magnetic field distortion, electromagnetic resonance, acoustic and ultrasonic inspection, Millimeter waves (MMW), Terahertz imaging, Infrared, X-ray etc. The advantages and disadvantages of these approaches are discussed and research challenges and perspectives are presented. The chapter is organised as follows: section 2.1 reviews and discuss individual methods working at different frequencies within the electromagnetic spectrum; section 2.2 discusses the advantages and disadvantages of these techniques; then research challenges and perspectives are presented in section 2.3.

2.1 Review of Current CWD Technologies

Current CWD approaches range from the EM spectrum based detection to X-ray imaging. X-ray imaging has been used for border control and luggage inspections in airports but, because X-ray is harmful to humans, this technique will not be discussed in this review.

2.1.1 Metal detection using Earth magnetic field distortion

This technology is based on the passive sampling of the distortion of the Earth's magnetic field. The local aberrations in the magnetic field produced by ferromagnetic objects such as guns and knives can be detected by extremely sensitive magnetometers. Detector systems based on this technology exist in walk-through type devices and portable devices, currently in development, which are called Gradiometer Metal Detectors [2].

The gradiometer metal detector system is a passive system and has been deployed as a permanently installed part of a secure entry system for courthouses. It is a walk-through type device that uses a series of vertically arranged gradiometers located on either side of its portal. A gradiometer consists of two magnetometers connected electrically in what is

called differential mode. The gradiometer responds to changes in the local magnetic field of the earth caused by a moving ferromagnetic object. The differential mode connection is required to reduce the effects of normal background fluctuations that would otherwise cause false alarms. The gradiometer portal is very similar to a zoned walk-through metal detector. Each gradiometer pair responds to the presence of the ferromagnetic object and, based on the magnitude of these interactions, the system displays the location of the metal object within the portal. The system responds to moving ferromagnetic metal objects so that placing the system near stationary steel objects will not affect its operation [3].

There are some drawbacks in the gradiometer systems:

1. The gradiometer systems become expensive if spatial resolution is an issue. The resolution is dependent on the number of pair of gradiometers.
2. Those systems can only detect ferromagnetic weapons. Obviously some metal weapons are not made of ferromagnetic metals. Knives made of stainless steel and thread weapons made of aluminium, copper or brass can not be detected.
3. The system needs to be deployed in a permanent installation to avoid vibration which could lead to false alarms. It may be possible to use extra-hardware to keep tracking of position of the magnetometers, but it implies extra cost. Portable devices intended to be carried by officers or mounted on vehicles are in development [4,5]

CWD and Classification based on Earth's magnetic field distortion is a new application of existing magnetometer sensors. Sensors in the system simultaneously collect data, providing a top-to-bottom profile of an individual. Reasonable suspicion will be dictated by the location and magnitude of the recorded magnetic anomalies. A database of magnetic signatures has to be established through the collection of magnetic profiles of a variety of weapons in differing locations and a number of non-weapon personal artifacts. These signatures will later be used in the analysis that will determine the presence, location, and potentially, type of weapons. Recent analysis schemes include advanced signal processing algorithms that perform pattern recognition and calculate the probability that the collected magnetic signature correlates to a known database of weapon versus non-weapon responses using neural networks. In [6] a method to reduce false alarms was developed by using a Joint Time Frequency Analysis digital signal processing technique.

From 2003, the Idaho National Laboratory (INL) has developed a new generation of CWD system – a passive portal that senses disturbances in the ambient Earth's magnetic field. It uses gradiometers to detect and locate position of metals. The CWD system uses 16 magnetic gradiometer sensors, arranged on both sides of the portal aperture. Data are collected from each of the gradiometers, and the change in the magnetic field over ambient background is determined. After the individual sensor responses are collected, the data from all of the sensors are processed to determine the location and size of a detected object.

Figure 2.1 shows the graphical interface of the INL portal provided to the operator. It uses freeze-frame video capture technology and places filled circles — dependent upon the number of items detected — over the video image indicating where suspected weapons may reside on a person. The circle sizes vary in proportion to the strength of the measured signal. This approach is normally used for a controlled environment e.g. walk through gates at airports.

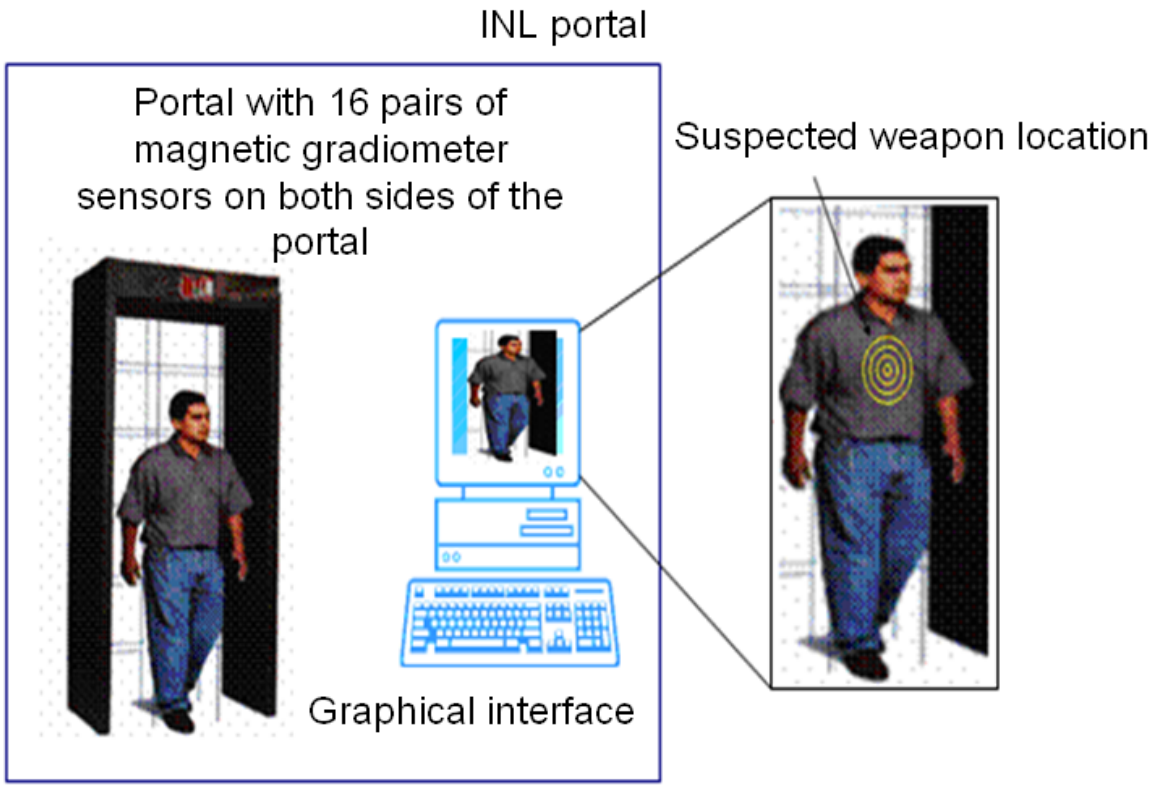

Figure 2.1. The CWD developed by INL [7].

2.1.2 Inductive magnetic field methods

The principle behind Electromagnetic inductive techniques for CWD is shown in Figure 2.2. An alternating current over the frequency range of 5 kHz-5MHz generates a time-varying magnetic field around the coil. This field induces currents in a nearby metal object which, in turn, generate a time-varying magnetic field of their own. These fields induce a voltage in the receiver coil which, when amplified, reveal the presence of the metal object or target.

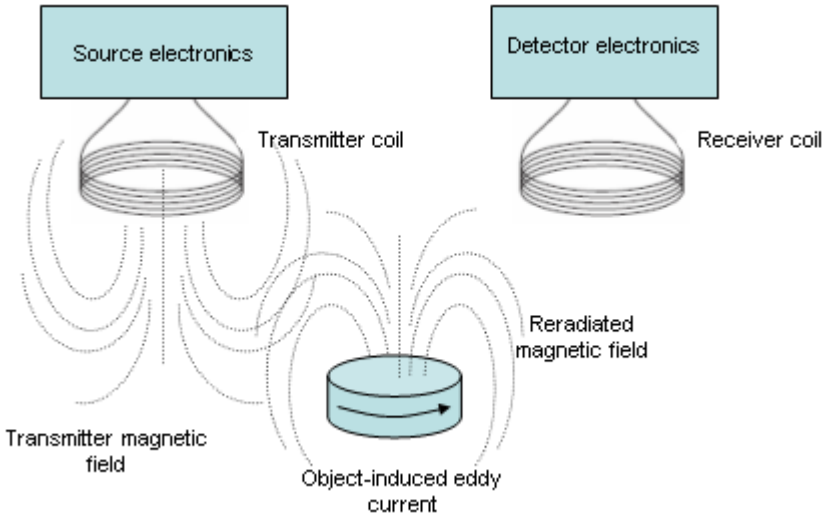

Figure 2.2. The principle of EMI technique for CWD [8].

There are two broad categories of EM induction approaches for CWD, which are classified by the type of magnetic field generated by its excitation coil: Pulse induction (PI) and Continuous wave (CW).

Pulse Induction (PI) detectors typically generate a transmitter current which is turned on for a time, and is then suddenly turned off. The collapsing field generates pulsed eddy currents in the target, which are then detected by analysing the decay of the pulse induced in the receiver coil. Conductive objects show a unique time-decay response, so a signature library of these objects can be developed. When concealed metals are encountered, its time-decay signature can be compared to those in the library and, if a match is found, the object can potentially be classified [8].

Continuous Wave (CW) detectors generate a transmitter coil current which alternates at a fixed frequency and amplitude. Small changes in the phase and amplitude of the receiver voltage reveal the presence of concealed metal targets.

Pulse Induction approach detects metal objects by analysing the time-decay response of the pulse induced in the receiver coil, whereas Continuous Wave approach does this based on changes in the amplitude and phase of the receiver coil voltage.

The following plots illustrate the two concepts of inductive metal detection methods by showing graphs of received signals with position on the horizontal axis. The scales are notional as the intention is just illustrate concepts. Figure 2.3 shows a change in decay rate of the signal received by PI detector (blue) with respect the reference signal (red) when passing over a metal located about position 10. Figure 2.4 shows a change in phase and amplitude of the signal received by CW detector (blue) relative to transmitted signal (red) when passing over metal located about position 10.

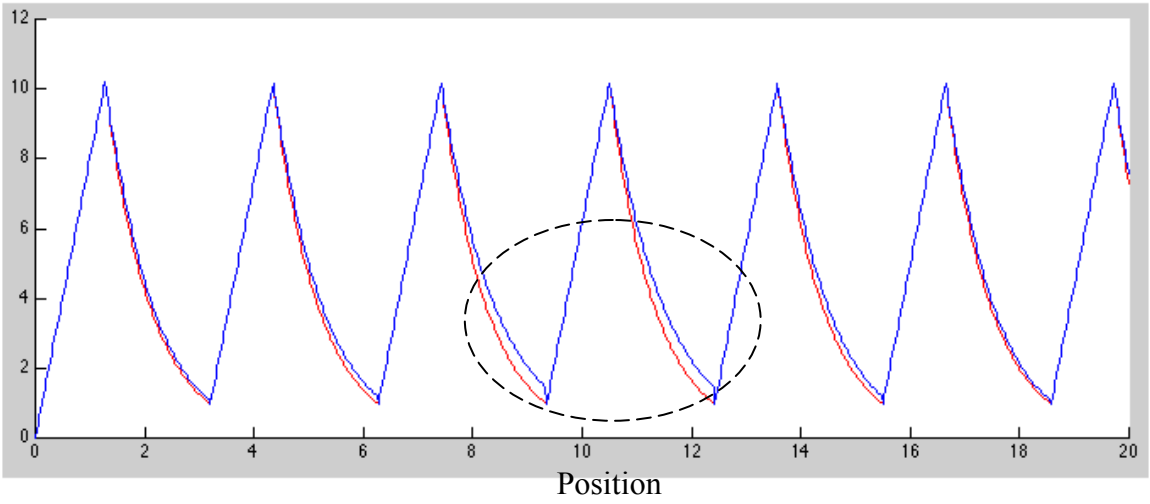

Figure 2.3. PI metal detection.

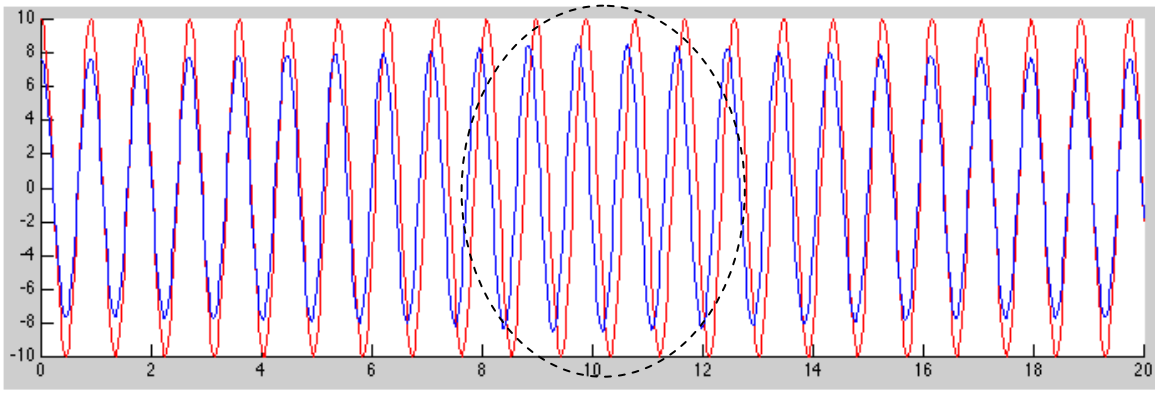

Figure 2.4. CW metal detection.

Most of these detection systems are used in airports throughout the world for weapon detection to protect restricted areas of the airports. Active Walkthrough Weapon Detectors like portal shown in Figure 2.5 belong to these systems. Figure 2.5 shows how signals from harmless objects are processed by active walkthrough metal detector. Pulsed magnetic fields produced by a transmitter (left panel) pass through the person being screened to the receiver panel. As a pulse passes through a metal object it causes eddy currents to be induced in its surface. Once the pulse passes beyond the object its field strength decreases and eddy currents in the metal starts to decay. As the currents decay they generate a low intensity magnetic field. This field is detected by the receiver coils with ferrite core to enhance the signal [9], and then processed into an electronic signal.

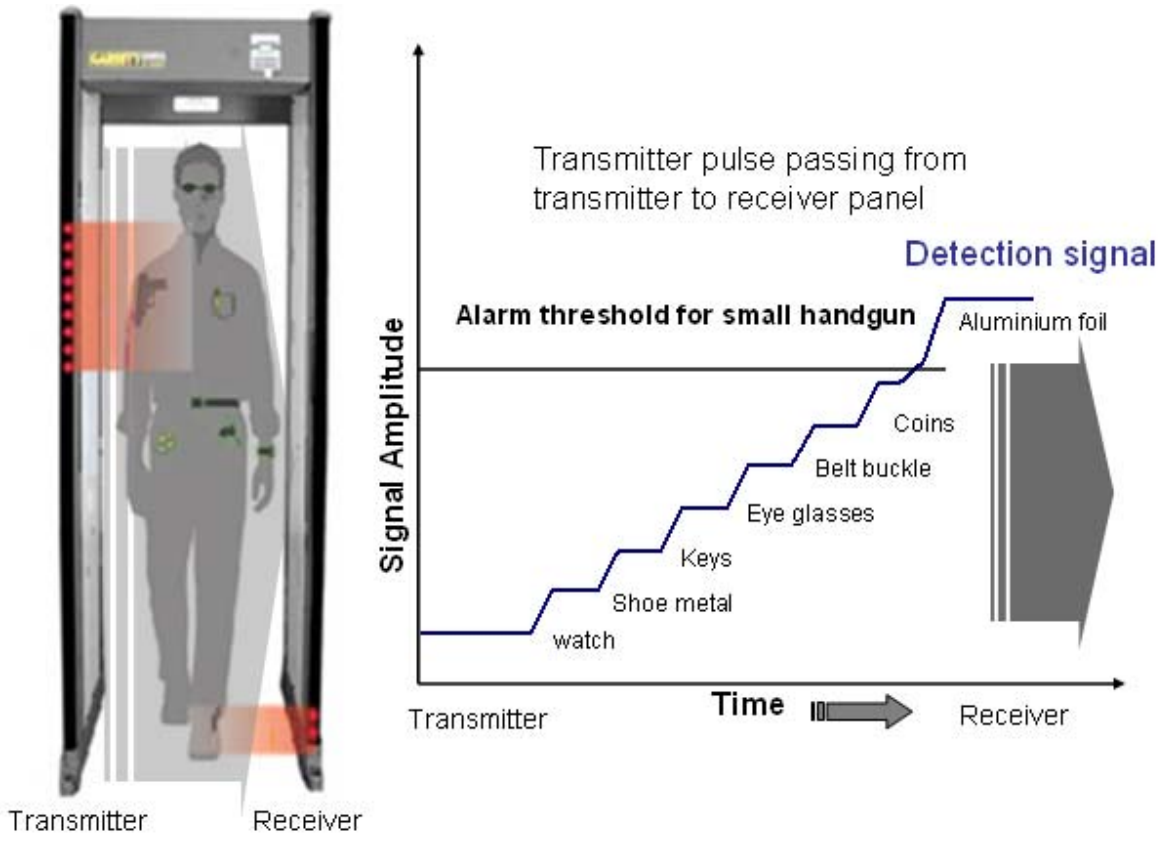

Figure 2.5. Cumulative signal effects in active walkthrough weapon detector.

Walkthrough weapon detectors based on inductive magnetic field differ from those based on gradiometers as they are active methods and can not identify the position of an object, whereas the latter ones are passive and can locate a hidden object.

CWD using this method has a problem with accuracy. A human body has a small conductivity thus the sensitivity of the detector cannot be high enough to be able to detect the magnetic field coming from the body. When dealing with materials that are not of very high conductivity (in general non-metallic materials) [10] or of very small dimensions, the human body could give a stronger signal than the material. This would cause the material to pass undetected. Thus, such CWD devices do not have a great reliability.

One of the most recent applications of inductive magnetic field approach is called Wide-Area-Metal Detection (WAMD) [11]. This is a CWD system which enables the detection of metal and can be used to locate people carrying metal weapons in a crowd that may require further investigation. WAMD use pulse induction to generate time varying magnetic field and use the time decay of the magnetic field in the target as a signature. WAMD system sensors use a 3D steerable magnetic field sensor (3DSMF) [12] to create and measure 3D time decay response of the magnetic field of the object. The strength of the magnetic field vector in 3D can be controlled by varying the current in each antenna element and employing superposition of the fields of each antenna. In this way false rate for classification decreases because most of target identification algorithms assume that target is excited with uniform field, which differs by far from complex magnetic field excitation of coil loops.

The WAMD sensor system is based on Horizontal magnetic field (HMF) metal detection antenna concept. This concept is based on sensors that attempt to generate three-dimensional magnetic fields and measure the target's 3D response by using magnetic field antennas that have complex spatial magnetic field distributions. The 3D steerable magnetic field sensor (3DSMF) (see Figure 2.6) orients the excitation magnetic field into the primary axis of the target. Once the primary axis is found, the antenna's magnetic field is rotated into the secondary axis of symmetric objects. For no symmetric objects, the 3DSMF sensor measures the object's response in 4π steradians. The classification algorithm then tries to match the object's 3D response to a target library.

To better understanding the above concept basic physics need to be reviewed. It is known that, for an infinitive conducting sheet current in free space, the magnetic field is in the direction perpendicular to the sheet current. Thus the sheet current is a horizontal magnetic field (HMF) generator or antenna. This magnetic field is constant. To take advantage of this feature, we create a practical approximation of an infinitive sheet current by placing closely spaced current-carrying wires in a plane (See illustration of three 3HMF in Figure 2.6). The result is a magnetic field with a relatively uniform horizontal shape.

To conceptualize the 3DSMF sensor, we need only to imagine two single-axes HMF antenna co-located at right angles to each other. This arrangement forms a 2D horizontal field-generating antenna. The third dimension to the magnetic field is created by adding a horizontal loop antenna to the two HMF antennas as shown in Figure 2.6. Thus a magnetic field in 3D is created by varying the current in each antenna and by employing superposition of the fields of each antenna.

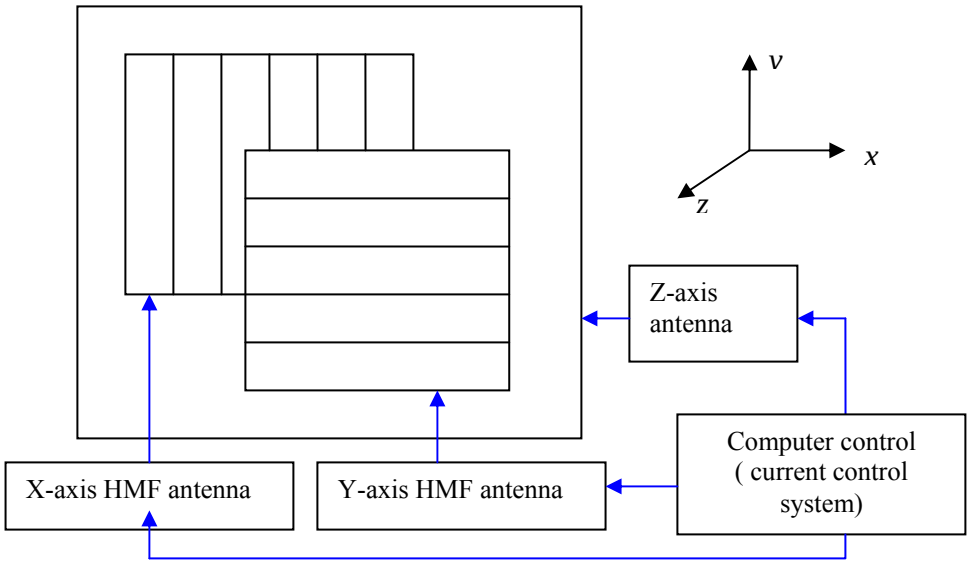

Figure 2.6. Block diagram of a 3D steerable magnetic field (3DSMF) sensor system [12].

2.1.3 Acoustic and ultrasonic detection

The detection of weapons using acoustic and ultrasonic detectors is dependent on the acoustic/ultrasonic reflectivity of materials that make up an object and the shape and orientation of the object. Basically, hard objects provide a high acoustic/ultrasonic reflectivity and soft objects a small reflectivity. The important detection parameters for these technologies are size of the target, diameter of the detector antenna, wavelength of the wave emitted, and the emitted power. The antenna size and wavelength affect the size of the smaller object that can be detected. Acoustic/ultrasonic power will not travel in a vacuum; it is attenuated less as its travels in dense medium (solids and liquids) and is

attenuated more as it propagates in the air. Also humidity in the air reduces the attenuation. The attenuation is frequency dependent; it is greater for higher frequencies. Therefore, there is a trade-off between the required spatial resolution and attenuation. Ultrasonic detectors operate from 40 kHz until frequencies well below 1 MHz because of increasing attenuation at higher frequencies. Acoustic detectors operate at audio frequencies.

Ultrasonic (high frequencies) detectors [13] have problems penetrating thick clothing whereas acoustic (low frequencies) detectors can propagate more easily through clothing and "see" a concealed object.

Conventional acoustic and ultrasonic based detectors are sensitive to hard objects in general, and thus, it can not differentiate between weapons and innocuous hard objects. Consequently devices based on these technologies produce many false-positive detections. Presently, there are hand held weapon detectors based on acoustic wave phenomena operating at 1m -5m distance. A combination of radar and ultrasound is being explored by JAYCOR, advanced-technology Company providing services to US Department of Defence. The system produces an ultrasound image and can operate at 5m-8m distance.

From the combination of the ultrasonic/acoustic approach, a nonlinear acoustic method (NAC) for CWD has been developed [14]. Figure 2.7 shows the principle. This technology uses ultrasonic beams of frequencies f1 and f2 to project sound onto a small spot area on a person at a distance and convert that energy probe from ultrasound to audio frequencies. The non linear interaction in the mix zone produces the following frequencies: f1, f2, f1-f2, f1+f2. The difference frequency (f1-f2), tuned in the audio range, is used to interrogate the subject with a beam able to penetrate clothing. Parametric acoustic arrays [15] can be used to produce nonlinear acoustic effects and the detection of a concealed weapon can be based on signatures. The nonlinear acoustic method for CWD uses correlation algorithms to perform patterns matching and classification to display the nature of a hidden weapon. In general this technique is harmless because does not involve ionizing radiation, is sensitive to metals and non-metals, and is able to penetrate clothing [13]. However, fast scanning is required for ultrasonic beams to focus on and find a target.

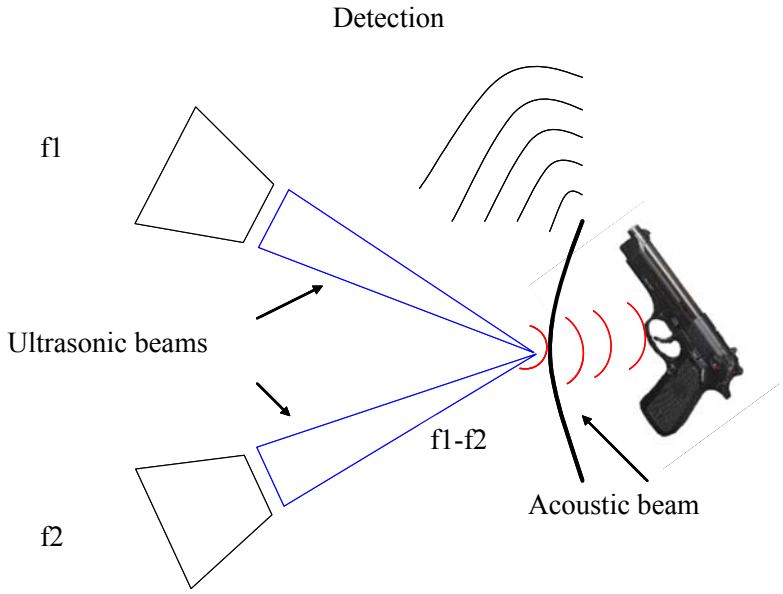

Figure 2.7. Non-Linear Acoustic CWD [14].

2.1.4 Electromagnetic resonances

This is an active technique which uses EM resonance as "fingerprints" or signature to distinguish weapons and nuisance objects. EM resonances in the objects are determined by its size, shape, physical composition. These resonances occur over the range 200MHz-2GHz. The detector uses radar to sweep through this range of frequencies and record the resonant response.

The radar return or resonance based scattering exhibits some features which makes it attractive for object identification schemes:

1. Scattering return is larger in the resonance region.
2. The natural resonances seen in a scattered return are independent of the orientation of the object.
3. A few natural resonances characterize an object over a large frequency band.
4. An object's resonance patterns uniquely identify it within a class of objects.

To induce a resonant response in an object, it is necessary to illuminate it in the frequency band of the natural resonances. The radar cross section (RCS) scattering falls in three regions, depending on the ratio of wavelength λ to body size *L*. The three regions are Rayleigh, resonance and optics corresponding to λ much higher than *L*, λ proportional to *L*, and λ much lower than *L* [16]. Figure 2.8 shows the RCS of a sphere of radius *a* as a function of its circumference measured in wavelengths, $2\pi a/\lambda = ka$, where *k* is the wavelength number. RCS has been normalized to the projected area of the sphere, πa^2. When the wavelength is much greater than the sphere circumference, its RCS is proportional to $a^2(ka)^4$, which shows that RCS increases as fourth power of frequency and sixth power of radius. When the circumference length is between 1 and 10 wavelengths the RCS exhibits oscillatory behaviour with several peaks which correspond to the natural electromagnetic resonance of the sphere [17]. When the circumference is large compared to a wavelength, the oscillatory behaviour fades out and the RCS is now independent of frequency and equal to physically cross section of the sphere.

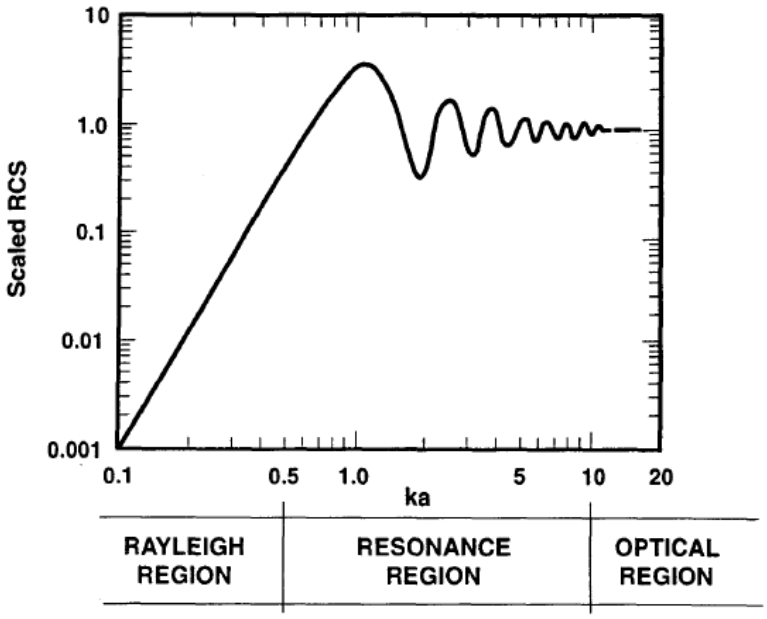

Figure 2.8. Enhancement of Radar Cross Section in the resonance region [17].

The theory of operation of this method is as follow. The target space can be illuminated by either a pulse or swept frequency source [2]. The signal reflected by objects in the target space provides an electromagnetic signature (EM resonances), a unique spectrum, for that object. The object signatures are then compared to known signatures to determine whether or not objects in the target space are threat items. Neural network processing is used to classify the difference between weapons and nuisance objects [18]. The person carrying the object will also exhibit a unique electromagnetic signature which must be subtracted from the composite person-object signature.

This method has an operation range of 6.096m, allows the detection of concealed weapons even behind a human body, operates at a safe limit power for human exposure and does not invade privacy of individuals.

The problem found with this technique is noise corresponding to the signature of people. Signatures of individuals vary from one to another and they also vary when a weapon is present. Unfortunately, the signature of an individual with a weapon is very similar to one without a weapon and so there is a problem with classification and a high rate of false alarm.

During 5th International Conference on Antenna Theory and techniques on May 2005 an approach based on EM resonance was presented incorporating circularly polarised, focused antenna arrays [19] to produce a very small common antenna beam footprint on the suspect under surveillance. This type of antenna makes the system less sensitive to the orientation of the concealed weapon. For the weapon classification, signal processing using Fourier or a Wavelet transform [20] is used.

2.1.5 Millimetre waves (MMW)

MMW based screening systems are basically of 2 types: passive and active. Passive sensors simply observe and report whatever detects in local environment. In the RF spectral range, natural surfaces will emit different amounts of radiation depending on parameters such as temperature and emissivity. In addition, metals are strongly reflective to RF, which reduces a metal surface's emissivity and allows it to produce reflections of other sources in the scene with the most significant being the sky. Passive sensors have the great advantage of producing valuable information without emitting any signals from people.

Active sensors typically stimulate the environment by generating and emitting known signals. These signals propagate out to the objects or targets of interest, interact with them, and reflect or scatter energy back to the sensor. Because the self-generated signals have known properties, it is often possible to use signal processing to extract very weak emitted target signals from competing sources of noise.

According to safety views, MMW systems utilise very low radiation power to generate detection capability. The system uses radiation power level 10,000 times less than that of a cell phone (maximum specific absorption rate (SAR) level of cell phone at 2009 is 1.6~2W/kg depending on region (see appendix B). The use of millimetre wave technology eliminates issues associated with use of ionizing radiation such as those seen with x-ray systems [21-23].

Figure 2.9 show how MMW images look. Passive millimeter wave (MMW) sensors measure the apparent temperature through the energy that is emitted or reflected by sources. The output of the sensors is a function of the emissivity of the objects in the MMW spectrum as measured by the receiver. Clothing penetration for CWD is made possible by MMW sensors due to the low emissivity and high reflectivity of objects like metallic guns.

Figure 2.9. MMW images (QinetiQ imaging system) [24].

2.1.6 Terahertz (THz) imaging

The THz imaging technique is based on the use of THz electromagnetic waves to spectroscopically detect and identify concealed explosives, chemical/biological agents, and metals through characteristic transmission or reflectivity spectra in the THz range. Generally, non-polar and non-metal solids are at least partially transparent and reflective to waves of frequencies 0.2 to 5 THz. Different materials have different effects on the THz wave. Typical clothing items and paper and plastic packaging should appear transparent in the THz regime whereas metals completely block or reflect THz waves. Ceramic guns and knives would partially reflect the THz signal. Skin, because of its high water content, would absorb nearly all T-Rays with the energy being harmlessly dissipated as heat in the first 100 microns of skin tissue. A THz reflection image of a person as shown in Figure

2.10 would show the outline of clothing and the reflection of objects beneath, such as weapons or key chains, but the person's skin would appear substantially dark [25].

Figure 2.10. THz reflection image of a person carrying a gun [26].

There are some advantages of this technique which are attractive for CWD:

1- The spatial resolution of THz waves is excellent for CWD. THz waves can separate objects less than 1mm apart, which is more than enough to tell a weapon apart from its surroundings. This resolution is roughly 10 times better then that of Millimetre Waves (MMW), due to the smaller wavelength.

2- Many materials of interest for security applications including explosives, chemical agents, and biological agents have characteristic THz spectra that can be used to fingerprint and thereby identify these concealed materials. .

3- THz waves are non-dangerous. The penetrating ability of THz waves may seem harmful to health, similar to the x-ray, but in actual fact, it is totally harmless as T-rays are non-ionizing - they do not alter molecules in the air or in humans. On the other hand,

x-rays can cause diseases such as cancer in humans if over-exposed and could cause damage to the eyes if shown directly [25].

However, THz imaging has some issues which have to be eventually solved:

1- The feasibility of the use of terahertz imaging for the detection of concealed weapons is questionable. The main issues are cost, processing and complexity. THz systems are expensive because it requires special power sources. The recent introduction of near infrared (λ=800nm) femtosecond laser as radiation source, has helped to bring the cost of such systems down below 50K Euros [27]

2- Though T-ray detection is already possible, it is not, by far, perfect yet. Using close range imaging, it is still difficult to develop video output because the scanning is still slow, leading to a poor frame rate.

3- The most significant limiting factor of the capabilities of T-ray imaging at stand-off range (3m to 100m) is the atmosphere which causes attenuation and turbulence to the waves [28]. However oxygen, water and other components of the atmosphere absorb THz power at specific frequencies only, leading to high attenuation at certain frequencies (Figure 2.11). Therefore, all stand-off THz imaging systems are tuned to use frequencies that are less attenuated.

4- Proper guidelines for using these imaging systems have to be finalised and put into action, as they might be harmful at some specific conditions of exposure [29] or have legal implications.

5- Privacy invasion issue, because T-ray can penetrate clothes.

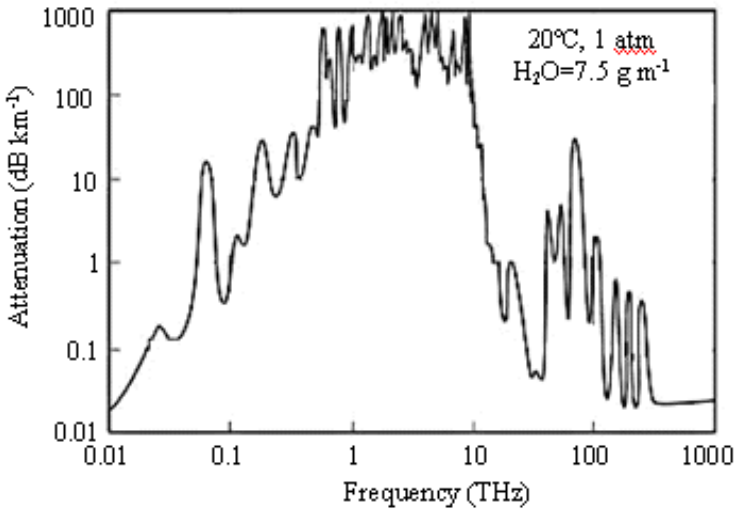

Figure 2.11. Atmospheric attenuation of THz rays against frequency [22].

2.1.7 Infrared imaging

Infrared imaging is another commonly used detection system. Human bodies as well as any other material emit radiation provided they are at a temperature above 0°K. The wavelength of the radiation peak is dependent on the temperature of the body, and the total power emitted from the body is dependent on the size and emissivity of the body. Most infrared sensors are designed to have peak sensitivity near the peak emission wavelength of human body which is 10 μm. This technology is normally used for a variety of nigh-vision applications.

Infrared radiation emitted by people is absorbed by clothing. This absorbed radiation heats the clothing and is then re-emitted by the clothing. Consequently, the image of a concealed weapon will be blurred, at best, assuming the clothing is tight and stationary. For normally loose clothing, the emitted infrared radiation will be spread over a larger clothing area thereby significantly decreasing the ability to image a weapon. The difficulty in observing an infrared signal of a concealed weapon becomes worse as the weapon temperature approaches that of the body [30].

2.1.8 Hybrid millimetre-wave and infrared imager

Hybrid millimetre-wave and infrared imagers are systems that exploit both mm-wave and infrared imaging techniques. The images from these two separate imaging subsystems are brought together algorithmically in what is called a fusion process. The fusion of the mm-wave and infrared images results in a fused image [31].

The fusion process requires that the images be aligned properly (Registration). Before alignment each image is filtered to remove extraneous or noisy data and enhanced to augment certain image features. This process is illustrated in Figure 2.12.

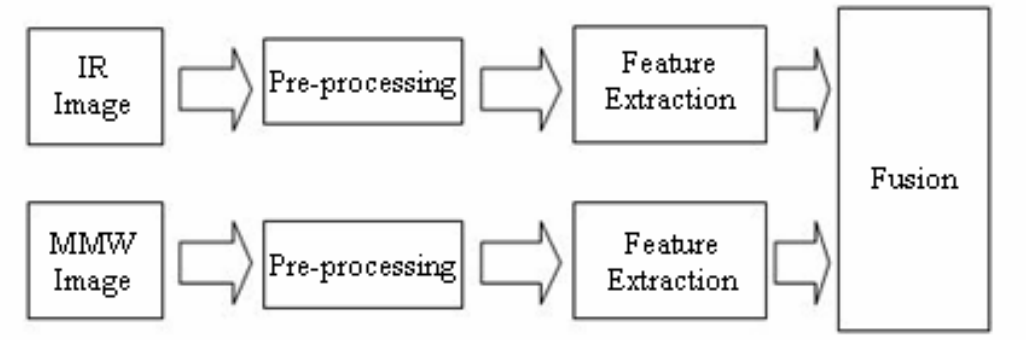

Figure 2.12. Image fusion [31].

The most straightforward approach to image fusion is to take the average of the source images, but this can produce undesirable results such as a decrease in contrast. Many of the advanced image fusion methods involve multi-resolution image decomposition based on the wavelet transform [32]. The fused data is the result of infrared and MM-wave images. If the infrared image cannot contain information on the concealed item, it will provide no useful information. In most situations, clothing will prevent acquisition of any information on a concealed weapon. Consequently, the fused image provides no further information on the concealed weapon than that provided by the MM-wave imager. MM-wave images take a few seconds to acquire and during this time the person must be stationary. The fused

image may exhibit no more than a MMW image of the concealed weapon with a high-resolution image of the surface of the clothing. However, the infrared image does facilitate location of human subjects, on which an object may be hidden, and this may accelerate the subsequent process of detecting a weapon on the subject.

2.1.9 Electromagnetic resonances and phased array

A portable CWD systems based on finding electromagnetic resonances was developed with relative good performance [17]. This concept can be adapted in order to screen people in an open area. This novel idea is based around a phased array located in the floor of the scanning place, with a sensor array in the roof and a phase shifter control system to steer the direction of the illuminating beam. Using a phased array [33] as a transmitter offers the advantage of illuminating the metal body in multiple directions and in any desired direction. This might give evidence of electromagnetic resonances as well as extra information regarding the location of the target. Hence, by finding electromagnetic resonances and keeping track of the beam as it scans, it should be possible to pinpoint the concealed weapon. The system could operate as shown in Figure 2.13. The arrays of sensors are distributed in a grid pattern in order to show the location of gun/knife carrying people.

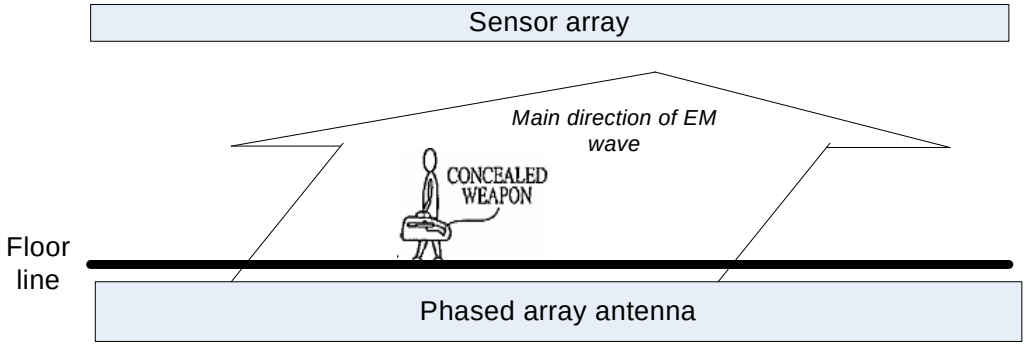

Figure 2.13. CWD system for open areas using phased arrays.

2.2 Discussion

After reviewing different detection methods for CWD, a summary is illustrated in Figure 2.14 and tables 2.1 and 2.2. Figure 2.41 shows EM spectrum used to illuminate the detection space by different CWD methods. Table 2.1 gives a brief summary of the technologies being developed for CWD, including issues such as type of illumination of the target, type of energy used for interrogation of the detection space, portability and proximity of use. Table 2.2 gives a summary of the main issues of CWD methods, including the parameter to be assessed, distance achievable, attenuation factor, depth of penetrability, and detectable weapons.

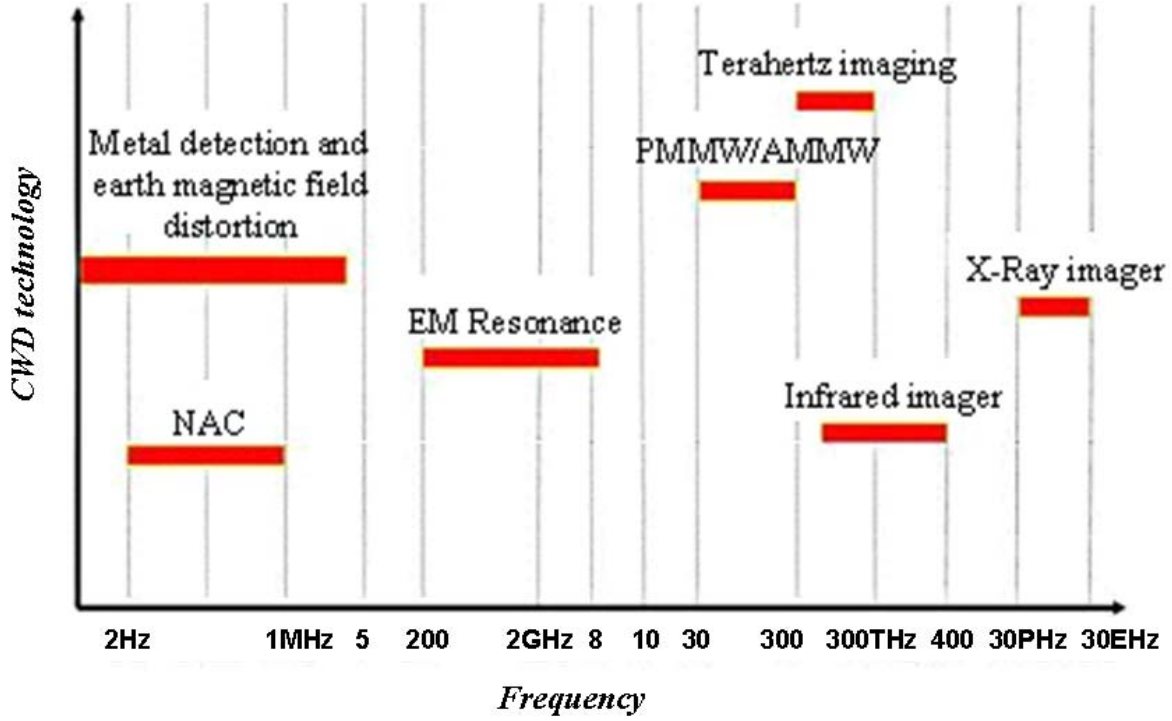

NAC: Non-linear acoustic concealed weapon-explosive detection
PMMW: Passive millimetre wave
AMMW: Active millimetre wave

Figure 2.14. EM methods for CWD in the EM spectrum.

Table 2.1. Summary of the Different Technologies being developed for CWD.

DESCRIPTION	ILLUMINATION	PROXIMITY	PORTABILITY
ACOUSTIC OBJECT DETECTOR	active	far [1]	portable
WALK-THROUGH METAL OBJECT DETECTOR	active	near [2]	portable
HAND HELD METAL OBJECT DETECTOR	active	near	portable
IMAGING PORTAL	active	near	portable
METAL OBJECT LOCATOR	passive	far	portable
PULSE RADAR/ SWEEP FREQUENCY DETECTOR	active	far	portable
THZ-WAVE IMAGER	active	far	portable
MM-WAVE RADAR DETECTOR	active	far	portable
EM PULSE DETECTOR	active	far	portable
MM-WAVE IMAGER	passive	far	portable
IR IMAGER	passive	far	portable

[1] More than three-meter-range

[2] Less that one-foot-range

Table 2.2. Summary of Main Issues of CWD.

CWD TECHNIQUE	ASSESSED PARAMETERS	OPERATING RANGE (M)	ATTENUATION FACTORS	PENETRABILITY	DETECTED WEAPON CONTENTS
EM RESONANCES	EM natural frequencies	> 10	Atmospheric conditions	wavelength dependent	metal and non-metal
NON-LINEAR ACOUSTIC	Impedance, resonance, non- linear acoustic interactions	~ 8	air	medium	metal and non-metal
TERAHERTZ IMAGING	THz radiation absorbed or reflected	3~50	water	medium/low	metal and non-metal
MMW	Emissivity and brightness temperature	4.5~7.62	water	high	metal and non-metal
INDUCTIVE METHODS, MAGNETIC SIGNATURE	Conductivity, permeability (magnetic signatures)	< 3	-	high	Metal objects

There is a large gap in the current detector market. Most pre-used gun detection is through intelligence and surveillance, along with targeted stop and search. CCTV does not often assist and is only really effective post event in providing identification and evidence, – i.e. it is not pro-active. The police do not have a deployable portable detector that can unambiguously determine whether someone is carrying a gun. Such a device would assist them in producing more effective stop and search strategies providing the number of false

positive events were kept within acceptable limits. Currently, research effort into developing a sensor is concentrated in large parts of the EM spectrum, plus acoustic and magnetic detectors. Focus now is on stand-off detection rather than proximity detection with portals or hand held metal detectors [34].

Wild [35] has developed a portable ultrasound concealed weapons detector that works at distances of up to 6m. There are reports of its partial effectiveness, and it is easily deployable. However, this makes no use of the resonant cavities present in a gun to generate a unique gun signature and it is falsely triggered by non-gun items such as leather wallets. Millimetre waves are known to penetrate clothing well, and both passive and active MMW imagers are being developed. These devices are generally large and more suited to portals at airports; although a passive MMW video surveillance camera has been developed [36]. Active through wall imaging systems, operating at 94 GHz, have been developed that are capable of identifying a gun in the hand of a suspect inside a room. At 94 GHz microwave radiation is attenuated but not scattered by building material. It is difficult to identify a weapon on MMW image, but some authors concentrate on fusing images of MMW and Infrared images to better reveal hidden guns [37] with some success.

THz sensing and imaging systems are currently being developed that are capable of forming 3D images of concealed weapons [38]. However, the penetration of THz through the atmosphere for stand-off detection and through some types of clothing leads to poor results (e.g. a wool sweater produces diffuse scattering of THz, leading to the blurring out of any concealed gun). Infrared imagers can potentially be used for detecting concealed guns at night. A challenge identified for infrared imager is clothing radiation absorption. The absorbed radiation heats the clothing and is then re-emitted by it, spreading over a large area and decreasing the ability to image the weapon.

Research is also ongoing into Wide-Area metal detectors designed to locate people in a crowd potentially carrying guns [39]. This technique utilises a pulsed magnetic field radiating across a large area, coupled with a receiver and CCTV to identify suspects. It does rely on CCTV operators to observe potential suspects once an alarm is triggered. At

the moment there is a terahertz imaging system commercially available which is sold by *TeraView Ltd*, in Cambridge, UK. The imager uses photomixing technology [40, 41] with a femtosecond pulsed laser illuminating low temperature GaAs as Terahertz source. Finally, work is ongoing on portable and handheld MMW radar detectors that utilise frequency modulated CW radar and complex signal processing to form an image of a concealed weapon [42]. A small body of work does exist that has systematically examined the opacity or otherwise of fabrics and other materials to microwaves and THz but these are not in a form that would easily assist the police in the deployment of suitable sensors for given conditions.

2.3 Challenges and Research Perspective

For development of deployable concealed weapon detectors, three issues should be solved: sensing distance, high penetration and weapon recognition. Enough sensing distance is required for open, outdoor environments e.g. high streets. High penetrations are required for detection of metals and explosive under clothes or garments. Alternatively, penetration is also required to detect targets beyond walls. Robust weapon recognition is required for various weather conditions and multiple objects or crowd environment. The above review has identified current detection methods are complementary approaches. No single approach can meet all the requirements for a comprehensive CWD.

To solve these issues, taking advantage of different CWD technologies, a combination of these is proposed.

Perspective of Research

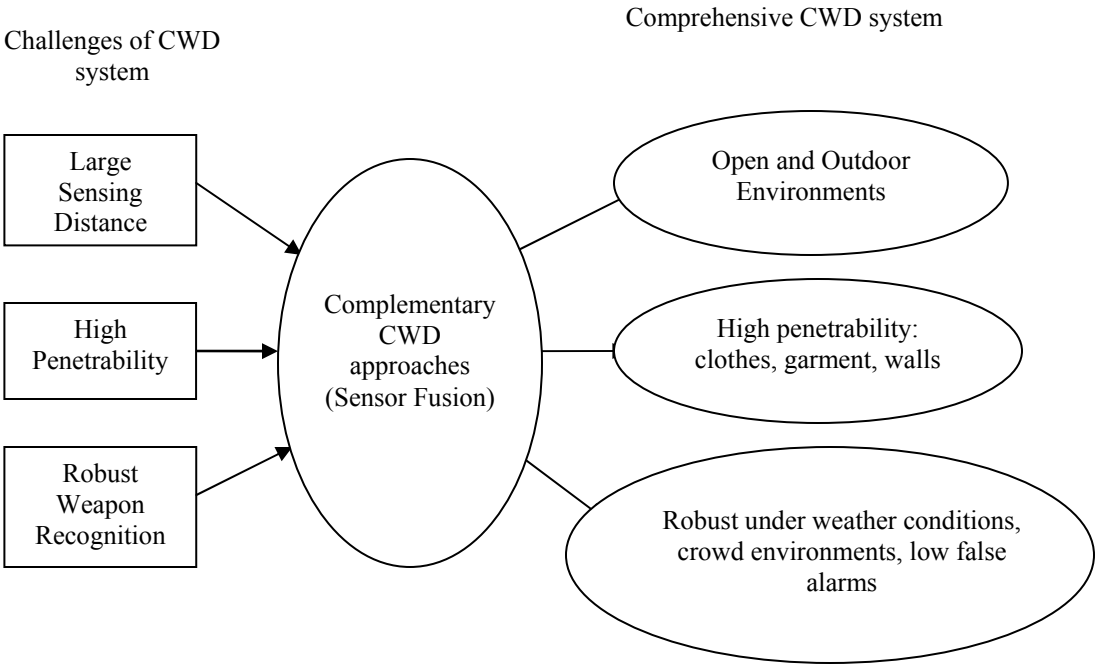

Figure 2.15. Diagram of challenges and research perspective of CWD.

Figure 2.15 shows a diagram of the CWD research perspective arising from challenges of a deployable CWD. Large sensing distance, high penetrability and a robust weapon recognition system can be achieved by using complementary approaches. A comprehensive CWD system is expected working in this direction.

To broaden and improve weapon recognition to explosives, chemical agents, and biological agents, the characteristic THz spectra of these threats can be exploited. The spectra can be used to fingerprint and thereby identify these concealed materials.

The literature survey has identified that current detection methods are complementary approaches and so the best approach is a combination of some of them. A tentative weapon detection system is showed in the next diagram (Figure 2.16). Complementary CWD approaches in low and high frequency of EM spectrum (EM induction methods, Earth's magnetic field distortion, and EM resonance) could be used to meet all requirements for comprehensive concealed gun/knife detection system

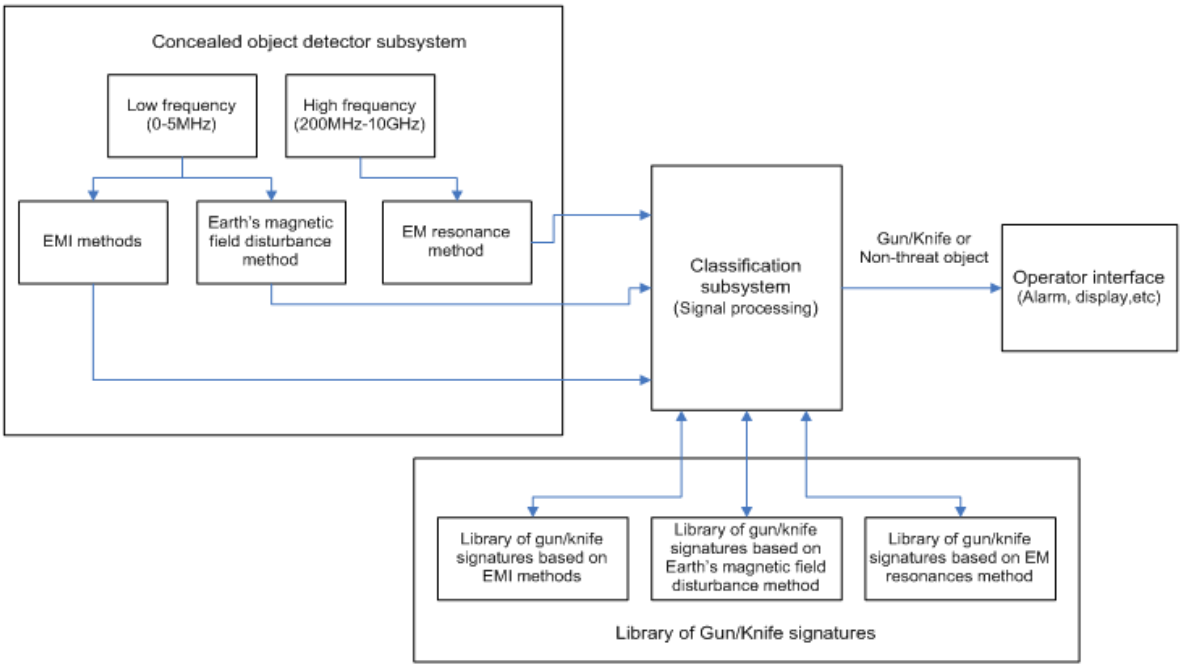

Figure 2.16. Diagram of a tentative weapon detection system.

2.4 Conclusions

A general concealed weapon detector collects data about the detection space and transmits this information to the operator. Different sensor technologies are employed to capture different sort of radiating energy (magnetic field, electromagnetic wave, acoustic wave, and ultrasonic wave) that contains information about the detection space or about objects in the detection space. Some technologies provide an image and other an indication regarding the objects inspected.

All technologies show advantages and disadvantages in issues such as operating range, material composition of the weapon, penetrability and attenuation factors. Each method has some advantages over another. It is clear that no single method can meet all requirements for a comprehensive CWD system. Most of the methods described here are complementary.

There are several challenges to the development of a comprehensive concealed weapon detector. Three issues are the most critical and must be solved: Detection at a distance for open and outdoor environments; High penetration for detection of weapons, explosive under clothes, back or even walls, and a robust weapon recognition for various weather conditions, crowd environment and able to discriminate accurately threat/non-threat items.

New CWD systems need to be an amalgamation of the techniques mentioned above permitting a reduction in the number of false-positive trigger rates.

Chapter 3: FEA OF GUNS AND KNIVES DETECTION APPROACHES

Following the review of recent technologies related to CWD, FEA is applied to study the detection capability of CWD technologies working with radiation of 0-1Ghz frequency, which is the part of EM wave spectrum that this research is focus on. In this chapter for the given EM spectrum, the study of two CWD technologies has been chosen. The first study is done on technology based on sensing disturbances in the earth magnetic field and the second one on technology based on Radar Cross Section (RCS) resonance response under EM wave illumination. In each case the sensitivity of the method to external and inner characteristics, and orientation of the weapon is analysed in order to study detection capability. To simplify the analysis and without loss of generality, gun barrels and knives have been modelled as uniform bars with different external and inner shape cross sections as shown in Figure 3.1.

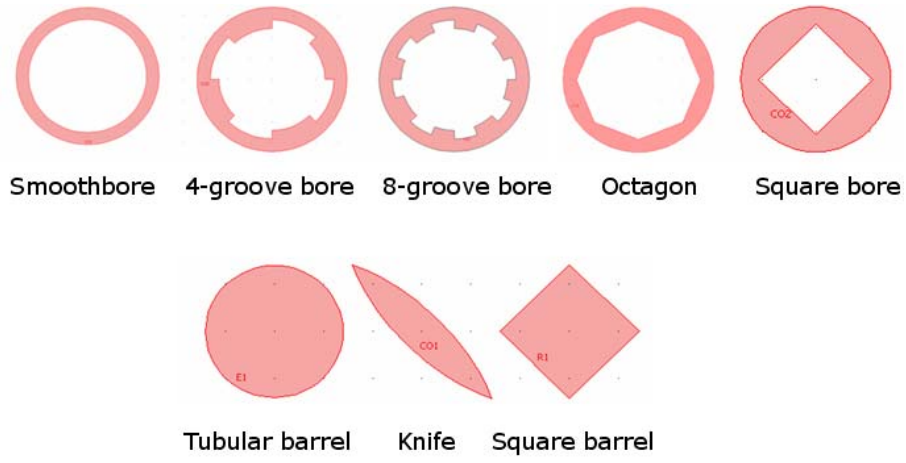

Figure 3.1. Cross sectional of the samples.

Figure 3.1 shows the samples used in this test. Top row show different cross sectional of gun barrels. Bottom row show external shapes: tubular barrels (diameter 17mm), knife (0.8mm width) and square barrel (17mm side).

3.1 Earth Magnetic Field Distortion Method

In this section the local disturbances in the Earth's magnetic field ($\approx 50\,\mu T$) arising from the presence of different sort of gun barrels and knives is analysed.

In order to emulate the Earth's magnetic field magnetic potential condition is applied to a finite volume (box: 1m x 0.5m x 0.5m). The top boundary is set to a magnetic potential of 1989A whereas the bottom boundary is set to a magnetic potential of zero (see Figure 3.2). This setting corresponds to a vertical magnetic flux density of about $50\,\mu T$.

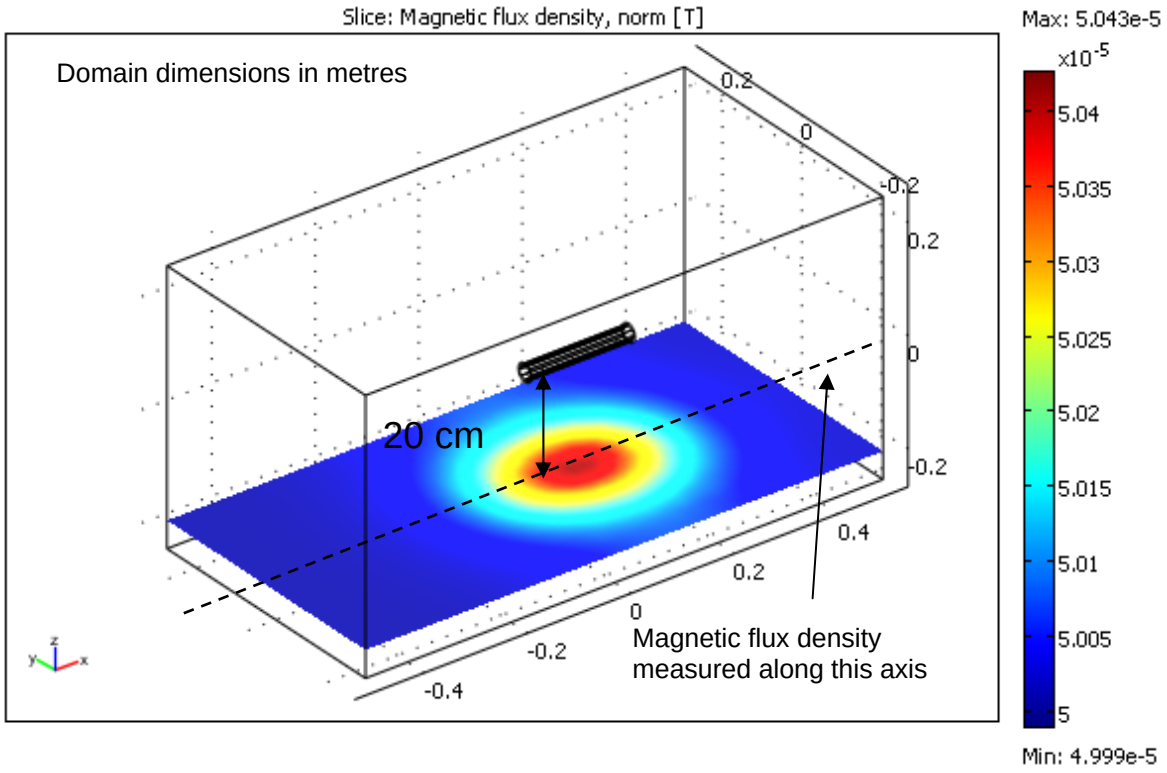

Figure 3.2. FE model of CWD based on earth field distortion.

Magnetic flux density norm is measured along a line in the axial direction of the interrogating weapon located 20cm below this (see Figure 3.2). Potential use of the resulting magnetic flux density profile as distinguishable magnetic signatures is analyzed in the next sub-sections.

3.1.1 Sensitivity to external shapes

Perturbations in the earth's magnetic field caused by weapons (bars for this model) with different external shapes show different amplitude pattern when magnetic flux density norm is measured. It could be used as a magnetic signature for weapons with different external shapes. Figure 3.3 shows Magnetic flux density pattern for three samples.

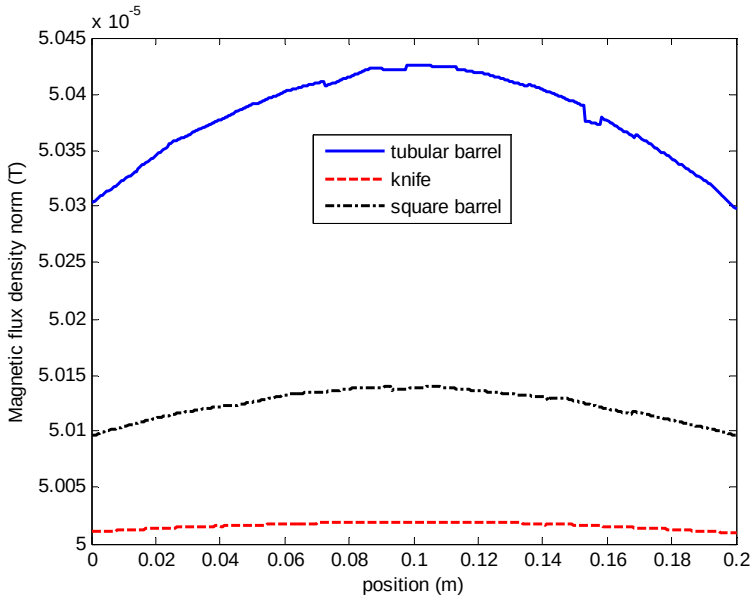

Figure 3.3. Magnetic flux density patterns of three samples with different outer section.

3.1.2 Sensitivity to inner shapes

Perturbations in the earth's magnetic field caused by gun barrels with the same external shape but different bore show a slight difference in amplitude pattern. This means the method is sensitive to inner shapes and could be distinguish different classes of guns. Figure 3.4 and 3.5 shows Magnetic flux density norm distribution for gun barrels with different bore shape.

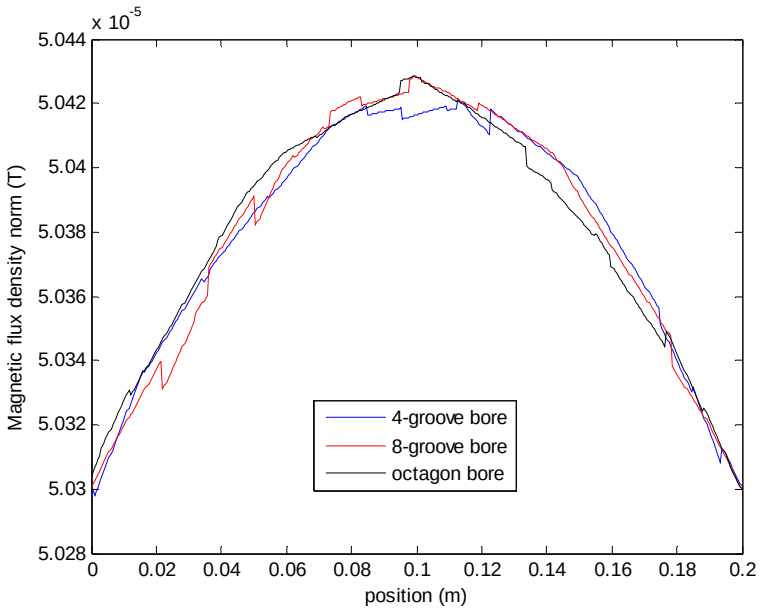

Figure 3.4. Magnetic flux density patterns of three samples with different inner section.

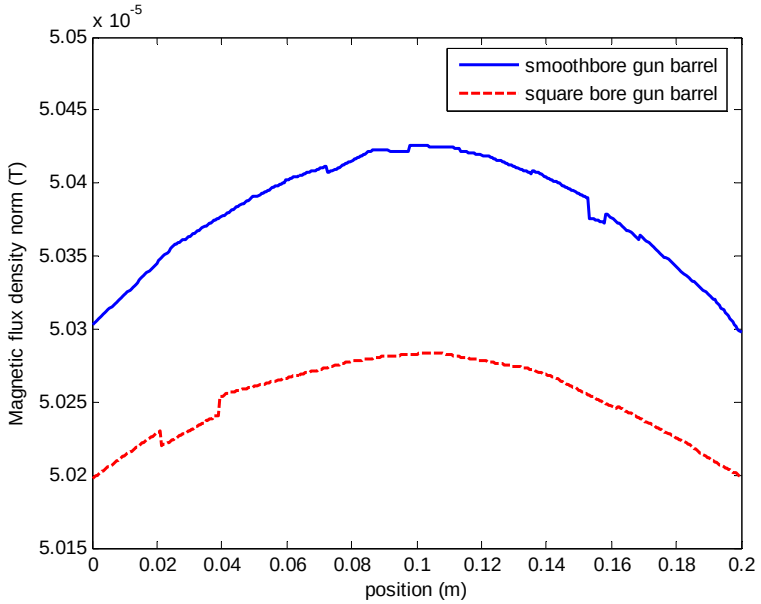

Figure 3.5. Target responses showing sensitivity to internal cross sectional change.

3.1.3 Sensitivity to orientation

The earth magnetic field distortion caused by a square gun barrel at 0 degree and 45 degrees rotation around its axial axis is measured as shown in Figure 3.6. The signals measured for these two scenarios show slight different pattern, especially in the middle of axial length. Thus this technology shows sensitivity to orientation of the weapon which makes more difficult weapon classification process.

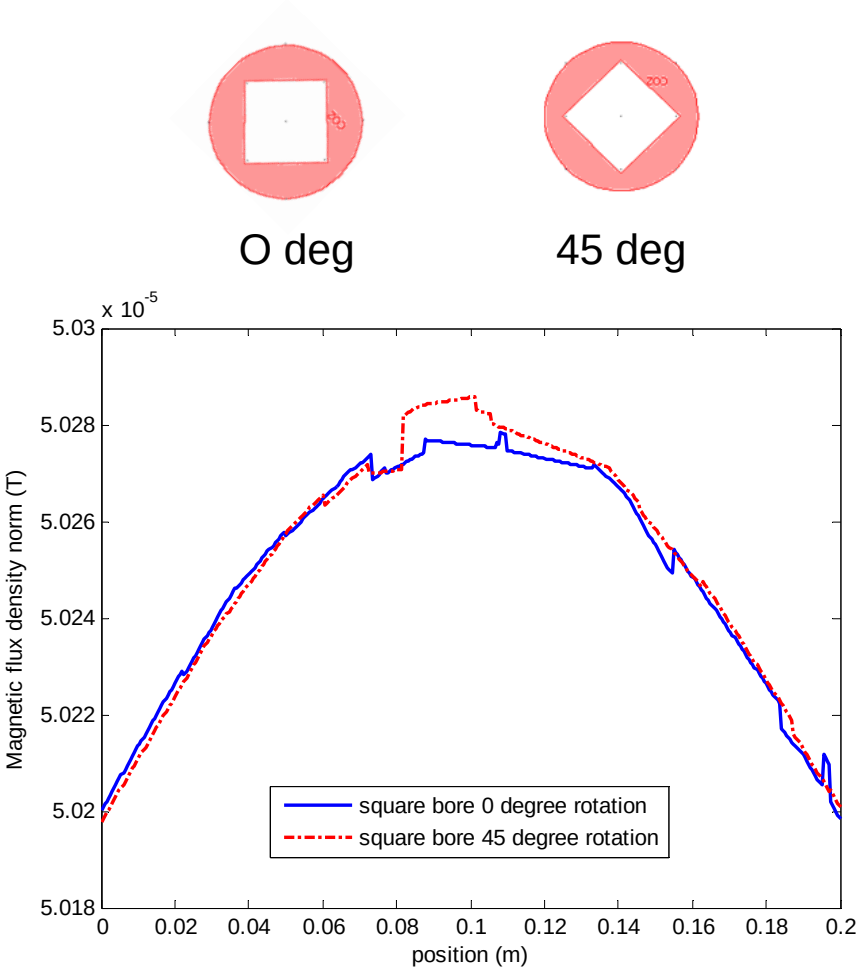

Figure 3.6. Signal response of a square bore barrel rotated 0 and 45 degrees.

3.2 High Frequency EM Wave Illumination Method

3.2.1 Investigation of EM wave in weapon characterization

The radar cross section (RCS) is a measure of sensitivity of an object to reflect illuminated signal in the direction of the receiver. In the next model RCS response is used to characterize guns and knives under EM wave illumination. The sensitivity of RCS respond at shapes (external and internal) and orientation is analyzed. Since the scattered wave from objects radiates in every direction, the 'perfectly matched layers' i.e. PMLs [43] are set up in cylinder coordinates. The modeling domain is 200mm by 200mm (see Figure 3.7). The frequency varies from 3GHz to 30GHz with a wavelength step of 10mm. The standoff distance is 90mm from the symmetric axis of gun barrel.

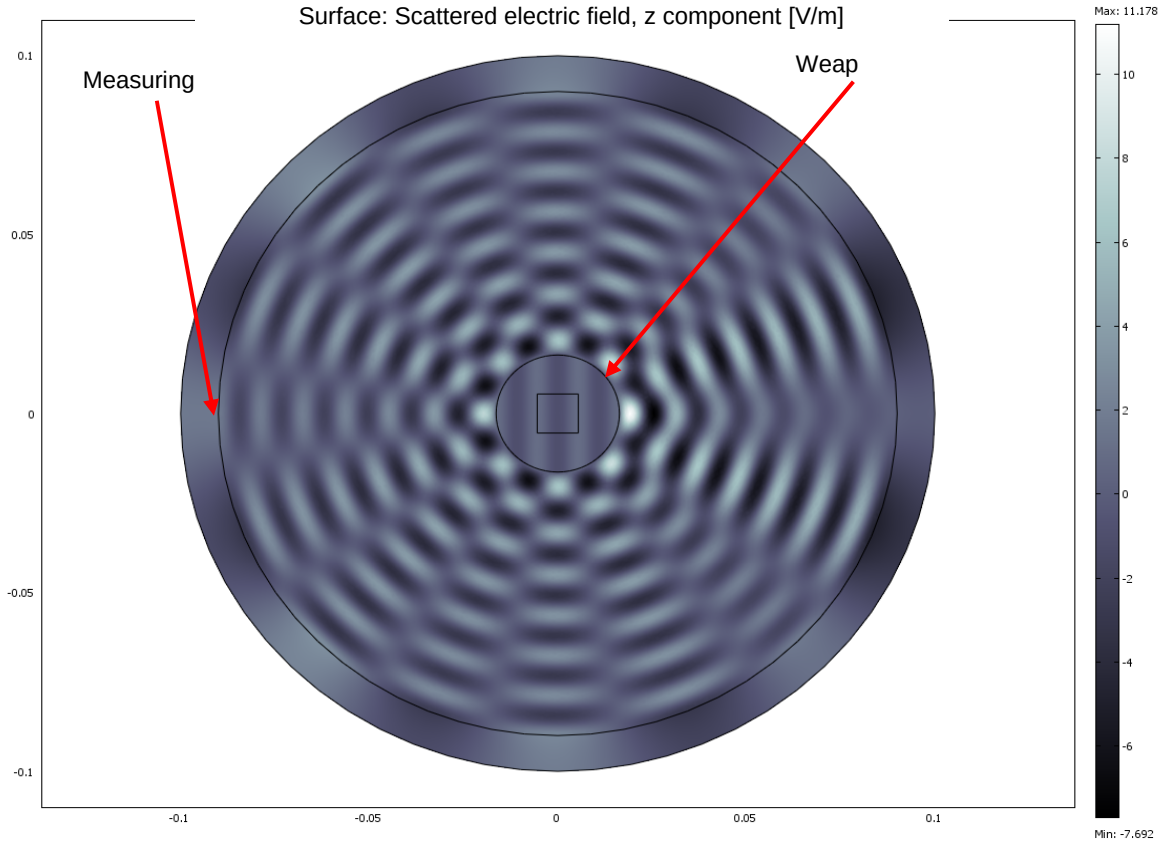

Figure 3.7. FE model to investigate weapon response to EMW illumination.

- **Orientation of inner shape vs. RCS**

The orientation of non-circular bore and material of gun against RCS pattern is analyzed. To simplify the problem, the bore shape is defined as a square. Two orientations i.e. 0 degree and 45 degree with respect to the radiation direction of incident wave are compared. The results are shown in Figure 3.8.

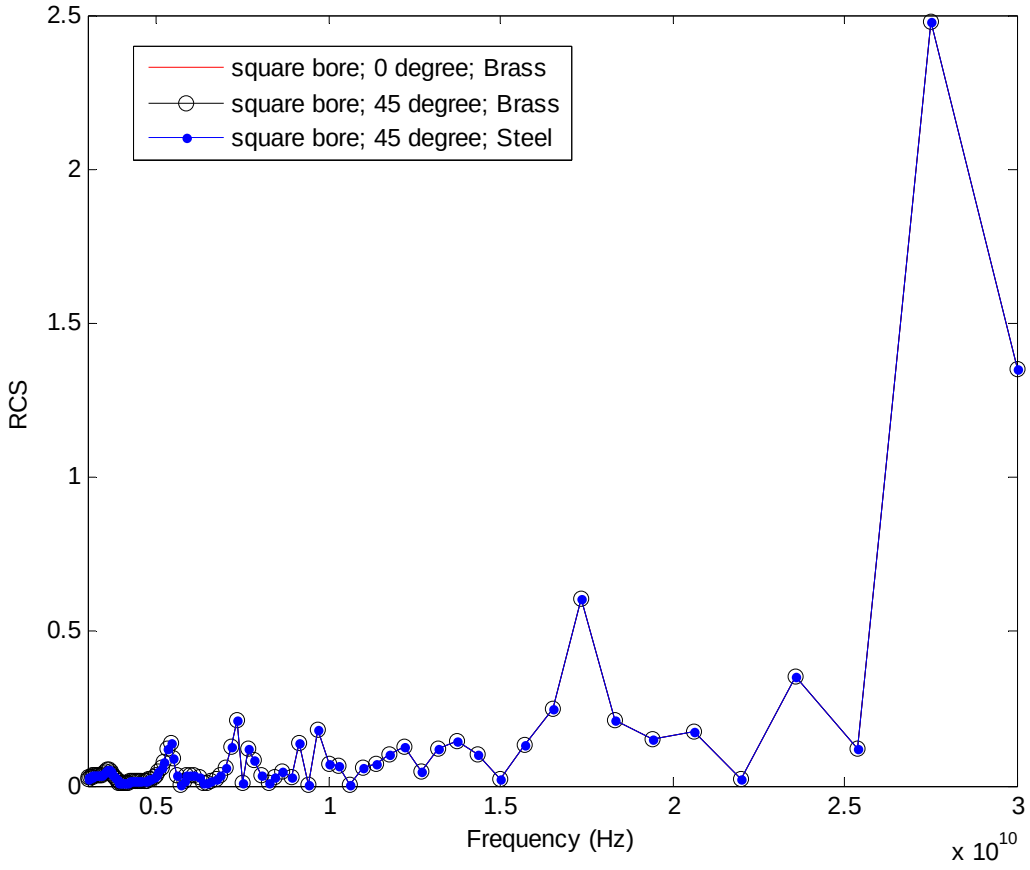

Figure 3.8. RCS response change of orientation of bore gun barrel.

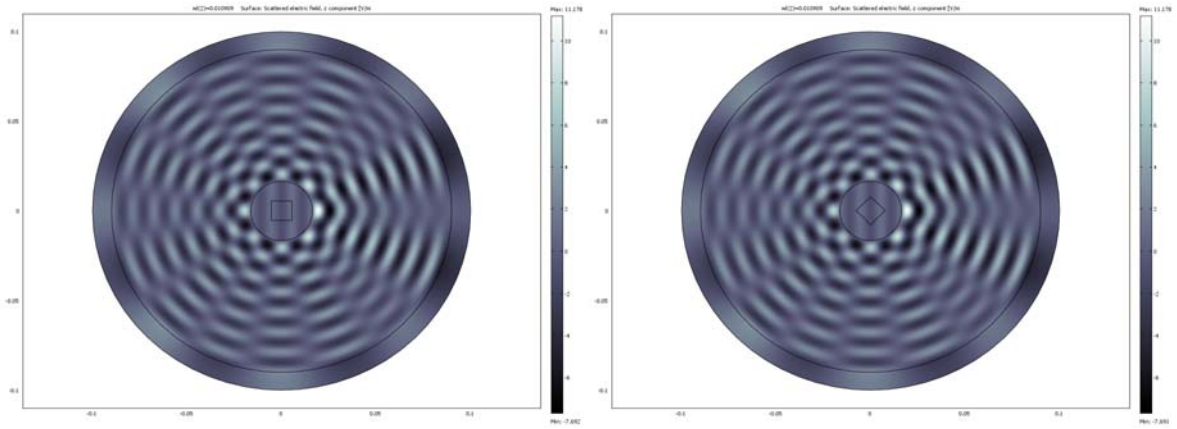

(a) (b)

Figure 3.9. Radiation patterns of scattered wave for (a) 0-degree rotated bore; (b) 45-degree rotated bore.

As can be seen in Figure 3.8, the RCS pattern is insensitive to material and the orientation changes of gun and barrel bore, respectively. It is because the conductive objects within EMW is quite reflective and can hardly penetrate into the barrel to interrogate the orientation or shape changes of bore.

- **Orientation of outer shape geometry vs. RCS**

The orientation of non-circular outer geometry of barrels against RCS pattern is investigated. The square barrel is modeled. Two orientations i.e. 0 degree and 45 degree with respect to the radiation direction of incident wave are compared. The results are shown in Figure 3.10.

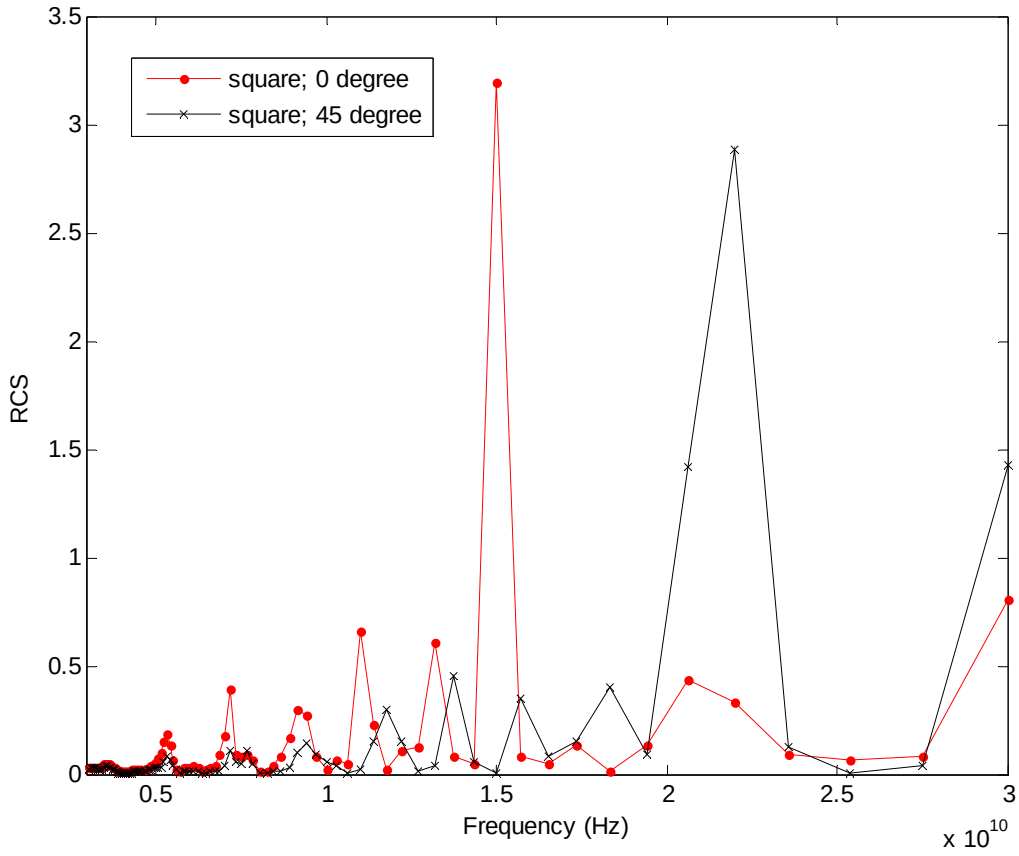

Figure 3.10. RCS response to change of orientation of external shape gun barrel.

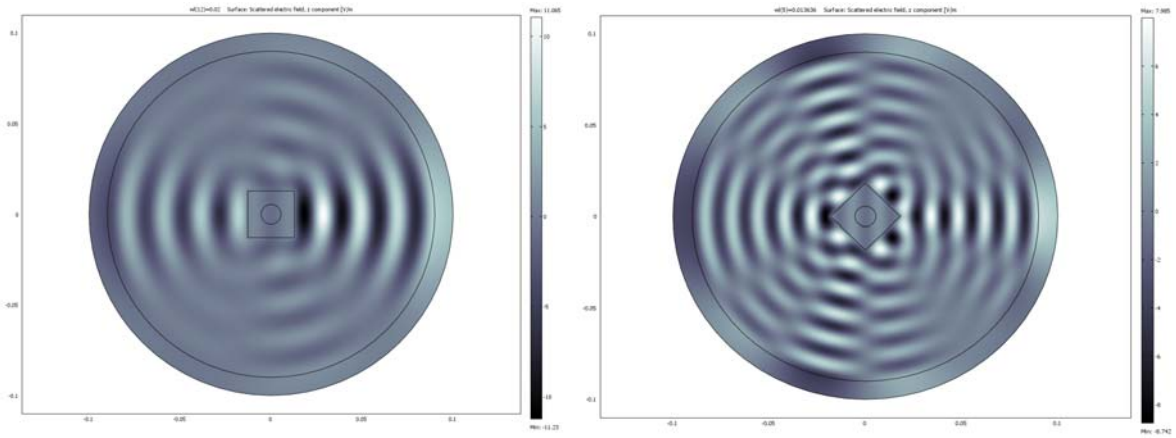

(a) **(b)**

Figure 3.11. Radiation patterns of scattered wave for (a) 0-degree rotated barrel; (b) 45-degree rotated barrel.

Unlike comparison illustrated in Figure 3.8, in Figure 3.10, significant variations in RCS pattern can be found with the orientation of non-circular barrel changed. The reasoning is readily obtained by looking into the radiation patterns of scattered waves from the object. The wave pattern is entirely changed when the reflective surface under wave illumination varies. Interestingly, the sharp section of reflective surface makes the resonance frequency of the entire object decrease when it is directly illuminated.

- **Shape changes in inner and outer geometry vs. RCS**

The RCS response to the shape of bore and outer geometry of barrel is compared. Three types of barrels are investigated: round barrel with round bore, round barrel with square bore, and square barrel with round bore. The comparison results are presented in Figure 3.12. From this Figure, it is noticeable that RCS pattern is insensitive to the internal shape variation of barrel. The RCS patterns for round bore and square bore nearly overlapped each other, though a little deviation can be found from 25GHz to 30GHz. In contrast, the pattern for square barrel is prominently distinctive from those for the other two scenarios.

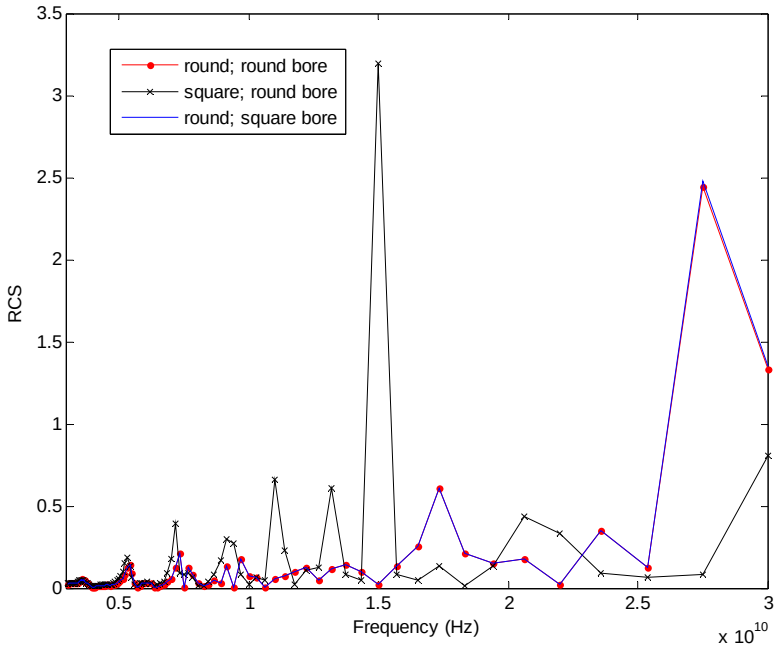

Figure 3.12. RCS response to barrel shapes.

3.2.2 Electromagnetic resonances

Section 3.2.1 has shown that RCS profile can characterize objects. In this section gun barrels with different cross sections will be illuminated with high frequency EMW (200MHz to 20GHz), corresponding to resonance region of most common weapons according to the literature review (section 2.1.4). The same 2- dimension model of 3.2.1 is set to sweep through 200MHz-20GHz and record resonance respond. Figure 3.13 shows the geometry the gun barrel (actually the cross section is employed for simulation) and cross section profile for the simulations.

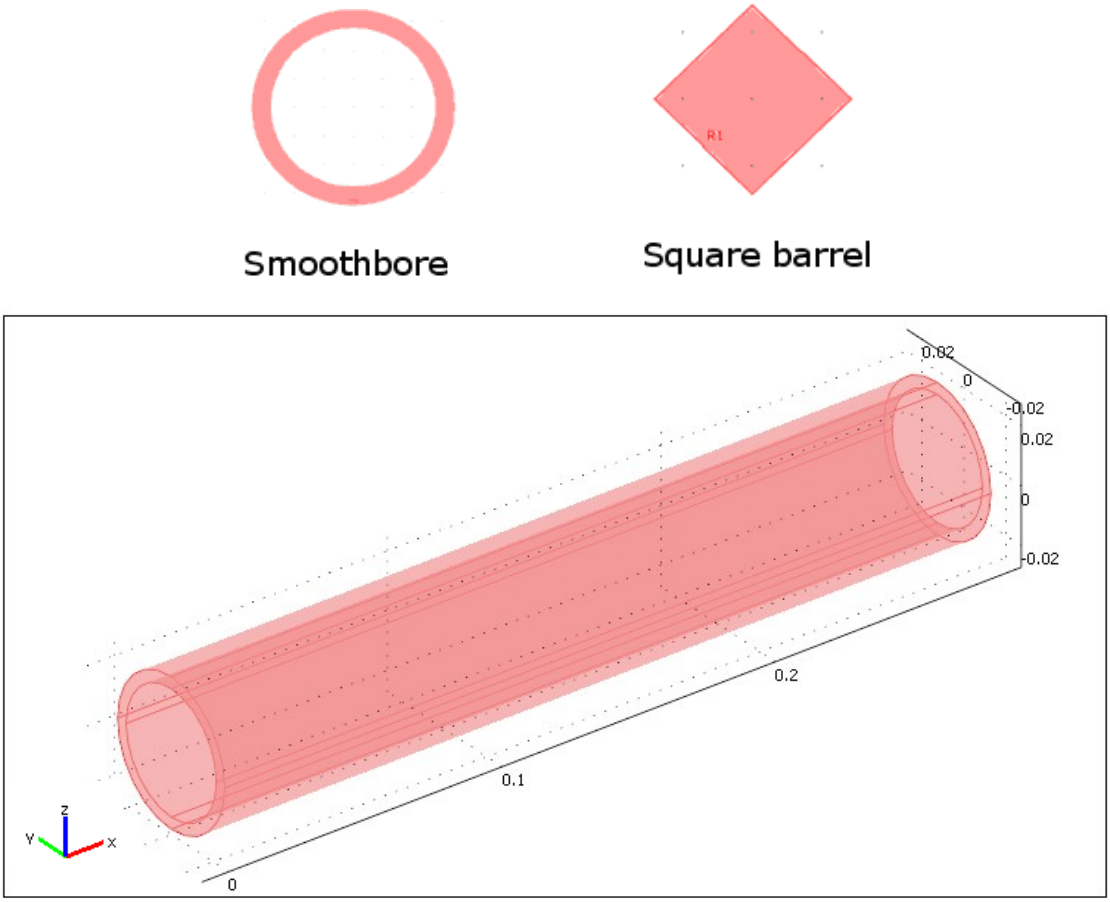

Figure 3.13. Cross section of gun barrels employed in the FE simulation.

In Figure 3.14 three smoothbore barrels with different diameter and a square barrel has been illuminated with EMW swept from 200MHz to 20GHz. The results imply the samples can be differentiated in terms of the fundamental resonance (around 500 MHz) and the magnitude of RCS

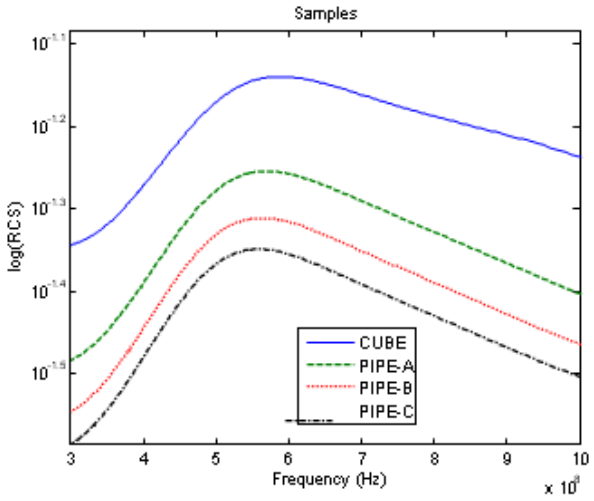

SAMPLES	FREQUENCY (MHZ)
Cube L: 50.25mm	588
Pipe A OD: 33.5mm ID: 26.5mm	571
Pipe B OD: 25.5mm ID: 21.5mm	564
Pipe C OD: 21.3mm ID: 14.3mm	560

Figure 3.14. The RCS values against frequencies for each gun barrel.

3.3 Conclusions

First study using FE simulations have shown that the presence of metallic objects in an interrogation space causes local distortion of amplitude of the earth magnetic field. This distortion field response is sensitive to geometry (external and internal shape) of the interrogated object and also to the orientation.

Measuring earth magnetic field distortion requires sensor technology with high resolution (order of microtesla) which implies high cost. Another drawback is the sensitivity to the object orientation which makes the detection more difficult.

Second study with FE simulations have shown the RCS of weapons under EMW wave illumination can characterize weapons. The sensitivity of RCS for weapons is larger in the resonance region (200MHz-2GHz) [17]. Thus RCS exhibits resonance when objects are illuminated by EM wave with frequencies in resonance region. Study has shown the sensitivity of RCS to outer geometry but insensitive to inner geometry, orientation and material composition.

Chapter 4: NEW PROPOSAL FOR THE DETECTION OF CONCEALED WEAPONS: EM WEAPON DETECTION FOR OPEN AREAS

4.1 Theory for Electromagnetic Weapons Detection and Identification

The detection and identification of the proposed method is based on the scattered magnetic field from a weapon when it is illuminated with low frequency electromagnetic fields. The computation of the scattered magnetic field is based on suitable solutions of Maxwell's equations. The subject has been analysed in detail by Kaufman and Keller in 1985 [44]. Rather than repeat details of the developments of the authors in [44], selected results pertinent with identification of CWD are described here.

To simplify the computation of the scattered magnetic field, a weapon is approximated by a sphere with radius "a" and conductivity "σ" and is irradiated with an electromagnetic wave in the form of step pulses. When the pulse occurs, the weapon is illuminated by a step change in the amplitude of the magnetic field vector which is considered to be planar in the vicinity of the weapon. The magnetic field in the vicinity of the weapon is defined as "H_0".

Figure 4.1 shows a sphere of radius "a" irradiated with an electromagnetic wave in the form of step pulses from group of energized wires.

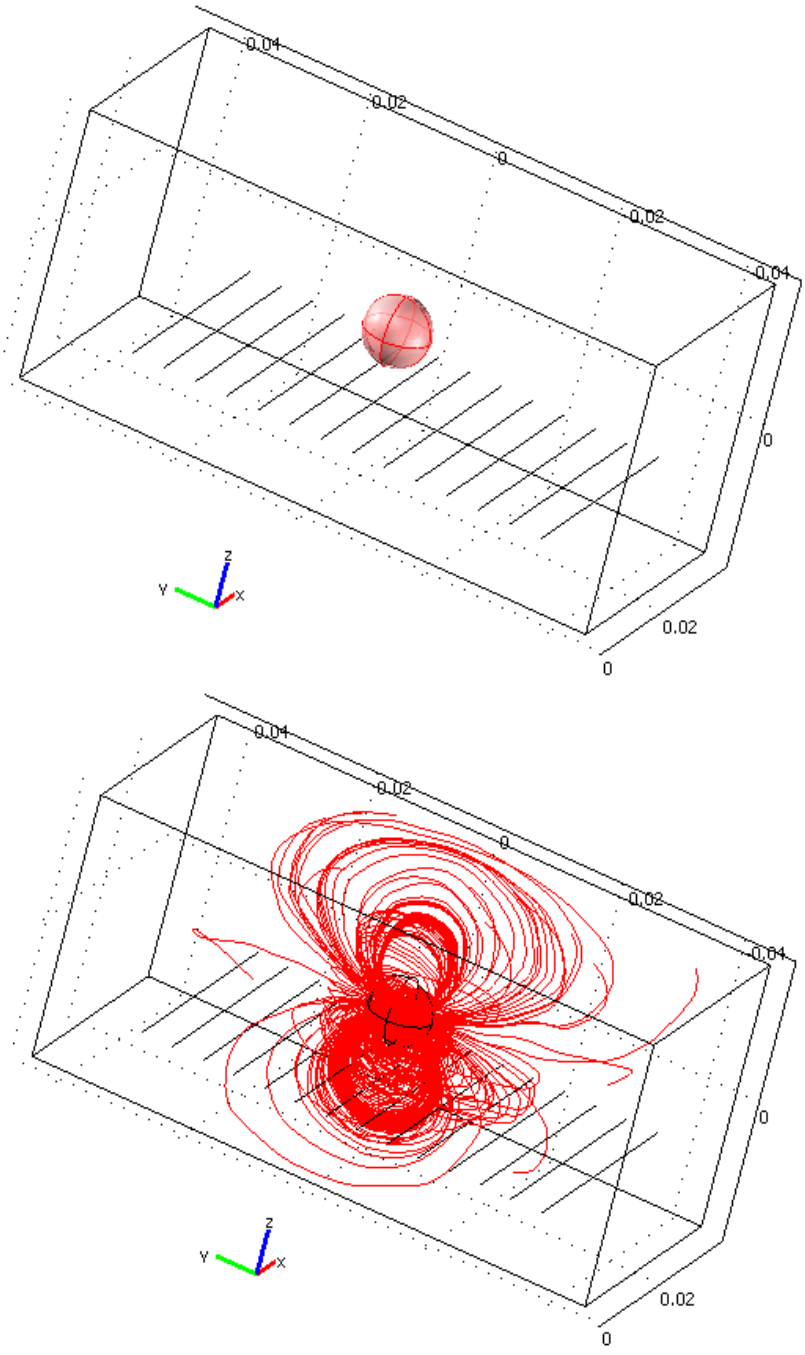

Figure 4.1. Sphere with radius "a" and conductivity "σ" irradiated with an electromagnetic wave in the form of step pulses.

Using a quasi-static solution of Maxwell's equations, it is found that the primary magnetic field around the sphere is increased by an amount due to currents induced flowing within the sphere and given by the following three equations:

$$E_{\phi}^{a} = \frac{3KB_0 a^3 \sin\theta}{R^2} \sum_{s=1}^{\infty} \frac{q_s e^{-q_s t}}{[k_s{}^2 a^2 + (K-1)(K-2)]} \tag{4.1}$$

$$B_{R}^{a} = \frac{6KB_0 a^3 \cos\theta}{R^3} \sum_{s=1}^{\infty} \frac{e^{-q_s t}}{[k_s{}^2 a^2 + (K-1)(K-2)]} \tag{4.2}$$

$$B_{\theta}^{a} = \frac{3KB_0 a^3 \sin\theta}{R^3} \sum_{s=1}^{\infty} \frac{e^{-q_s t}}{[k_s{}^2 a^2 + (K-1)(K-2)]} \tag{4.3}$$

where E_{ϕ}^{a}, B_{R}^{a}, B_{θ}^{a} are the only components of the anomalous fields caused by currents induced in the sphere. These components are expressed in a spherical coordinate system centred on the sphere, with "R" being in the direction of the incident field as shown in Figure 4.2.

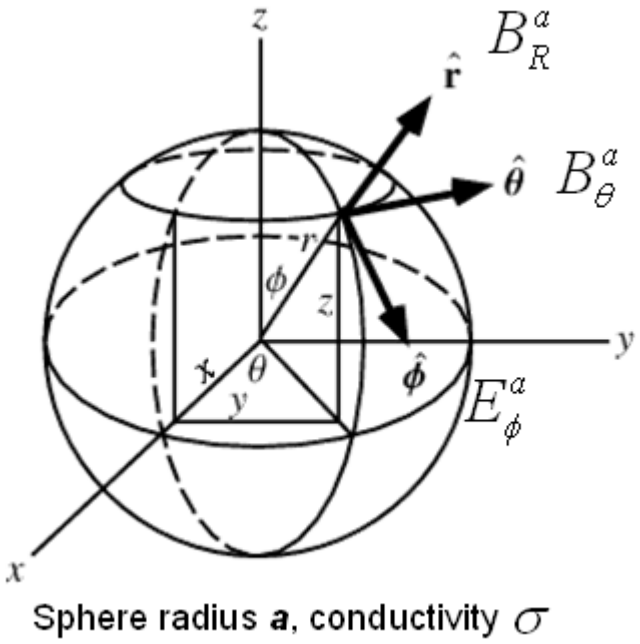

Figure 4.2. Components of the magnetic fields caused by currents induced in the sphere.

The other quantities in the equations are defined as:

$K = \mu / \mu_0$ (The relative magnetic permeability of the weapon) (4.4)

$q_s = k_s^2 / \sigma\mu$ (4.5)

$k_s = \pi s / \alpha$ $(s=1, 2, 3, \infty)$ (4.6)

and "t" is time, following the initiation of the current step.

The form of each electromagnetic field component is that of a sum of exponentially decaying transients. The asymptotic behaviour of these transients is now examined. During the early part of the transient response of the electromagnetic field (t→0), the expressions for the anomalous magnetic field components are as follow:

$$B_R^a = B_0 (a/R)^3 \cos\theta [1 - 6/\sqrt{\pi}(\alpha t)^{1/2}] \quad (4.7)$$

$$B_\theta^a = B_0 1/2 (a/R)^3 \sin\theta [1 - 6/\sqrt{\pi}(\alpha t)^{1/2}] \quad (4.8)$$

During the late part of the transient decay, the field is almost entirely determined by the first exponential terms:

$$B_R^a = \frac{6B_0}{\pi^2}\left(\frac{a}{R}\right)^3 \cos\theta e^{-\frac{t}{\tau_0}} \quad (4.9)$$

$$B_\theta^a = \frac{3B_0}{\pi^2}\left(\frac{a}{R}\right)^3 \sin\theta e^{-\frac{t}{\tau_0}} \quad (4.10)$$

$$E_\phi^a = \frac{3B_0 a}{\tau_0 \pi^2}\left(\frac{a}{R}\right)^3 \sin\theta e^{-\frac{t}{\tau_0}}, \text{ where } \tau_0 = \sigma\mu\alpha^2\pi^2 a \text{ is a time constant.} \quad (4.11)$$

The computation of step-response decay curves of a sphere with parameters: radius a=0.2m, K=150, σ =3.54e6 S/m is shown in Figure 4.3. Four terms of equation (4.1) and the summation of first 8100 terms have been computed. The full step response decay curve shows three zones: early-time behaviour (flat), intermediate-time behaviour (power-law), and the late-time behaviour (exponential decay).

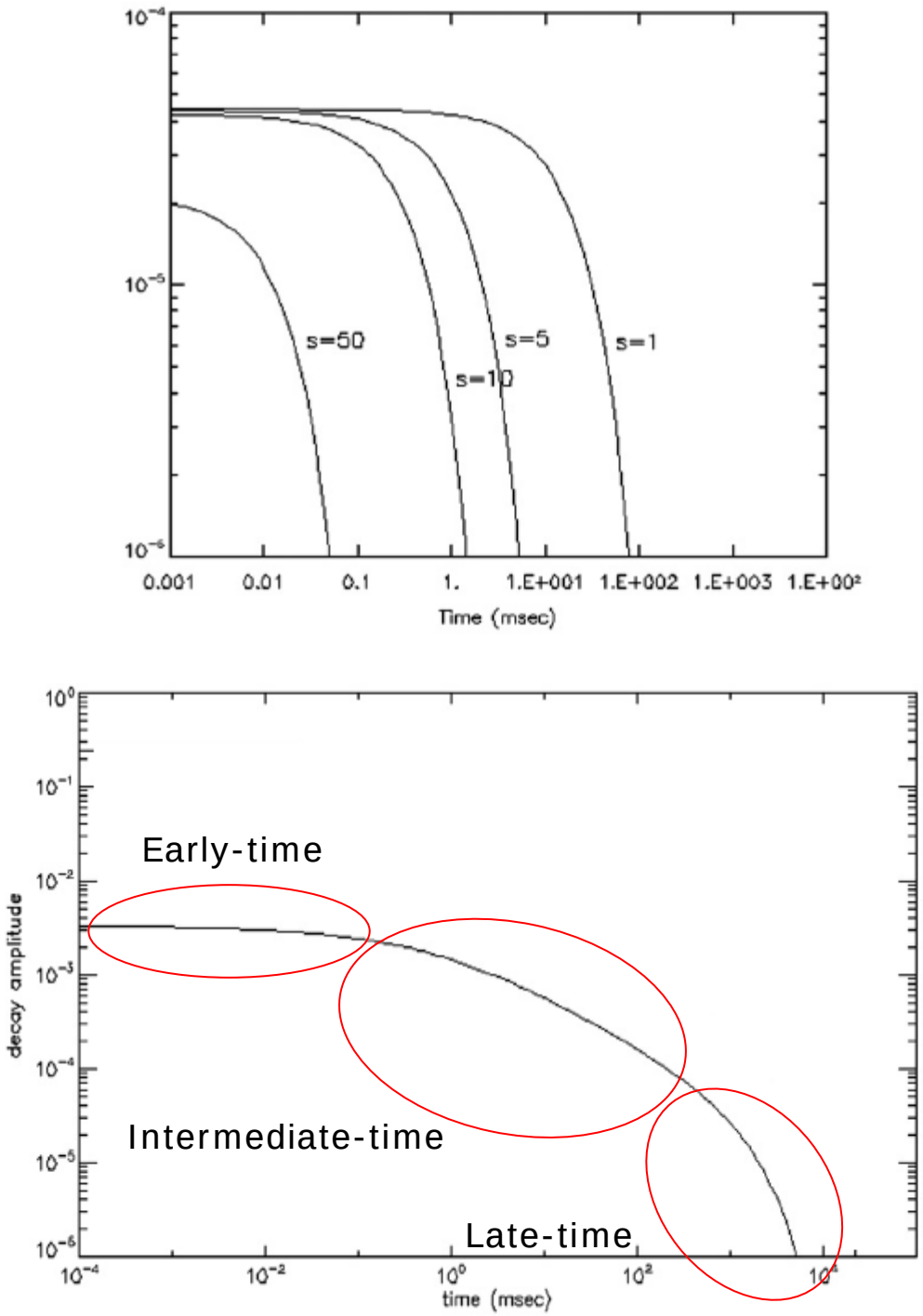

Figure 4.3. Four terms of Eq. (4.2) for s=1, 5, 10 and 50 (top). The full step-response decay computed for summations of 8100 terms of Eq. (4.2) [45] (bottom).

These results are the basis for the design of a highly effective weapons detection system. Each of the three expressions for field components is of the form of a product of two terms,

the first term of which involves only the geometry and magnitude of the primary field in the vicinity of the weapon, and a second term involving a time constant, but independent of the geometry and strength of the field incident on the weapon. Measurement of the time constant provides a means for weapon detection which is free of false alarms due to variations in primary field strength.

A time constant can be determined from a plot of the transient magnetic field with amplitude in logarithm scale (the slope of the curve is the time constant as shown in Figure 4.4.

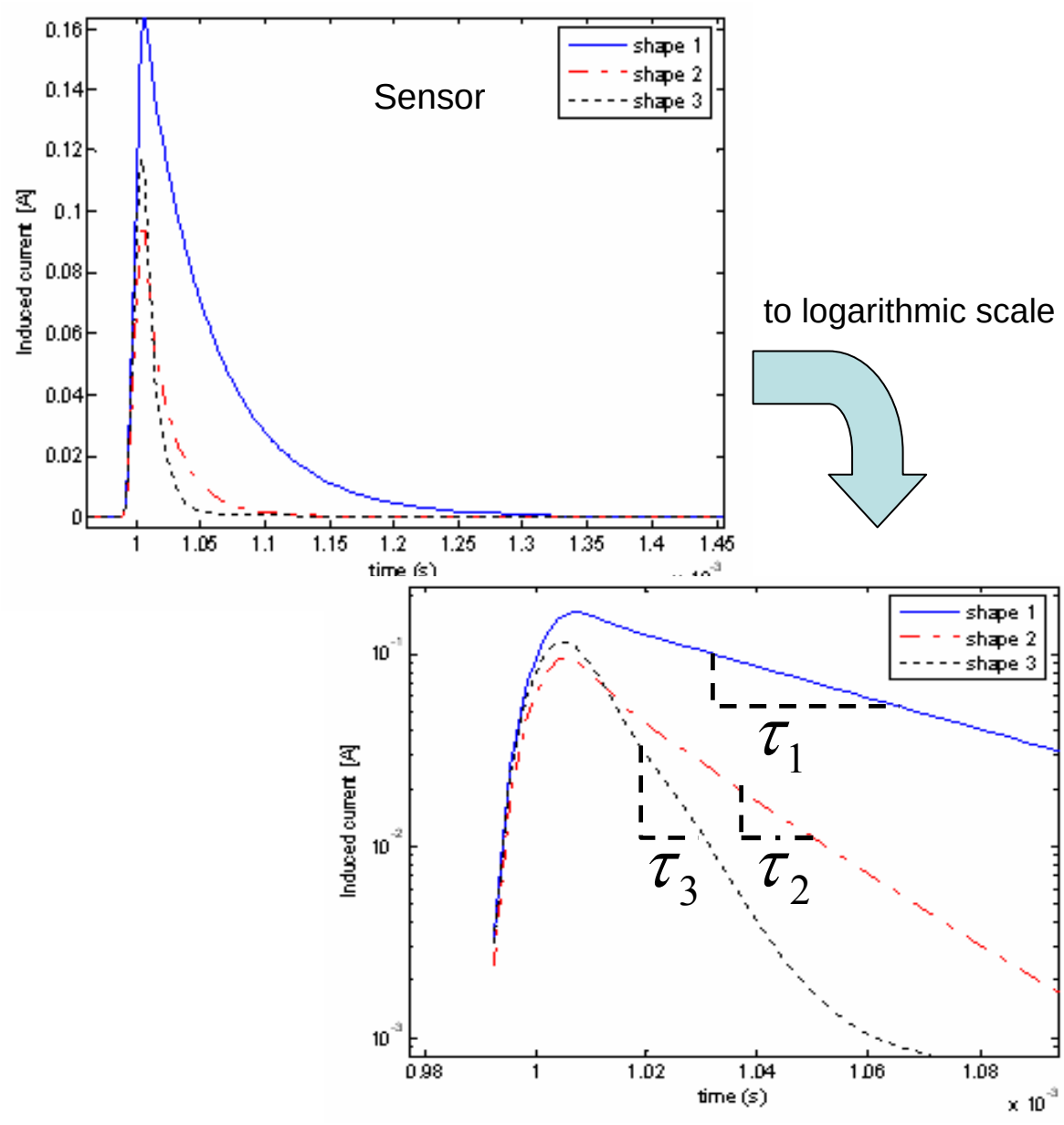

Figure 4.4. Time constant from sensor signals in logarithm scale.

The time constant can also be determined from the expression:

$$\tau_0 = -\frac{B_R^a}{\partial B_R^a / \partial t} = -\frac{B_\theta^a}{\partial B_\theta^a / \partial t} \qquad (4.12)$$

Weapons have a complex geometry, so a question arises as to whether or not conclusions for simple geometries extend to more complicated shapes. Kaufman and Keller (1985) extended the analysis to axial symmetry and arrive at an expression for the scattering time constant as follows:

$\tau_0 = \sigma\mu a^2 / q$,

where "q" depends on the shape of the conductive body. (4.13)

The expression shows the potential of using the time constant in identifying a specific weapon of an even more complicated shape. All weapons of the same size, shape and metallic composition will be characterised by a scattered electromagnetic field. Time constant will be the same, no matter what the strength of the incident field or the distance of the weapon from the transmitter or the receiver array. Thus weapons can be classified at least within the precision with which the time constant of the decaying magnetic field can be determined.

The appropriate way to determine the time constant for a real weapon is by illuminating that weapon with an electromagnetic field using step pulses and measuring the time constant from the decaying field. Usually the weapon will be carried on the body of a person. However the time constant associated with the human body might obscure that of the weapon. An estimate as to whether this will happen can be made by substituting numbers in the expression (4.13). For example, assume that the conductivity-permeability of the steel in a weapon is of the order of 1 SHm^2, the radius of the sphere enclosing a weapon is 0.1m, the form factor "q" is 10 (the more convoluted the shape of the metallic object the greater will be the form factor). With these numbers, the order of magnitude estimate for the time constant of the hypothetical weapon is 1 millisecond. In the human body, flesh and bone are conductive and the conductivity-permeability product for a human

body is of the order of $10 SHm^2$. Thus the corresponding order of magnitude time constant for a human body is $0.1\ \mu s$. Although these are only estimates, the two time constants are so different that there is no likelihood that one will obscure the other.

4.2 Proposed Concealed Weapon Description

The system comprises a Uniform Magnetic Field Generator (UMFG), consisting of a group of parallel current carrying cables located below a walking surface to produce a horizontal magnetic field and arrays of magnetic field sensors located within the sensing area as can be seen in Figure 4.5. The system works based on pulsed-EMI technique. Currents in the UMFG flow for a sufficiently long time to allow turn-on transients in the sensing object to dissipate. The current in the cables are then turned off. According to Faraday's law, the collapsing magnetic field induces an electromotive force in the metal target. This force causes eddy currents to flow in the metal. Because there is no energy to sustain the eddy currents, they begin to decrease with a characteristic decay time that depends on the size, shape, and electrical and magnetic properties of the metal object. The decay currents generate a secondary magnetic field, and the time rate-of-change of the field is detected by magnetic field sensors. The time decay response is used for classification. The arrays of sensors are distributed within sensing area in a grid pattern in order to show the location of gun/knife carrying people.

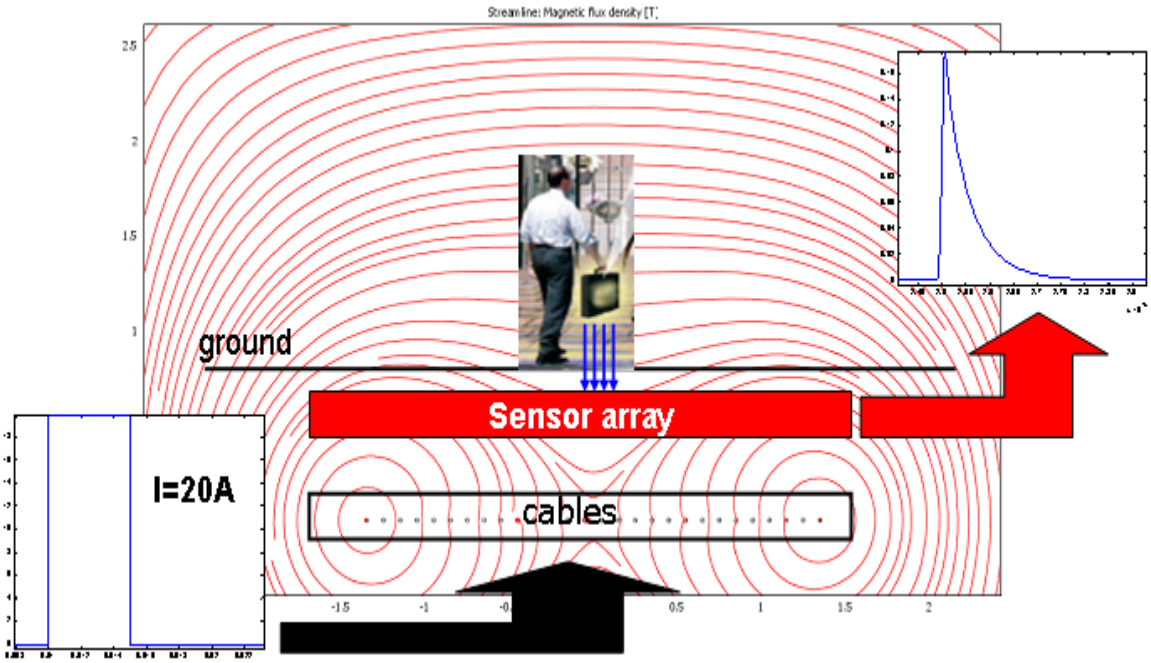

Figure 4.5. Functionality of the proposed CWD system.

4.3 Proposed Design

The new proposition of CWD system comprises:

1. Metal detector subsystem.
    - UMFG, Switches and Pulse control
    - Sensor arrays

2. Control subsystem.

3. Detection & classification subsystem.

4. Operator interface.

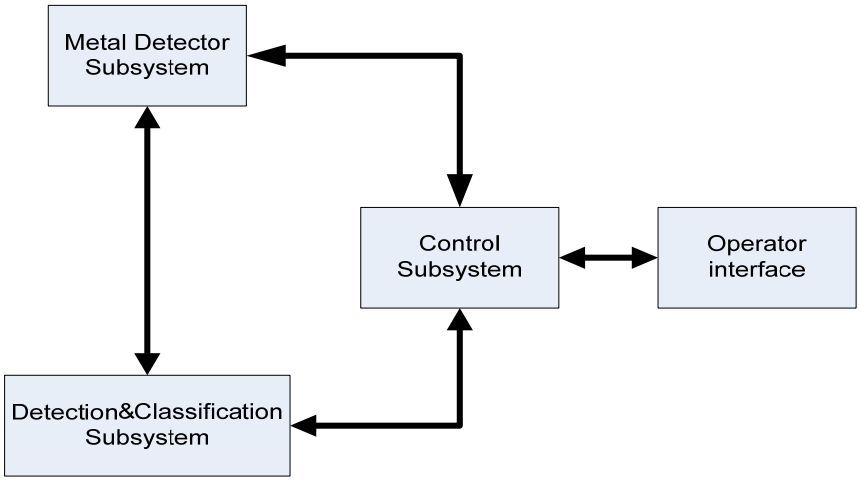

Figure 4.6. Proposed CWD structure.

4.3.1 Metal detector subsystem

- **Uniform Magnetic Field Generator (UMFG)**

It is known from basic physics textbooks that for an infinite conducting sheet current, the field in the direction parallel to the sheet is given by:

$$B = \mu_0 v / 2 \qquad (4.14)$$

Where v is the current density in the sheet and μ_0 is the permeability of free space ($\mu_0 = 4\pi\times10^{-7}$ N·A^{-2}).

The magnetic field perpendicular to the sheet is zero. It implies that the sheet current is a horizontal magnetic field generator. Sheet current can be approximated by closely spaced parallel current carrying wires. The important feature of (4.14) is the fact that the magnetic field is constant, a feature that improve weapon detection as it will be shown in the next section.

An approximation to a sheet current is created by a series of closely spaced parallels wires (see 4.3.1). These wires form the active surface of UMFG. The UMFG consists of a single cable AWG10 (American Wire Gauge, 2.58 mm diameter) wiring around a box forming rectangular 20 loops (3 m x 0.60 m), 2cm between loops in the way showed in Figure 4.7.

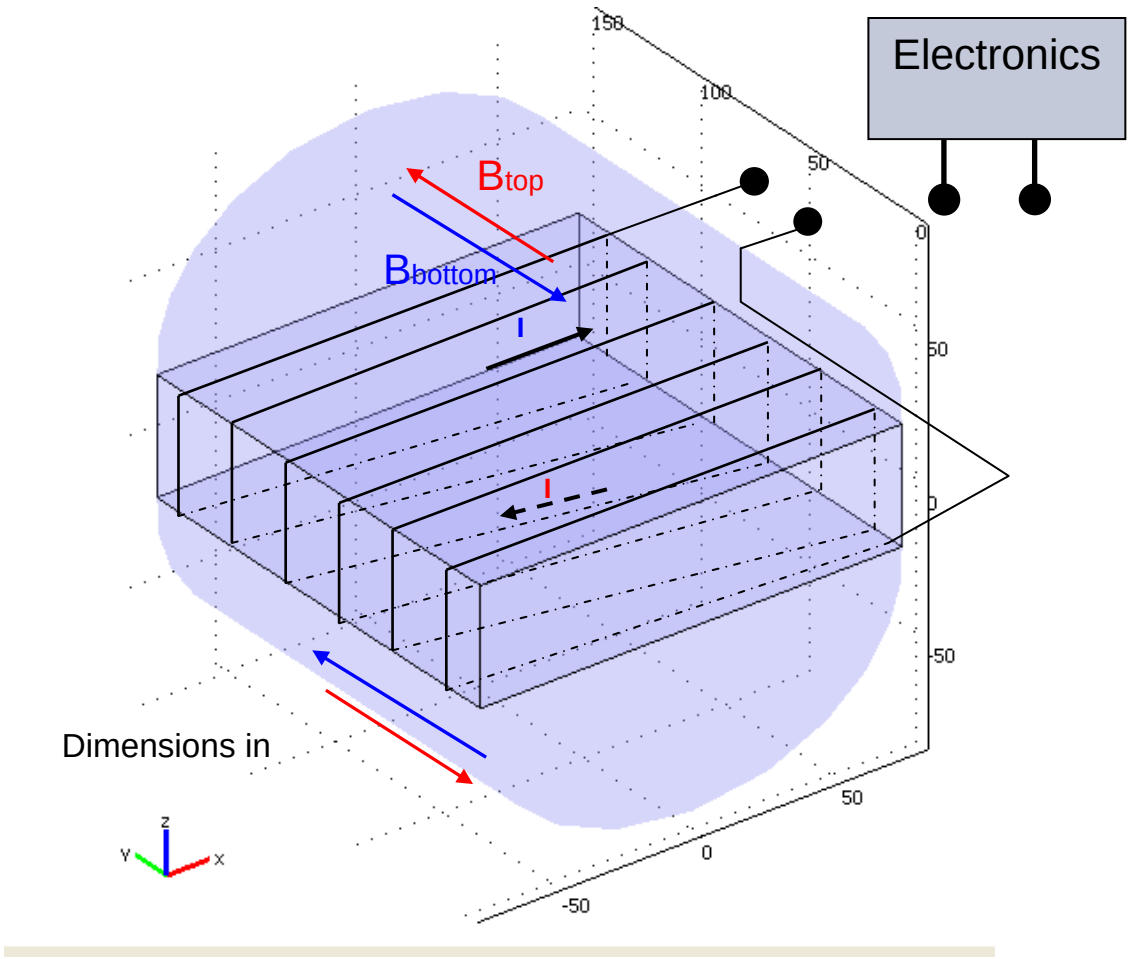

Figure 4.7. Magnetic field covering area from active part of UMFG (top plane) and return path (bottom plane).

In Figure 4.7 the cable is connected to high-speed electronic (turn-off delay time 180ns) switches. A single power supply provides current to the UMFG. The excitation field is generated by the plane of wires closest to the ground (top of the box). However the primary field is reduced by the superposition of the opposite magnetic field generated by the return path (bottom of the box). The effective magnetic field covering area is shown in Figure 4.8.

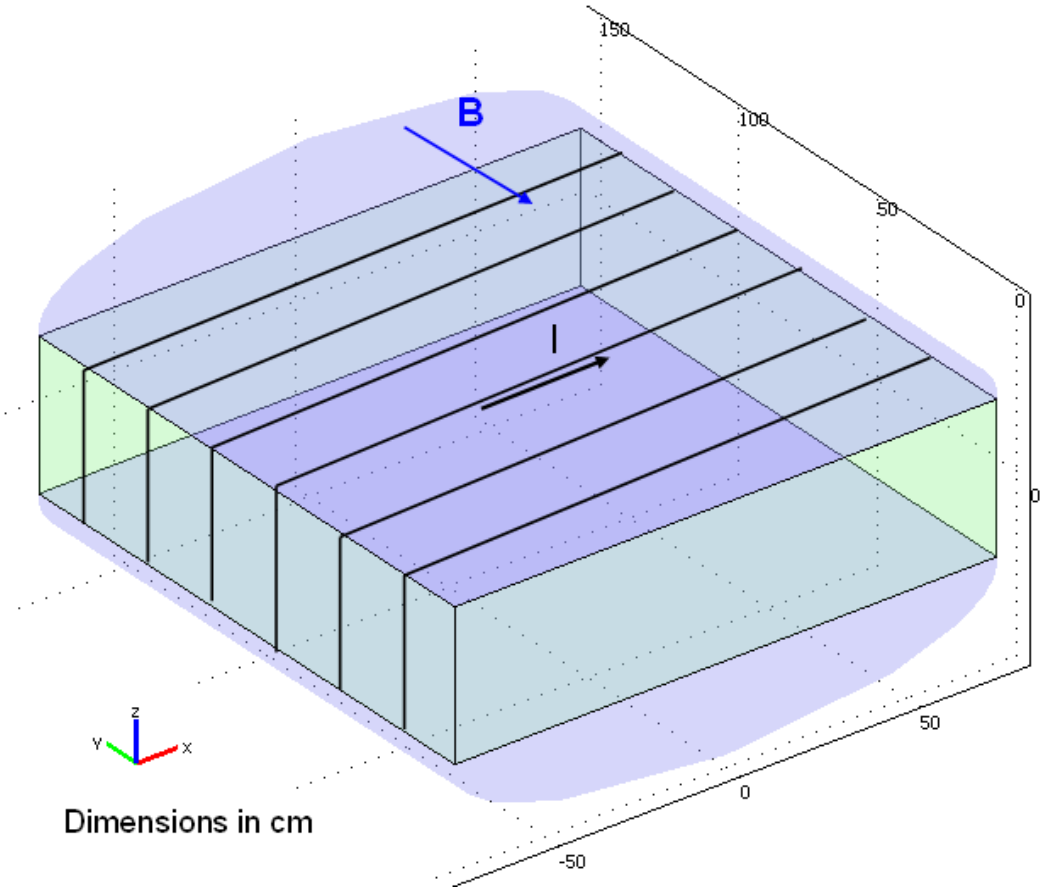

Figure 4.8. Effective magnetic field covering area.

Magnetic field covering area will not be reduced if magnetic shielding is added to the return path. An alternative solution without using magnetic shielding is to route return path to the sides of the box instead of the bottom as shown in Figure 4.9.

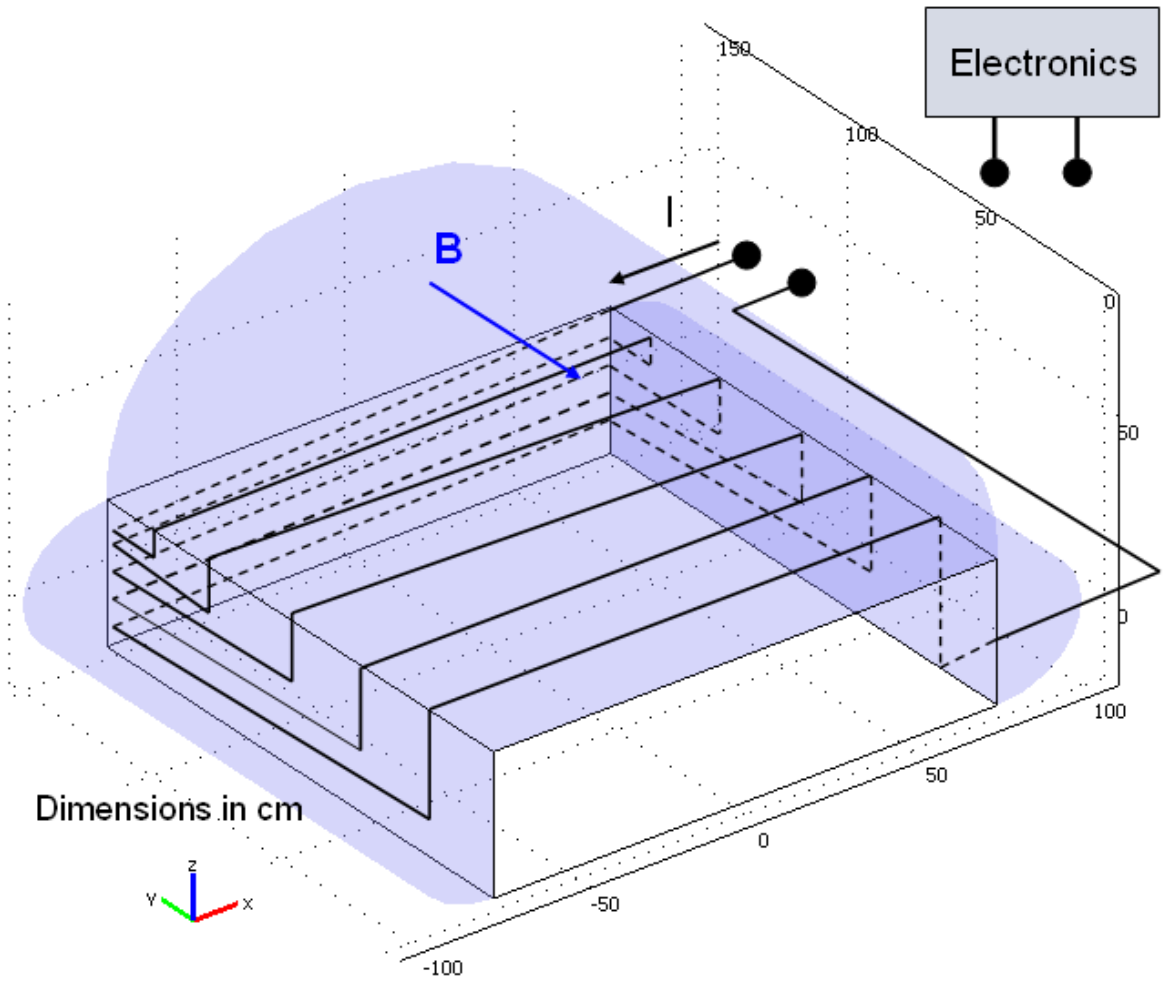

Figure 4.9. Routing the return path to the sides of the box maximizes the effective magnetic field covering area.

The current in the UMFG is controlled by the electronic switches. The switches are power MOSFETs (IRF150). A pulse generator controls the opening/closing of the switches. The circuit is shown in Figure 4.10. The circuit consists of low power pulse generator (LM555 set a 20Hz, 10% duty cycle in order to not overheat the wires.) switching a power MOSFET (IRF150) in order to drive 6.7A into the UMFG. To prevent electrical failures the low power circuit (pulse generator) and MOSFET are decoupled by an opto-isolator.

To protect the MOSFET from back electromotive force (EMF) a flywheel diode series with three Zener diodes are connected across the ends of UMFG wires. Besides protecting the MOSFET the set of diodes reduce considerably the switch off time whose effect on target is to enhance the signal back to the sensors.

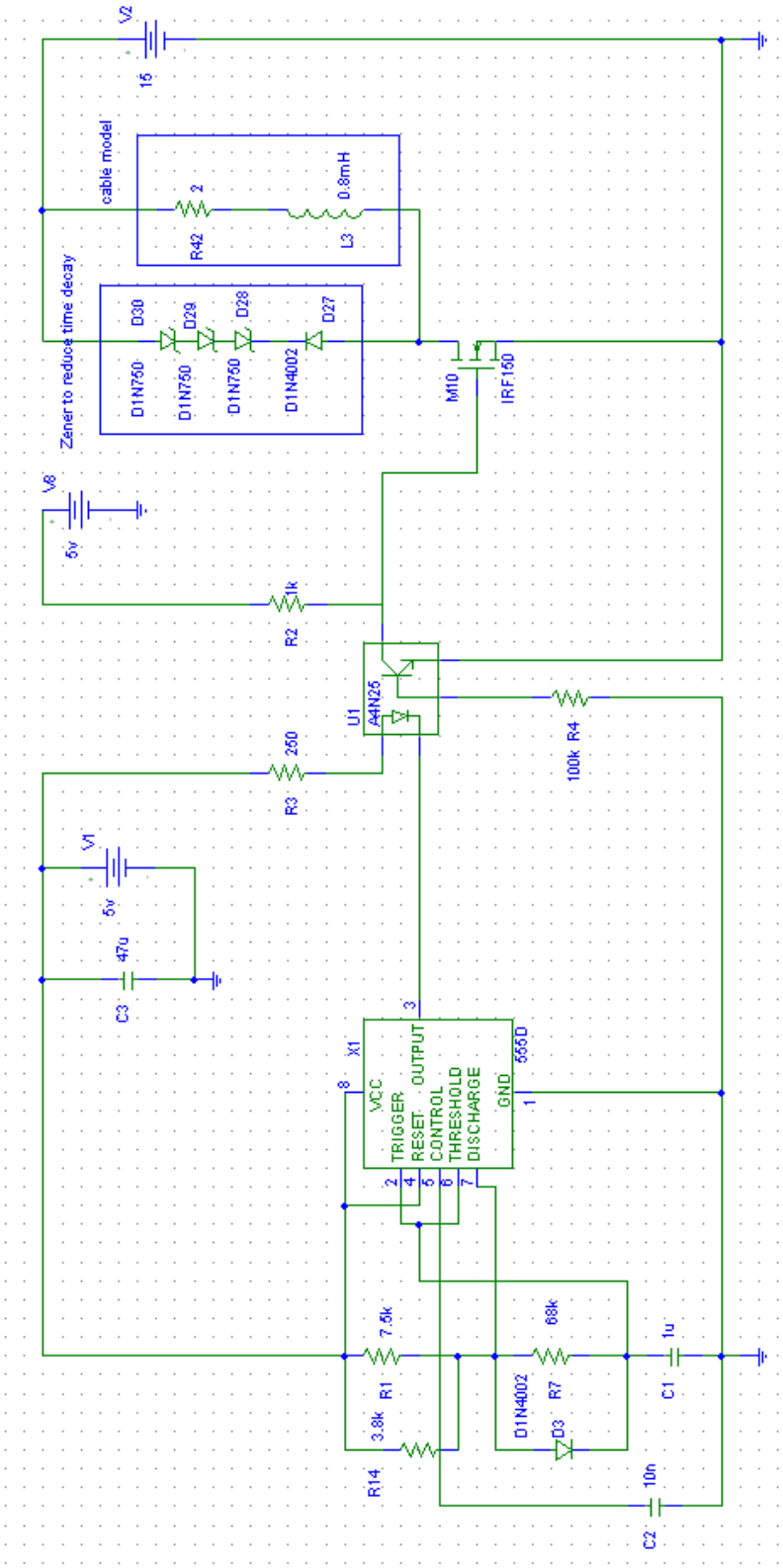

Figure 4.10. Pulse Control Circuit.

The proposed weapon detection system needs to cover a larger area. To accomplish that an option could be to use a single UMFG with a longer wire; however doing this maximizes the magnetic field collapse time, inducing weaker eddy currents in the metal and making detection difficult. In the time domain, the strength of the excitation magnetic field is dependent of rate of change of its collapse time. The decay of the excitation magnetic field is governed by the decay of the current in the wires after the switch is opened. Thus a way to use a longer wire in which currents decays in a short time needs to be found.

Ignoring capacitive effects, the decay time on the UMFG is given by L/R, where L is the inductance of the loop and R is the resistance of the loop. For this application, L can be minimized using several shorter loops. L decreases more than R so the reduction of R does not prevent the minimization of the time decay.

For the proposed weapon detection it is planned to use five of UMFG (144mx5) connected in parallel as shown in Figure 4.11 with sensor arrays in between to cover an area of 3x3 m. This block area could be used as a module for a larger system. In the whole system each UMFG has its own switch because each UMFG will be excited sequentially as shown in Figure 4.12 by a pulse controller. It improves the detection by giving location of the target and avoiding exciting other metal in the vicinity.

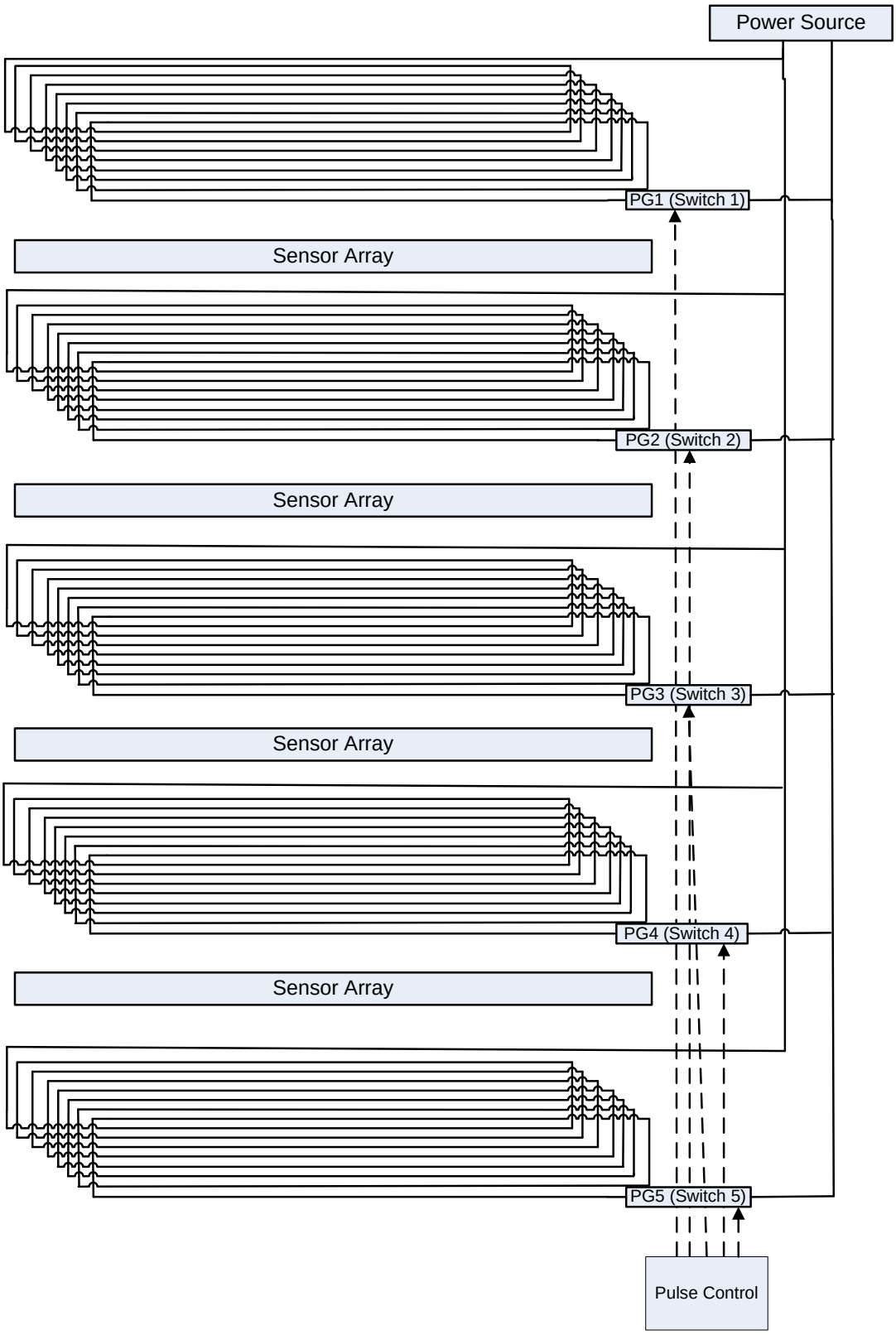

Figure 4.11. Layout of a block of intended CWD system including five UMFG.

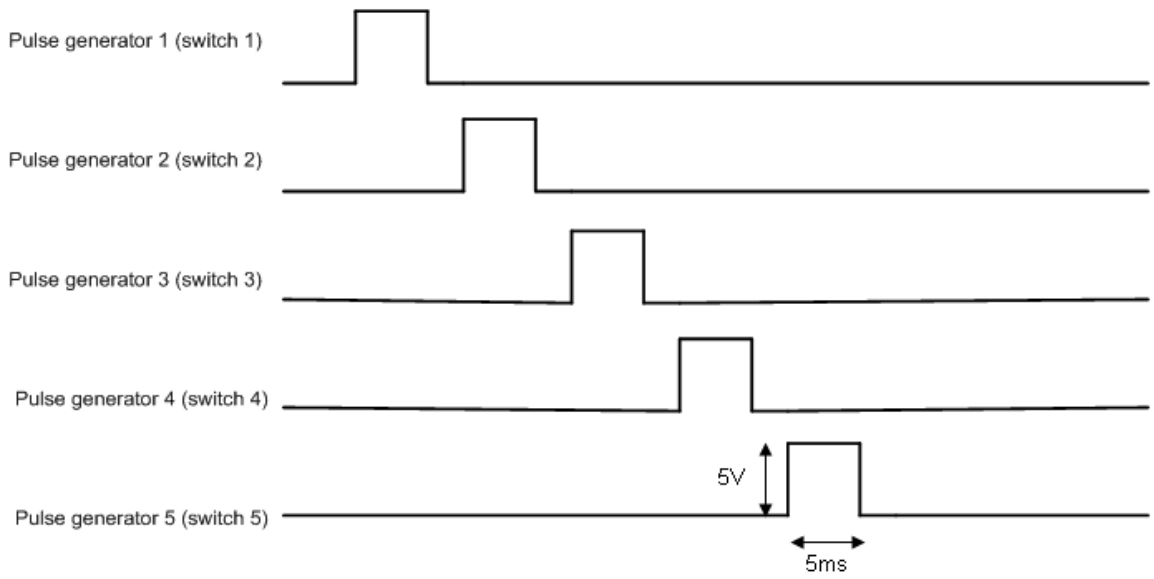

Figure 4.12. Time diagram of switch trigger signal (LM555 set a 20Hz, 10% duty cycle).

- **Advantages of uniform excitation magnetic field**

There are some advantages in terms of detection and classification according to the way that targets are excited. Targets could be illuminated by magnetic field generated by a large coil (3m diameter) or group of parallel wires. Figure 4.13 shows streamlines of magnetic field density from a loop (a) and those from closely spaced current carrying wires (b**)**

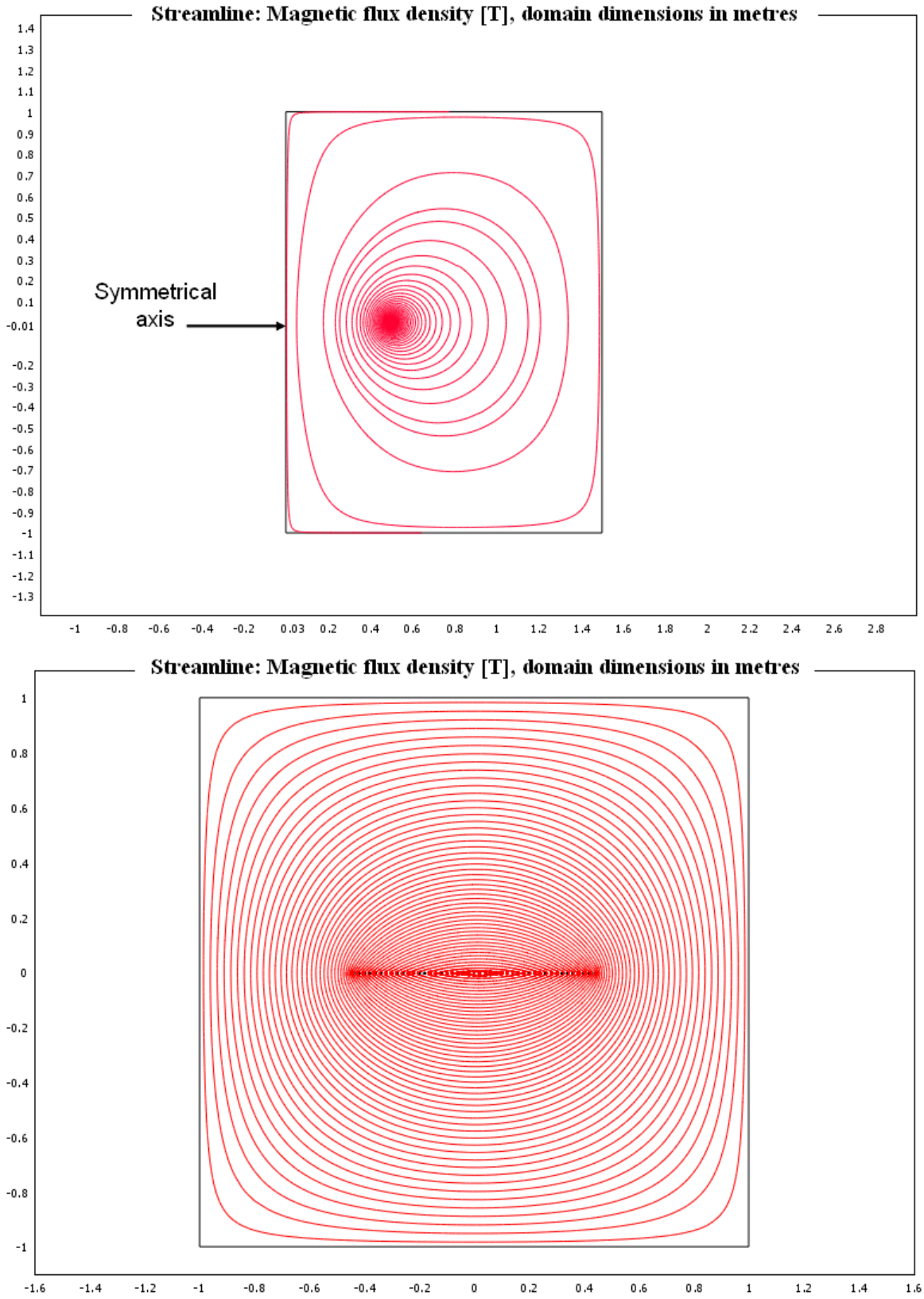

Figure 4.13. Cross sectional view of magnetic field from a coil loop (top); Cross sectional view of magnetic field from UMF (bottom). Current flow into the paper.

Illumination of objects with uniform magnetic field makes easier the classification process and provides a strong source of illumination.

[1] **Improvement in target classification**

The advantages of exciting an unknown metal with uniform magnetic field can be better explained by a description of the basic physics of the problem. Consider a simplified extended target model made of two separated dipoles as shown in Figure 4.14. Each dipole decay time constant is modelled as a single exponential decay and the sum of the two dipole time decays is the target's decay signature. Dipole 1 has a decay time constant τ_a and amplitude A_a and dipole 2 has a decay time constant τ_b and amplitude A_b. This signature is an inherent property of the target and is used for classification. Now let's consider the case as showed in Figure 4.14a, where exciting the target with a spatially varying (non-uniform) magnetic field that excites the two dipoles with different magnetic fields, B_1 and B_2, the target signature is dependent on the excitation field and is not simply the sum of two exponential decays. This potentially makes target classification more difficult. In Figure 4.14b, the excitation magnetic field is uniform (B_u) over the target. In this case the theoretical response of the target is preserved because the magnetic field can be factored out of the target response equation. So target signal expression still contains decay properties, independent of the strength of the uniform magnetic field.

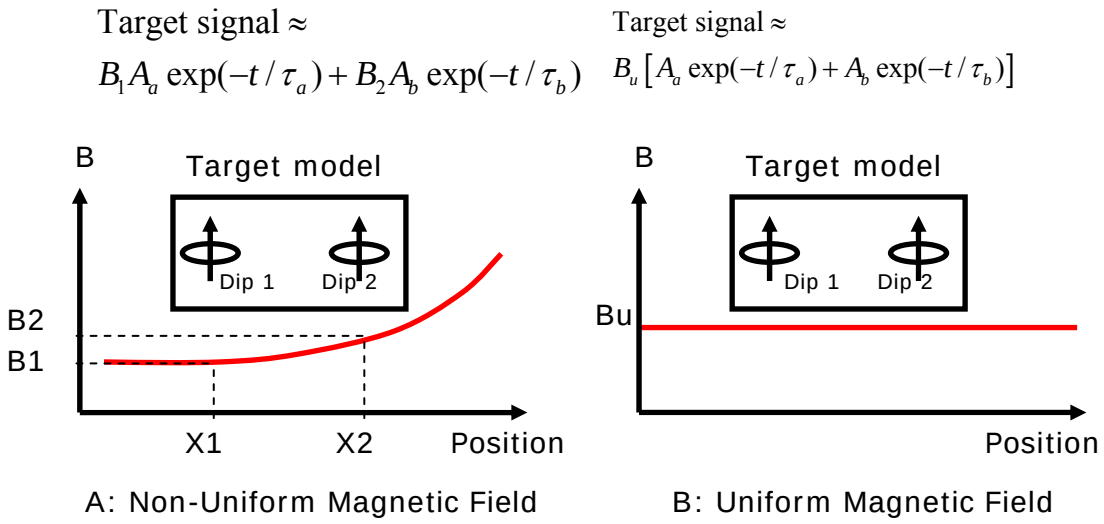

Figure 4.14. Magnetic field uniformity and Target signal response [12].

[2] **Slow reduction of field strength with distance**

The uniform magnetic field generator has a stronger magnetic field intensity compared to that of conventional loop coils as a function of distance from the plane of the magnetic field generators [11]. Figure 4.16 shows a plot that compares Bx from the Uniform magnetic field generator UMFG (1m x 3m) to Bz of a loop coil (1m of diameter) versus distances from the plane of UMFG. The magnetic field for each case has been normalized to one at the distance of 10cm to show the relative field intensity fall-off with distance.

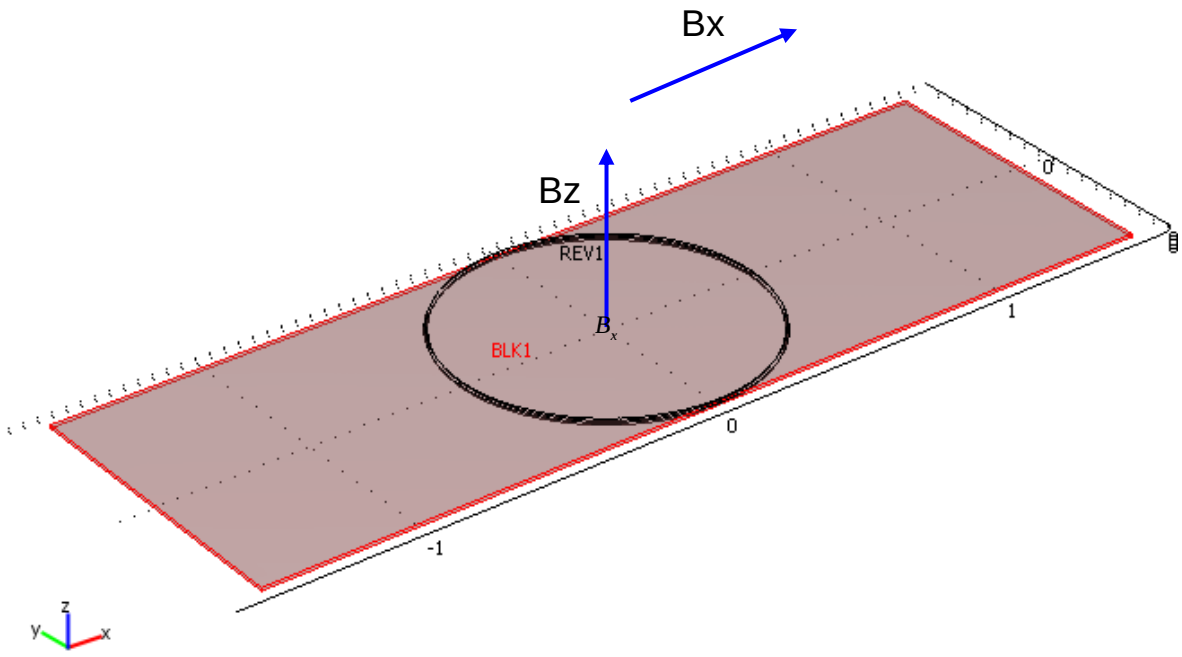

Figure 4.15. UMFG and Loop Coil.

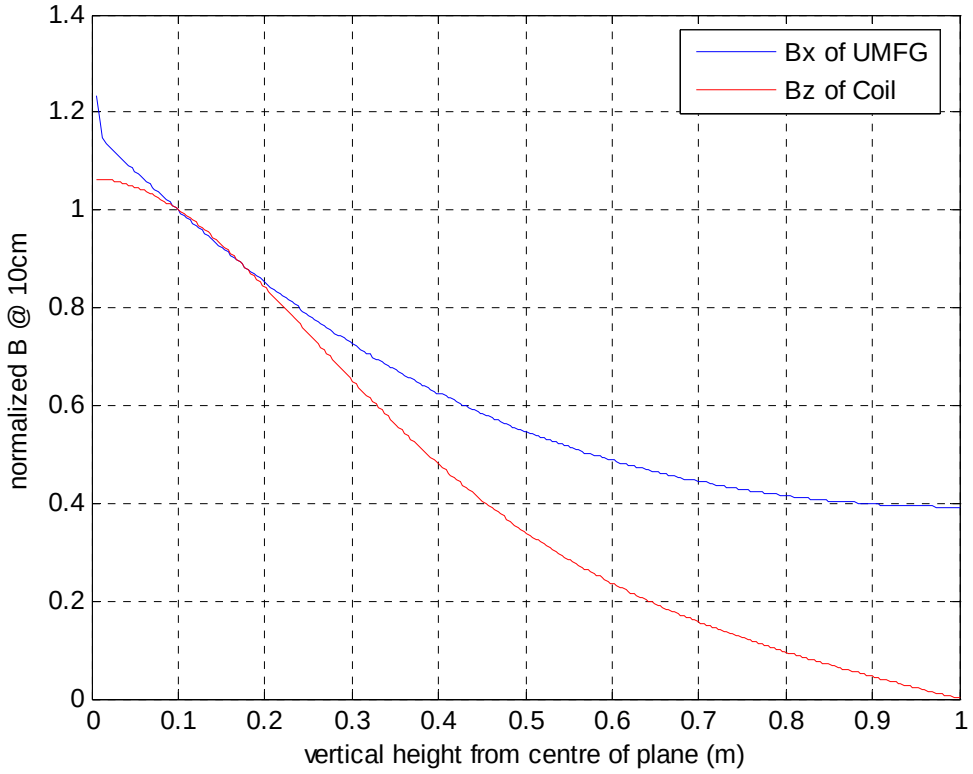

Figure 4.16. Magnetic field from UMFG and a loop coil.

- **Sensor array**

The magnetic field strength for the proposed weapon detection system is in the order of microtesla (10^{-2} gauss). Looking on table 4.1 there are plenty of magnetic field sensor technologies which can cope with this requirement [46]. Some sensor technologies have more advantages than others in term of minimum detectable field, cost and circuit complexity. For this research three magnetic sensor technologies could be suitable: search coil, hall-effect devices and magnetoresistive devices.

Table 4.1. Magnetic Sensor Technology Field Ranges [46].

Magnetic Sensor Technology	Detectable Field (Tesla) 10^{-12} 10^{-8} 10^{-4} 10^{0} 10^{4}
1. SQUID[1]	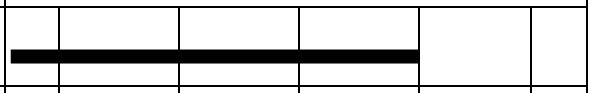
2. Fiber-Optic	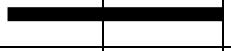
3. Optically pumped	
4. Nuclear-procession	
5. Search coil	
6. Anisotropic Magnetoresistive	
7. Flux-Gate	
8. Magnetotransistor	
9. Magnetodiode	
10. Magneto-Optical sensor	
11. Gian magneto-impedance	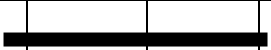
12. Hall-effect Sensor	

[1] Superconductive Quantum Interference Device

Table 4.2 shows an analysis of capabilities of those sensor technologies for the present work.

Table 4.2. Performance of Sensor Technologies.

Characteristics	Search coil	Hall device	Magnetoresistive (AMR)
Resolution (T)	10^{-12}	10^{-4}	10^{-10}
Cost[1]	Low	Moderate[2]	High
Size	~cm	~mm	~mm
Temperature Stability	Good	Poor	Acceptable
Input Power	0	~mW	~mW

[1] Cost depends on the scale of manufacture; the relative cost here is estimated for large-scale manufacturing.

[2] Relative cost include bias magnet.

In the proposed weapon detection the array of sensors are distributed within sensing area in a grid pattern in order to show gun/knife carrying people location as shown in Figure 4.17.

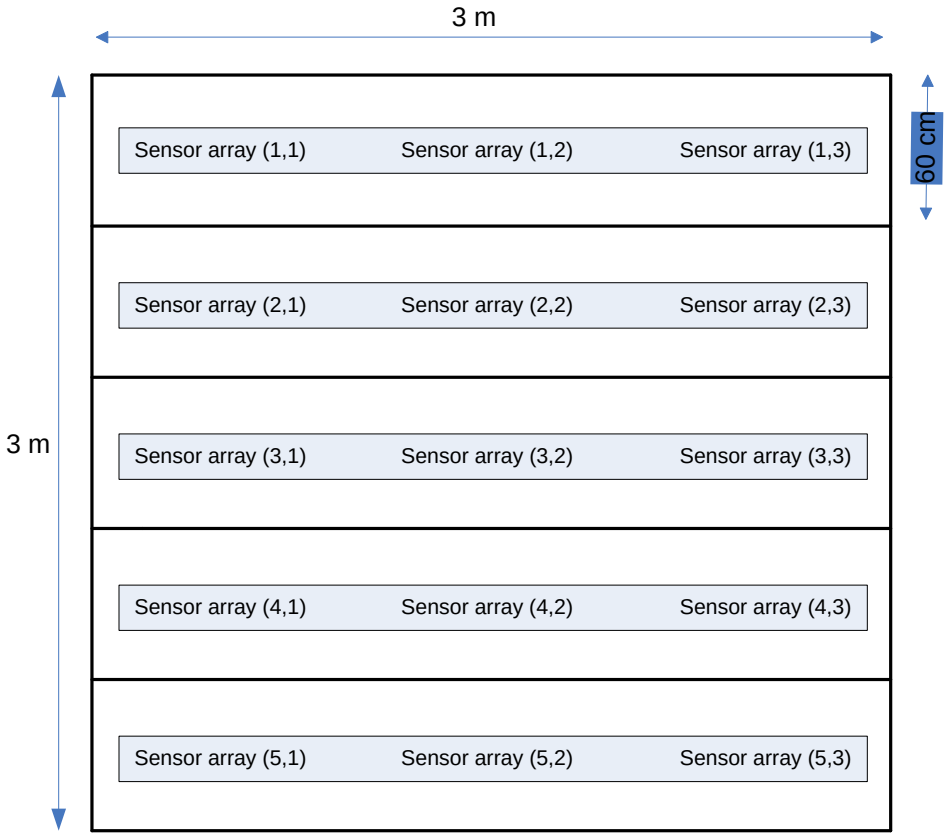

Figure 4.17. Sensor array distributions for the proposed CWD system.

4.3.2 Detection & classification subsystem

The eddy currents excited in the metal body take the form of an exponentially decaying transient immediately following sudden changes in the exciting magnetic field. This decay curve can be used to obtain a time constant of the current decay. It has been found (G.V. Keller, 1985) that time constant decay is independent of the strength of the field incident magnetic field and highly dependent on the size, shape and material composition. For gun/knife classification a library of potential threat metal objects can be developed. When a metal body is encountered in the field, its time decay response can be compared to those in the library, and if a match is found, the metal body can be classified. If an unknown target's

response signature is significantly different from any weapon signature in the library, the target can be considered a clutter.

In the proposed system each UMFG and sensor array needs to be excited and read independently following a given order. This facilitates finding the location of the suspect and saving memory and computation time for classification. This process is shown in Figure 4.18.

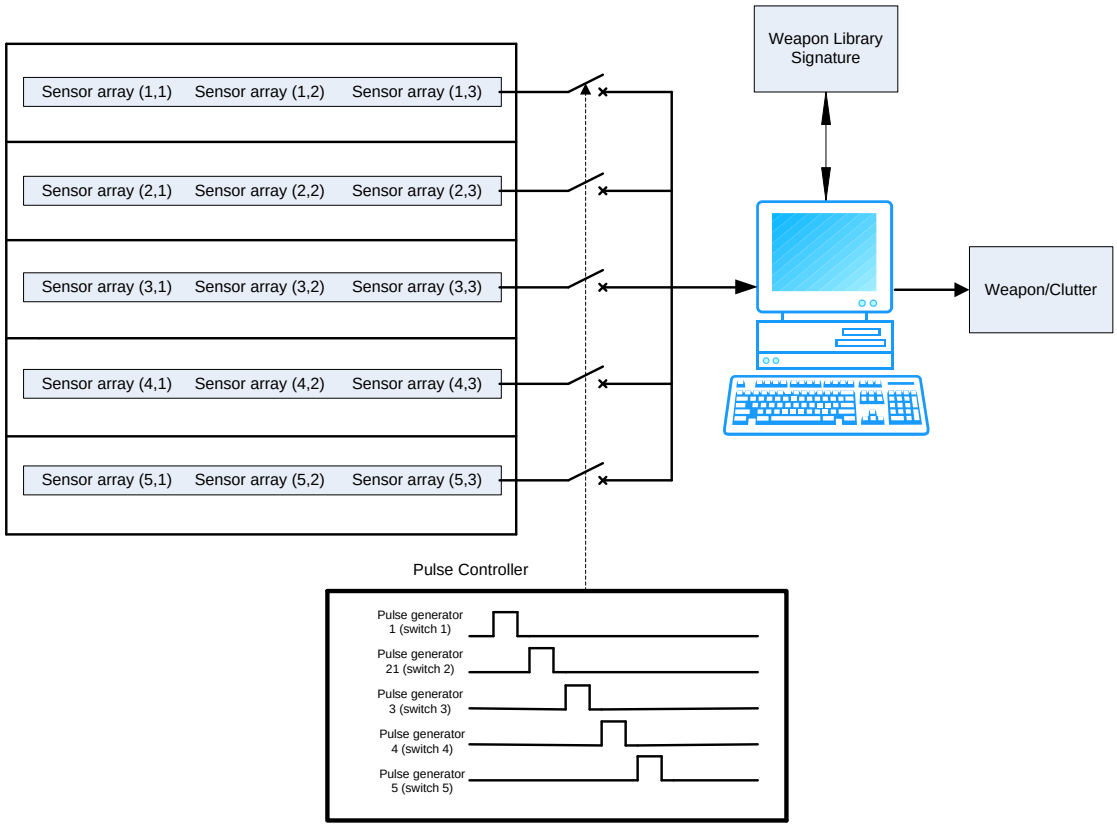

Figure 4.18. Scanning of interrogation area for detection and classification.

- **Extraction of time constant decay**

One of the proposed algorithms for the determination of a time constant consists of transformation of the signal strength by using the logarithm of the signal. With this transformation, an exponential decay curve appears as straight line, with the slope being the

time constant. The time constant (slope of the line) can be extracted by curve fitting (best-fit one –parameter linear function) of the transformed data. This process is illustrated in Figure 4.19.

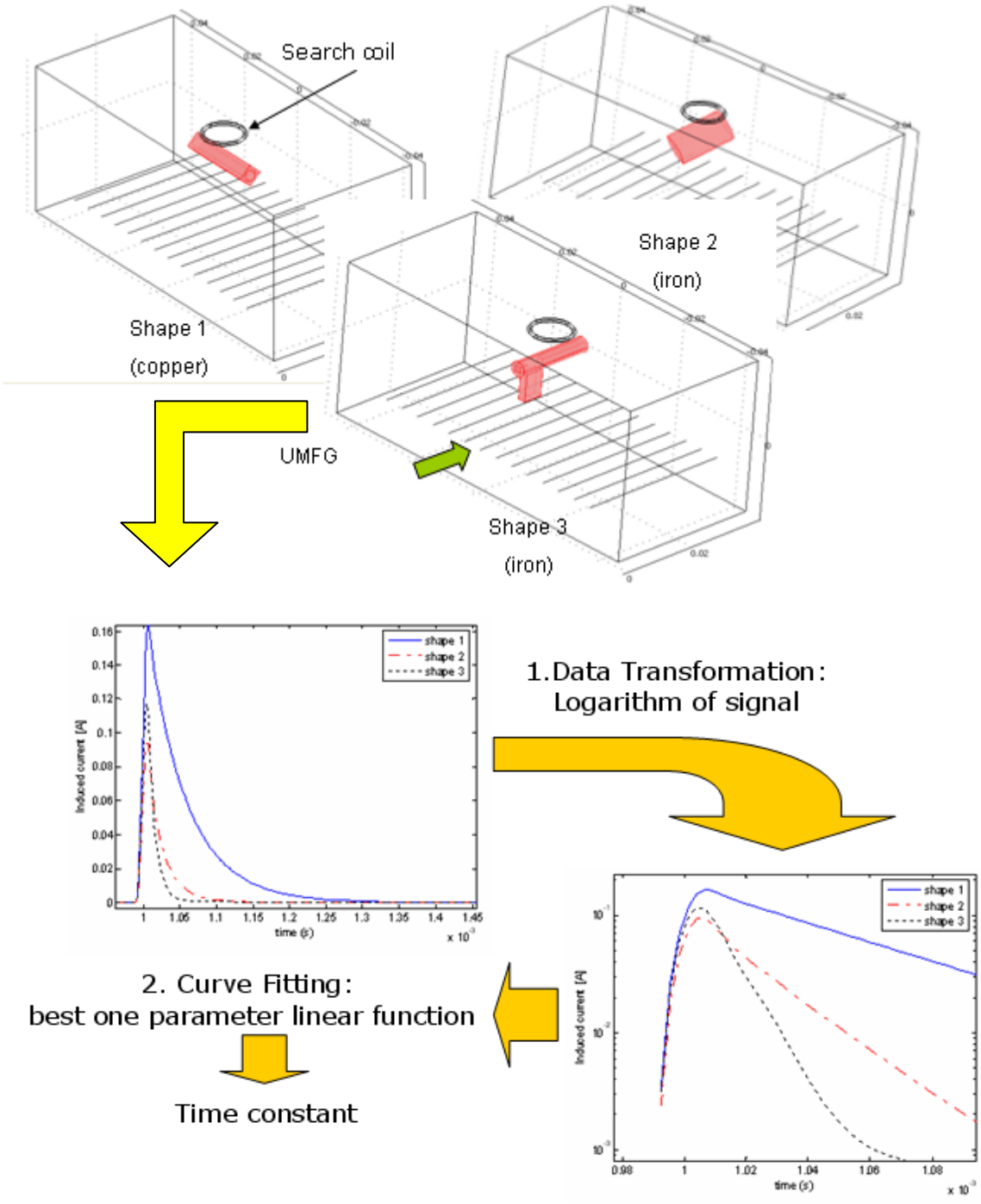

Figure 4.19. Proposed algorithm for extraction of the Time Constant.

4.3.3 Control and operator interface subsystem

The control subsystem gives the sequence order for the UMFG excitation, reads the sensors, and performs the signal processing for the detection and classification.
Set of alarms, location indicator, video monitors and displays interfaces with the operator giving the result of the detection and classification.

4.4 FEA Simulations

To test the proposed method, a simplified 3-D model in COMSOL 3.3 (finite element analysis and solver software package) as shown in Figure 4.21, has been used. The model consists of a UMFG (20 parallel cables laid on the floor, 3cm in between) for transmitting step pulse of current of 10A, 1.5ms width pulse, falling time 170us, causing eddy currents to flow in a nearby metal object. The eddy currents scatter a signal that will be detected by a three-axis magnetic sensor array (hall or magneto-resistive sensors) placed between the cables. Parameter values used in the model are based on previous studies and simulations performed to achieve a strong enough magnetic field. Simulations have been run to analyse the sensitivity/insensitivity of the target response to changes in shapes, orientation, sizes and material composition of interrogated objects. A study of target response at different stand off is also included.

4.4.1 Sensitivity to outer shape

Four different samples: Gun1 with smooth barrel and smooth bore, Gun2 with square barrel and smooth bore, and two knives with different cross section as showed in Figure 4.20 are tested respectively. In Figure 4.22, the magnetic flux density (B) along z-axis and y-axis is sensed from a distance of 35cm from the object along perpendicular line between object and floor. Following the intended algorithm for time constant extraction, the logarithm of magnetic flux density is plotted against time in order to show more clearly the time constant for each interrogated object.

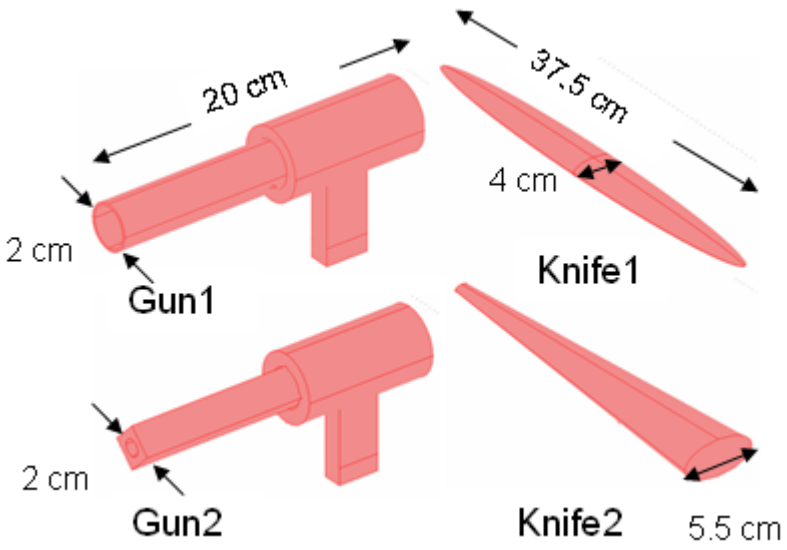

Figure 4.20. Samples for test.

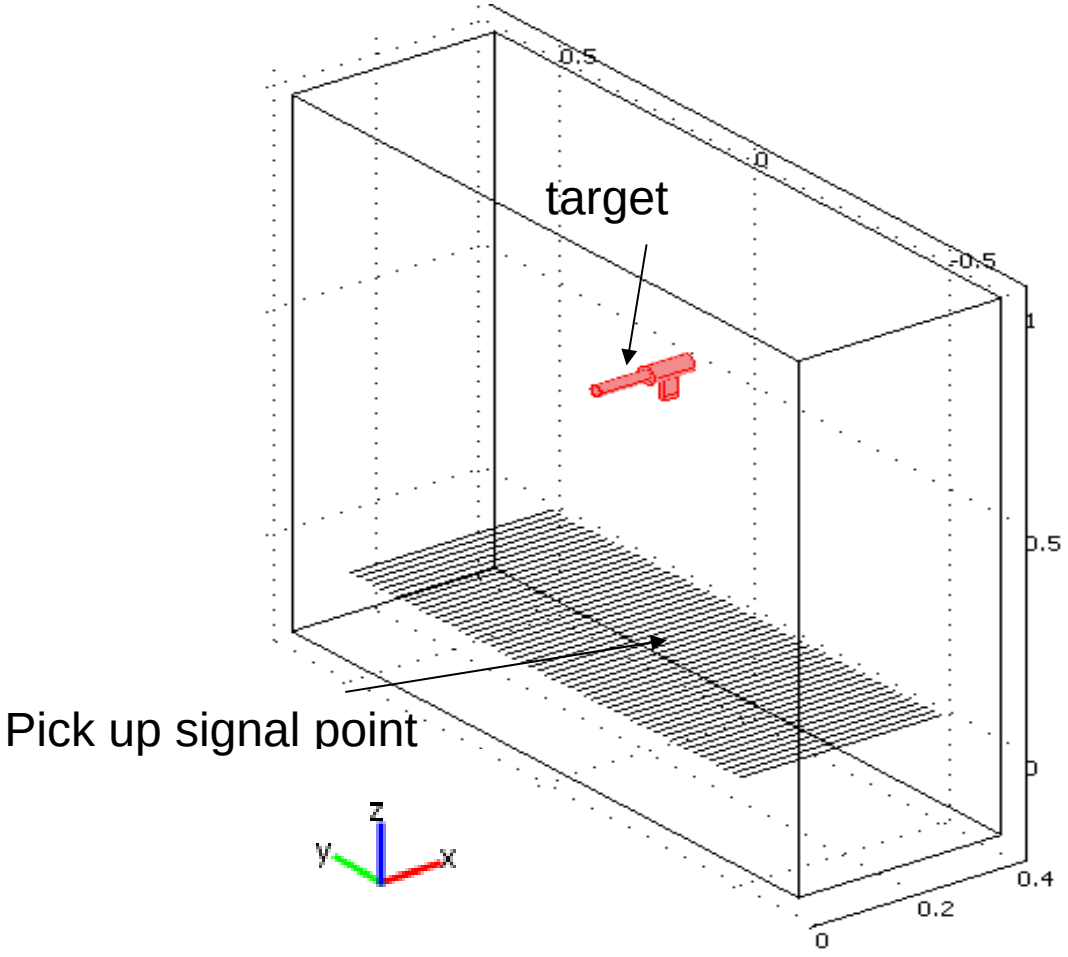

Figure 4.21. 3-D Model (dimensions in metres).

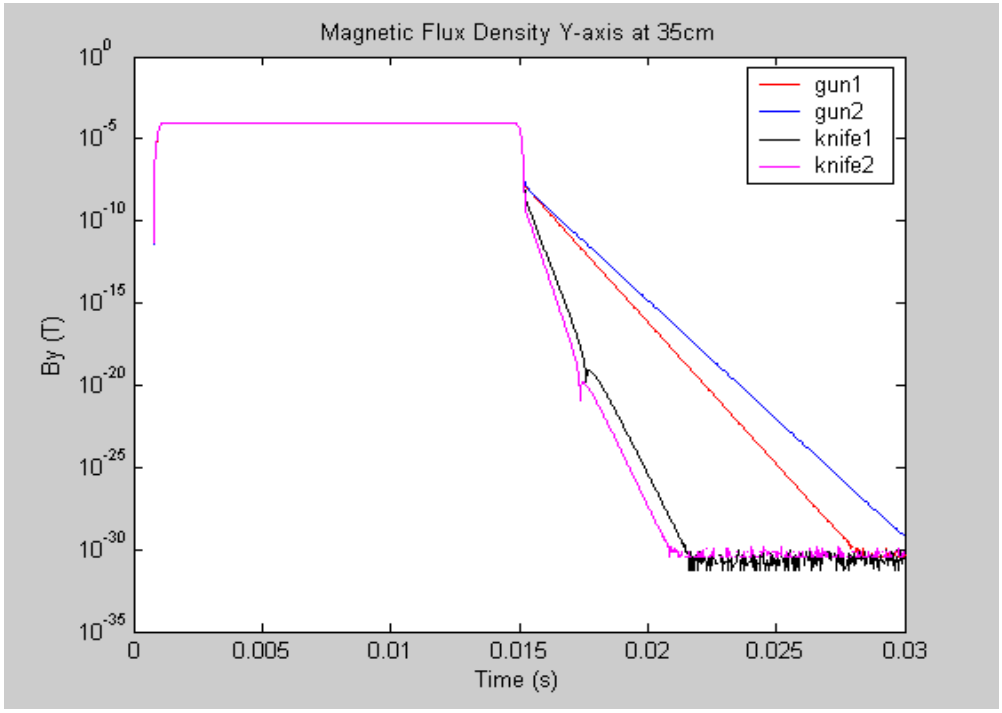

Figure 4.22. Scattered magnetic field on y-axis (top) and z-axis (bottom).

4.4.2 Insensitivity to object orientation

In the following test a gun (steel) is oriented in three positions as seen in Figure 4.23. Results showed that even if the amplitude of the signal changes, the time of decay stays invariant. Also measurements have been taken at different distance from the gun (15cm and 35cm as shown in Figure 4.24) to show how the time constant is independent of the strength of the field incident.

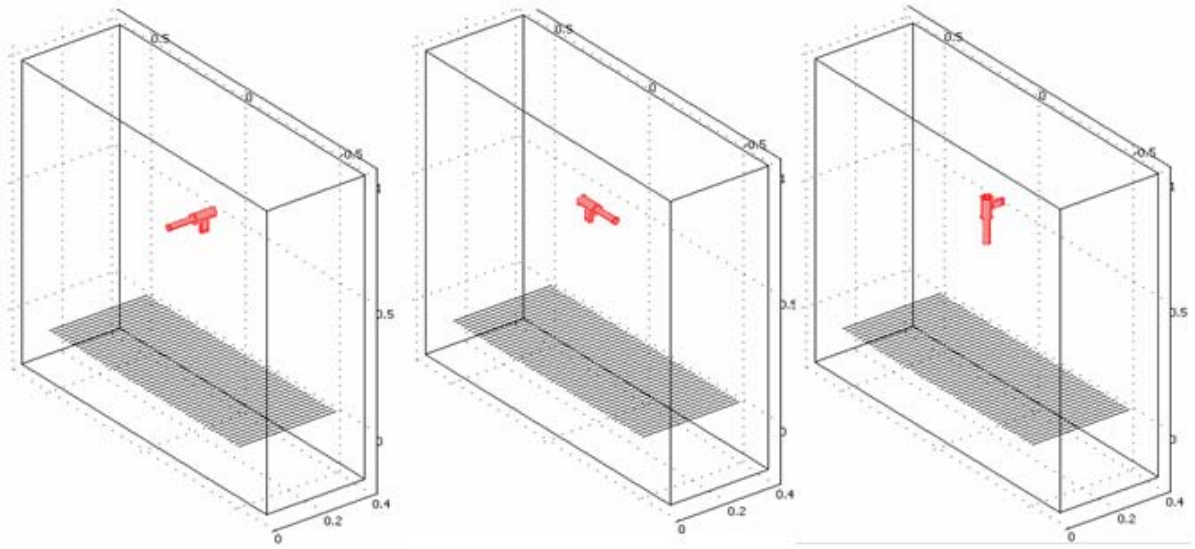

Figure 4.23. Model to test sensitivity to weapon orientation (domain dimension in metres).

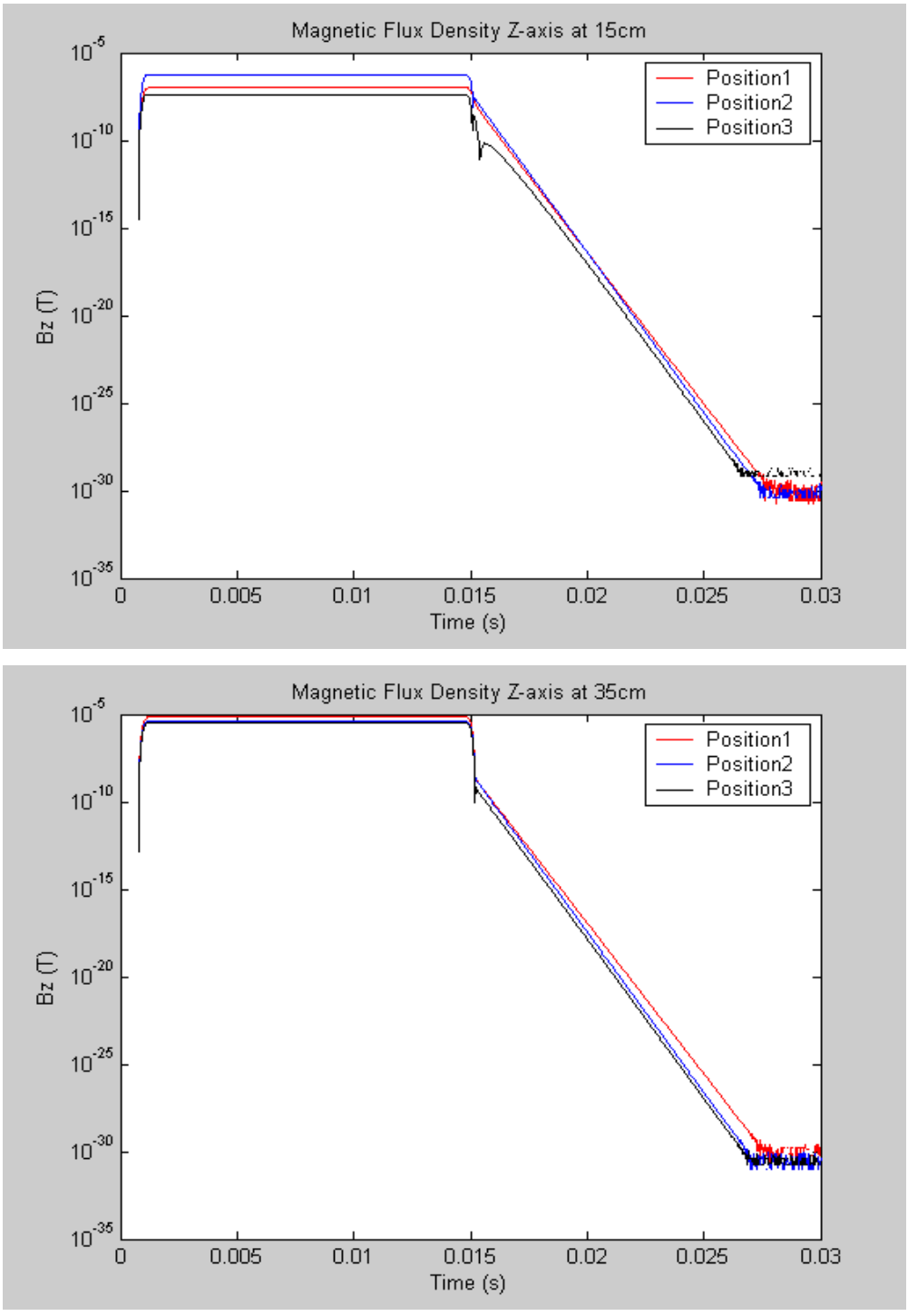

Figure 4.24. Scattered magnetic field sensed from a distance 15 cm (top) and 35 cm below the gun (bottom).

4.4.3 Sensitivity to size

Three guns of the same type but different sizes are tested. In this test a coil is added to the model to sense the time decay of induced current in the target caused by the abrupt change of the magnetic field. Results in Figure 4.25 show that time constant is a function size of the sample. Because large metallic objects store more energy than small ones, the time decay of collapsing magnetic field (or induced current in the coil) takes longer. This characteristic could be potentially used to discriminate object size.

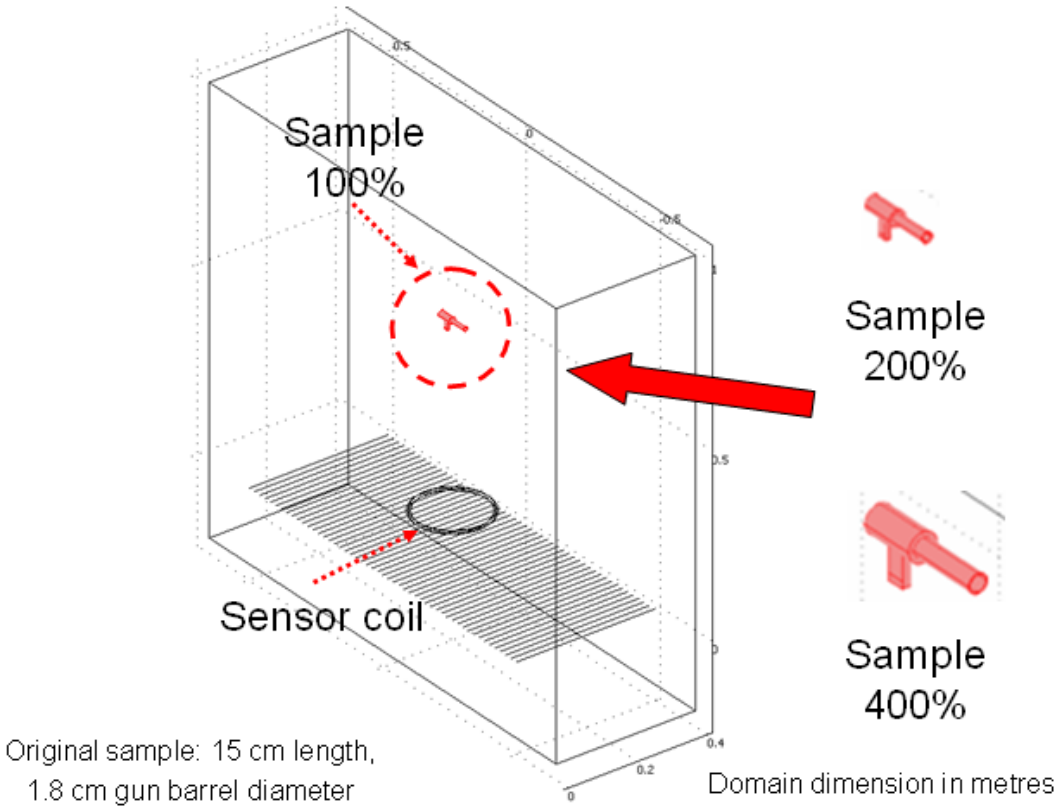

Figure 4.25. Model to test size sensitivity.

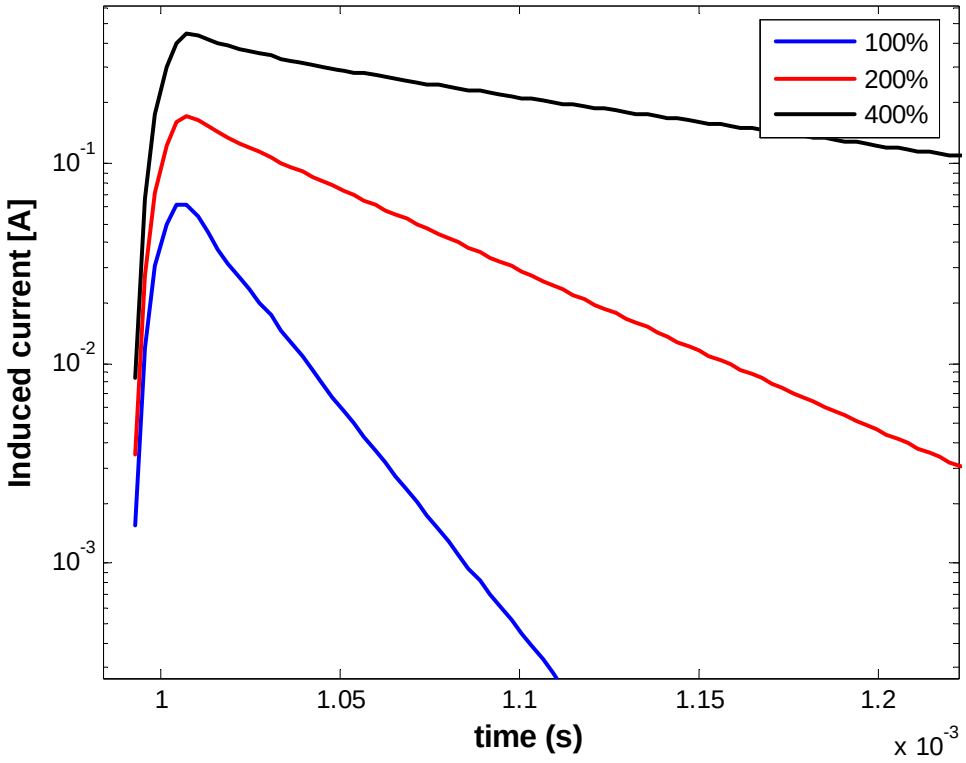

Figure 4.26. Time constant response to size of guns.

4.4.4 Sensitivity to material composition

The same sample as Figure 4.25 with different material composition (copper, iron, and steel) was tested. The time constant profile is clearly different for each case confirming the potential of the new weapon detection system to identify objects with a different material composition.

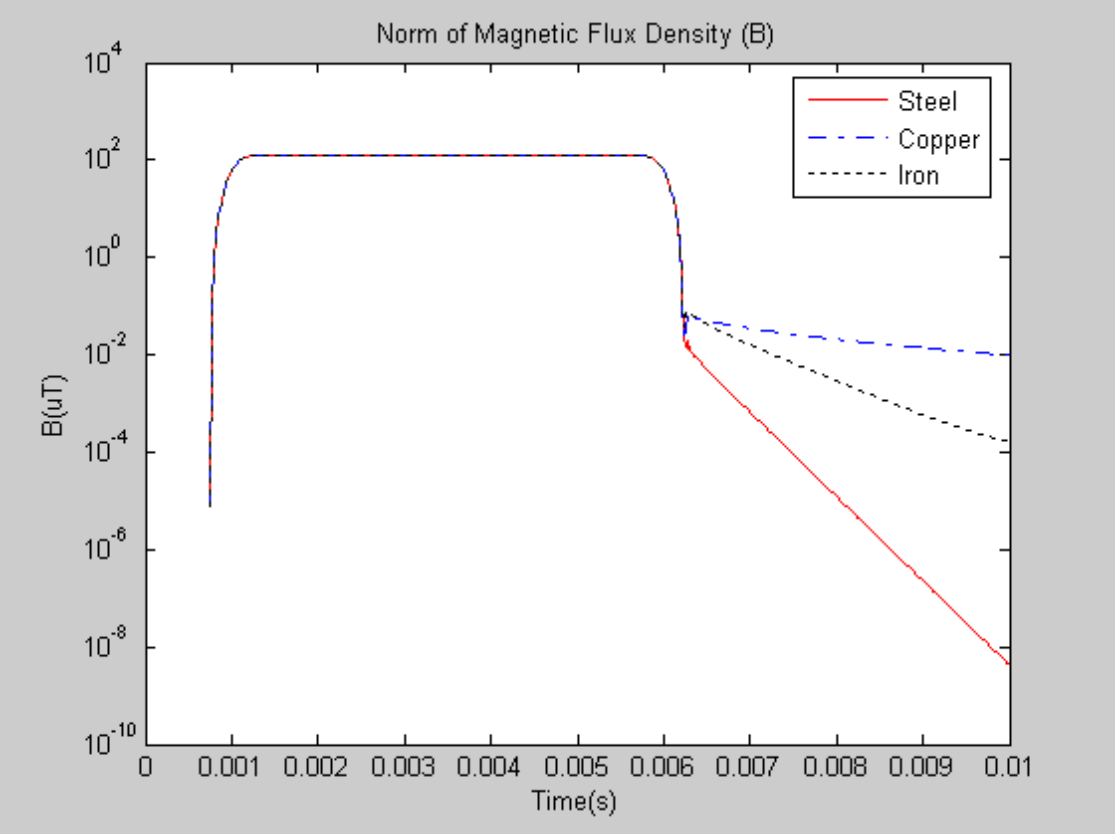

Figure 4.27. Time constant profile of a gun made of steel, copper and iron.

4.4.5 Target response to stand off

The measurements are taken in a point located over the cables. The target (aluminium) is placed at different distances (15mm, 25mm, 35mm, 45mm and 55mm) from the sensor as shown in Figure 4.28. The signal measured by the sensor without the metal object has been subtracted from all measurements.

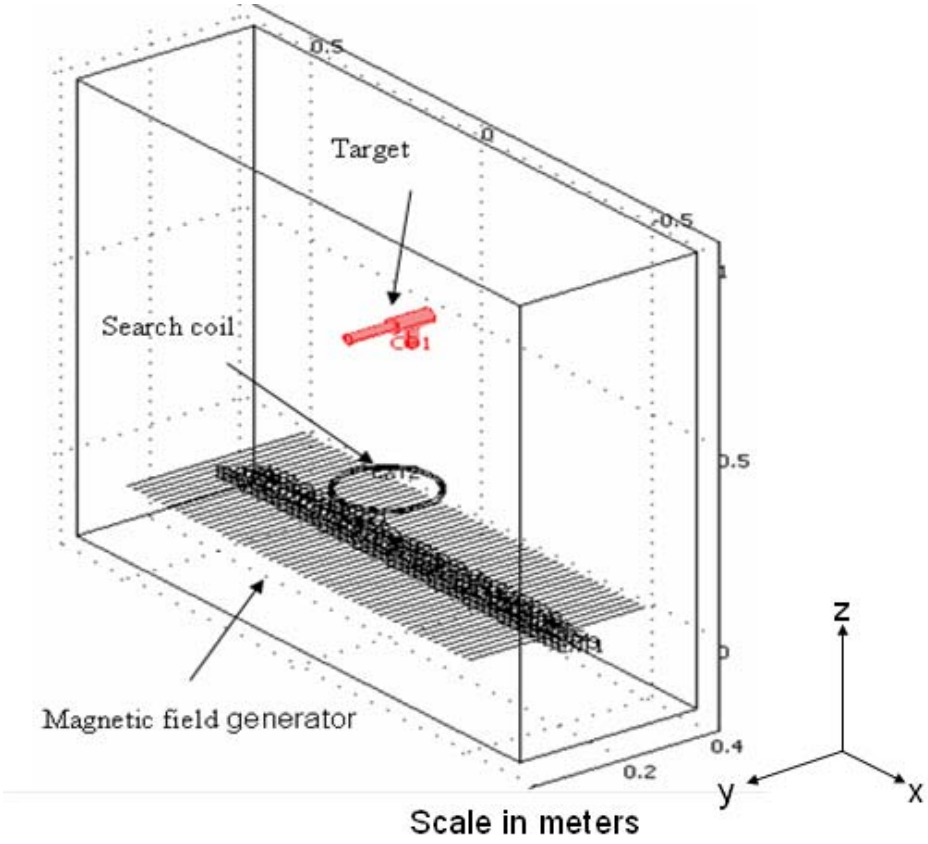

Figure 4.28. Model to measure target response at different stand off.

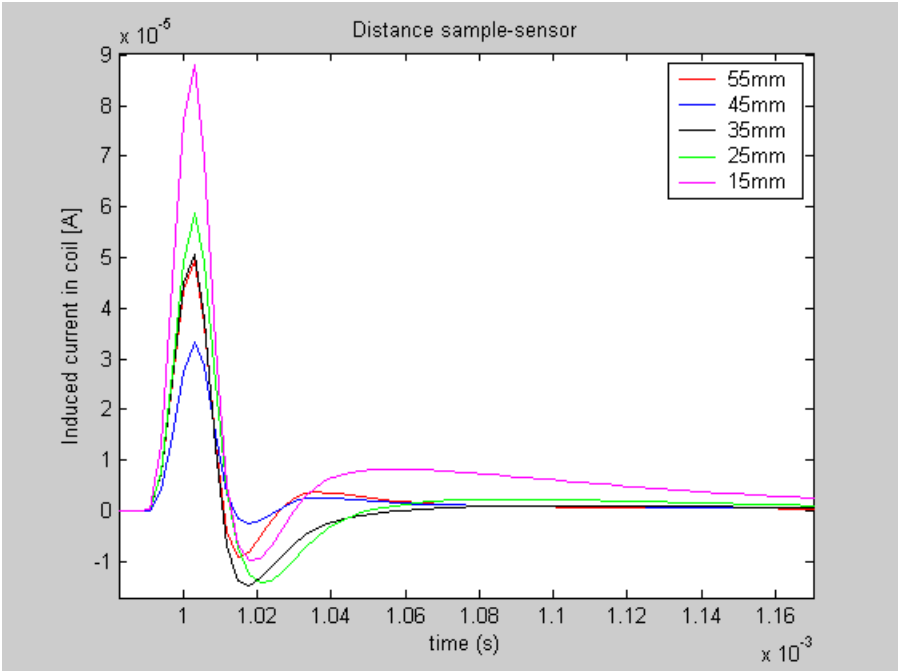

Figure 4.29. Signal amplitude of the target at different stand off.

Figure 4.29 shows how peak amplitude of induced current in a search coil is proportional to target location.

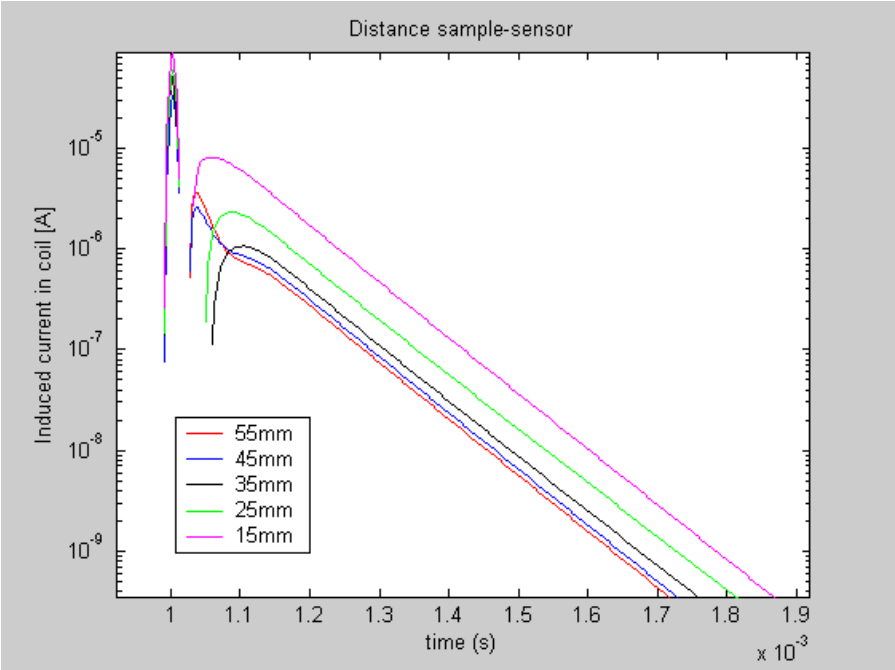

Figure 4.30. Gradient of target signals response at different stand off.

From Figure 4.29 and 4.30 it can be seen that even though amplitude of the signal response changes at different stand off, the time constant remains invariant. This simulation proves that time constant is independent of the strength of illuminating and scattering magnetic field.

Tests have shown that time decay measurements obtained from simulations of the proposed weapon detection system are sensitive to the shape, size, and material composition of the target. Furthermore, the time decay profile is independent of the strength of the illuminating magnetic field. Measurements taken in any direction also show an agreement in time decay profile. All the mentioned are requirements of a comprehensive CWD system, so the results look promising in terms of effectiveness and reduction of false alarm level.

4.5 Experimental Work

4.5.1 Driver circuit for UMFG

To improve the detection the UMFG needs to induce eddy currents in the target with sufficient strength to generate magnetic fields strong enough to be measured by sensors. UMFG has to excite the target with a magnetic field with strength and rate of change high enough to sense distance targets and induce strong eddy currents. Thus UMFG needs to carry enough current and switch faster to meet those requirements.

Based on FE simulations the UMFG needs to carry a current 6~10A and switch in around 250us to induce strong enough eddy currents in the target such that the magnetic field back to the sensors is in the order of μT . A driver circuit for the UMFG consists of a MOSFET IRF150 that can carry the required current and a step pulse generator to switch the MOSFET at a frequency adjusted to the acquisition and signal processing time of available hardware (in this research the frequency used is 20Hz).

Figure 4.31 shows the first design for the driver of the UMFG. The pulse generator (low power circuit) and the MOSFET (high power circuit) connected to the UMFG are electrically decoupled by an opto-isolator to prevent electrical failures. The pulse generator consists of timer LM555 set at 20Hz, 10% duty cycle in order to not overheat the wires.

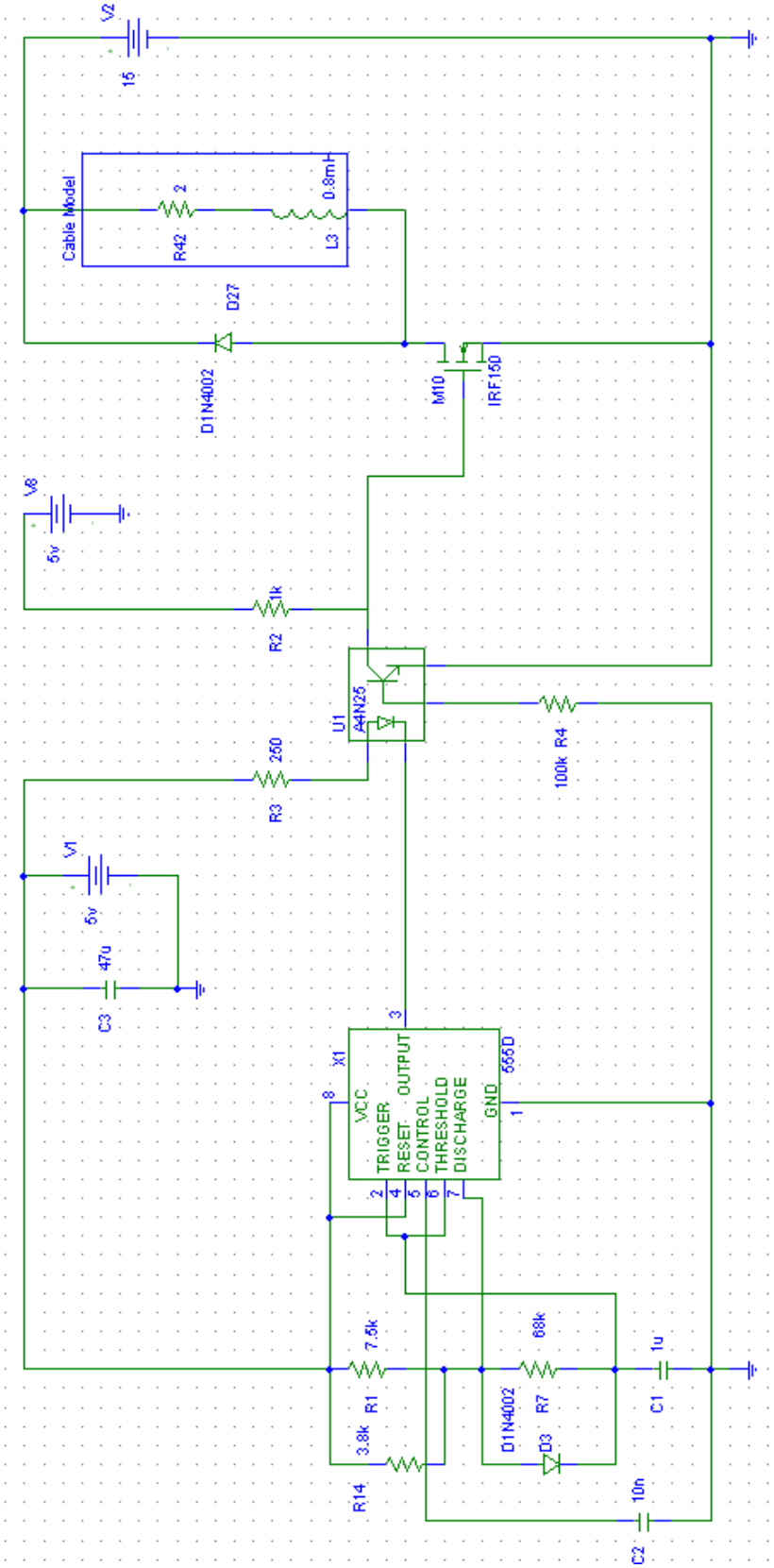

Figure 4.31. Driver circuit for UMFG (design 1).

To prevent back electromotive force (EMF) in the MOSFET a flywheel diode is connected across the wire. The pulse signal obtained from the 10 turn cable has a fall time of 1.2ms and amplitude 6.7A. As explained before the MOSFET needs to be switched off in less than 250ms to induce high eddy current density in the target. The clamped voltage and the current are shown in Figure 4.32.

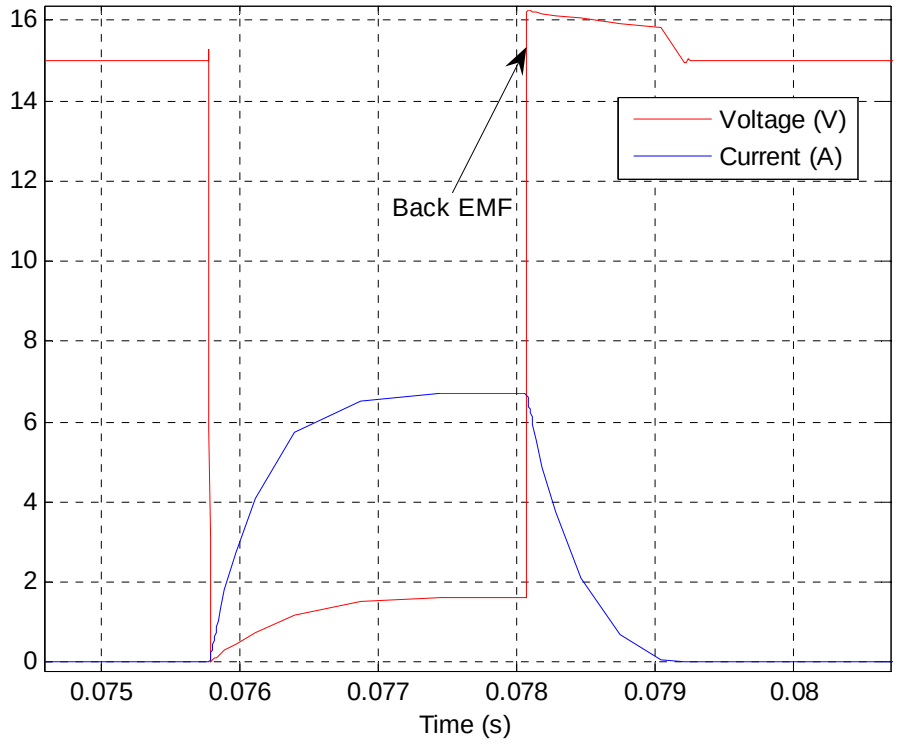

Figure 4.32. Current and Voltage in UMFG during one excitation pulse (design1).

To speed up the fall time a modification in the circuit was done (Figure 4.33). Three Zener diodes were added to the fly-back diode in order to reduce energy stored in the inductance L and allows it discharge faster. The fall time is now 200us with amplitude 6.7A. The reverse transient voltage is raised but not enough to damage the MOSFET (IRF150 has a VDss=100V). Voltage and Current in the new design are shown in Figure 4.34.

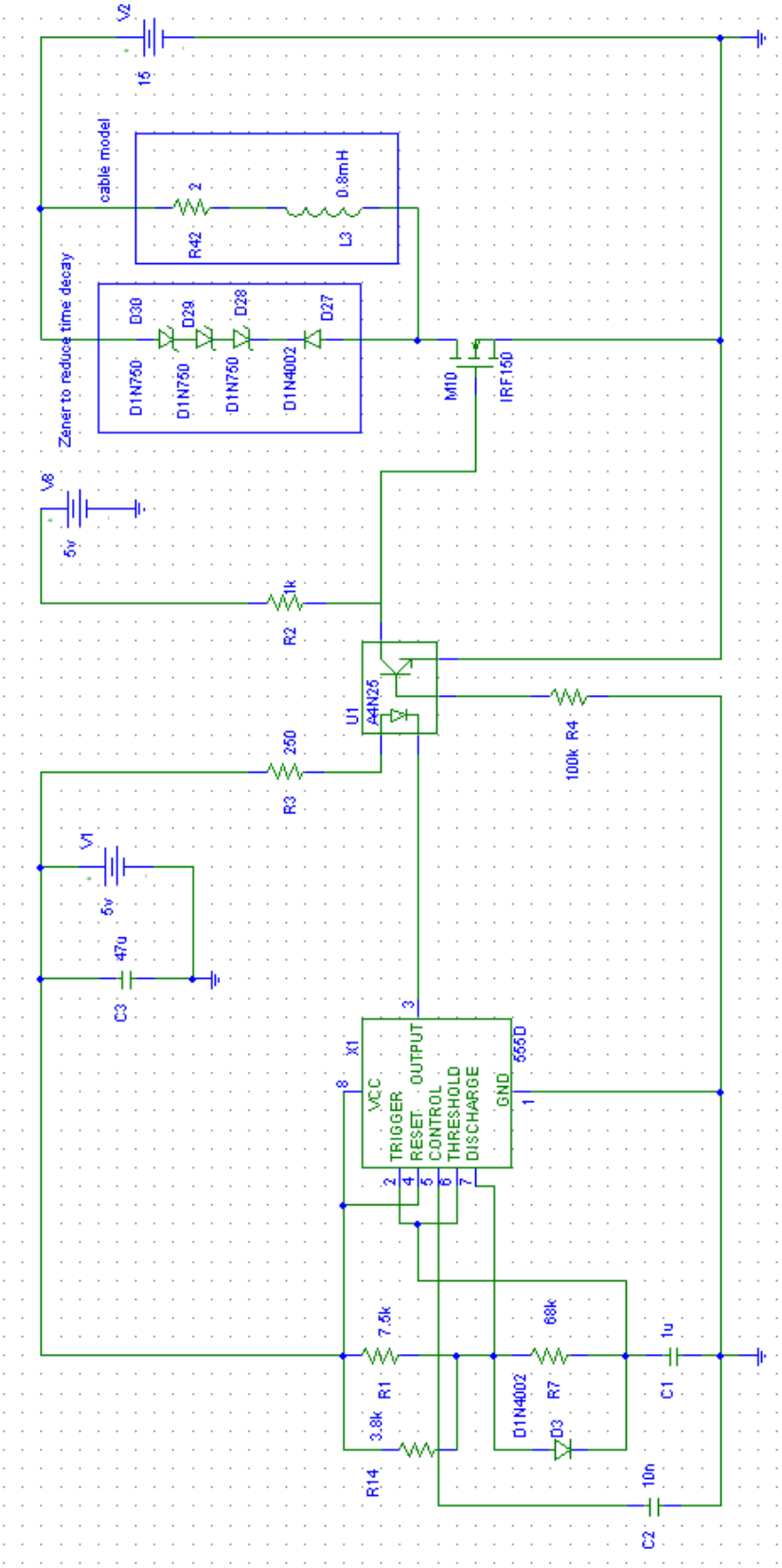

Figure 4.33. Pulse current generator (design 2).

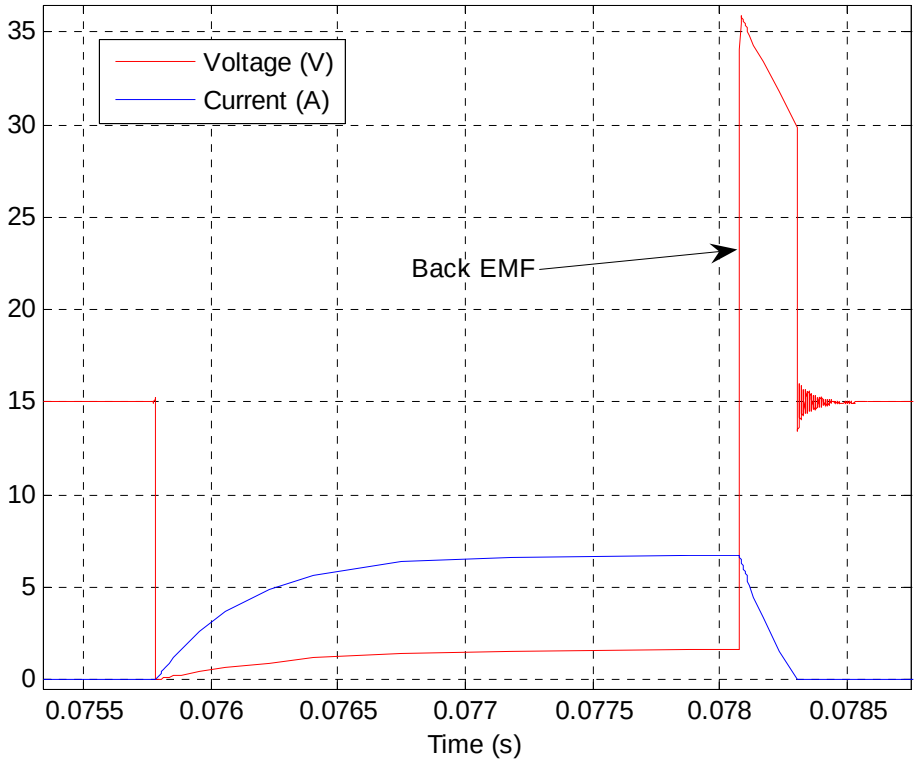

Figure 4.34. Current and Voltage in UMFG during one excitation pulse (design2).

Changes in transient voltage and current of UMFG as a consequence of adding three Zener diodes series with original fly-back diode are shown in Figure 4.35 and 4.36. Figure 4.35 shows the increasing of the reverse transient voltage as price to reduce switch off time. Figure 4.36 shows the substantial reduction of MOSFET turn off time after design changes.

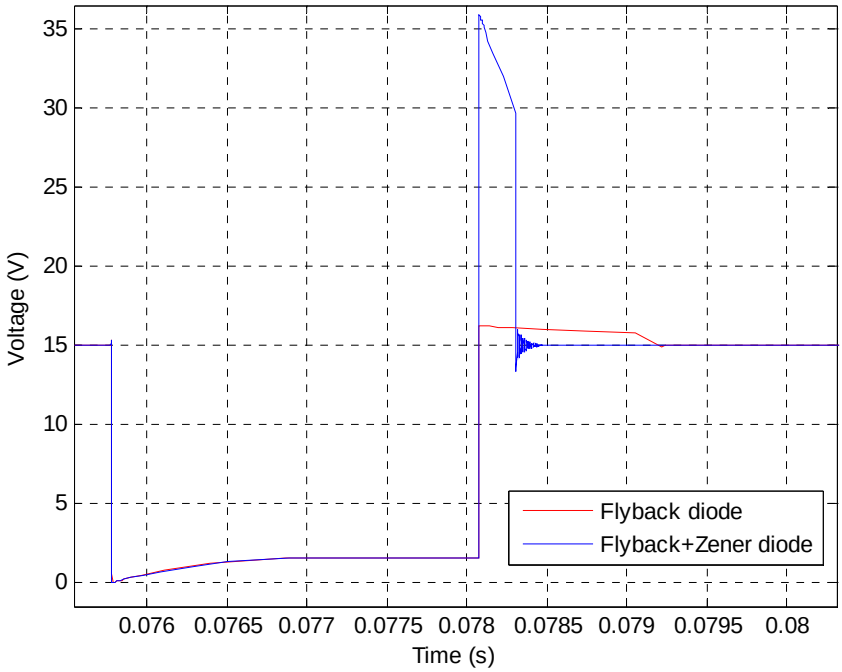

Figure 4.35. Back EMF reduction comparison between design 1 and 2.

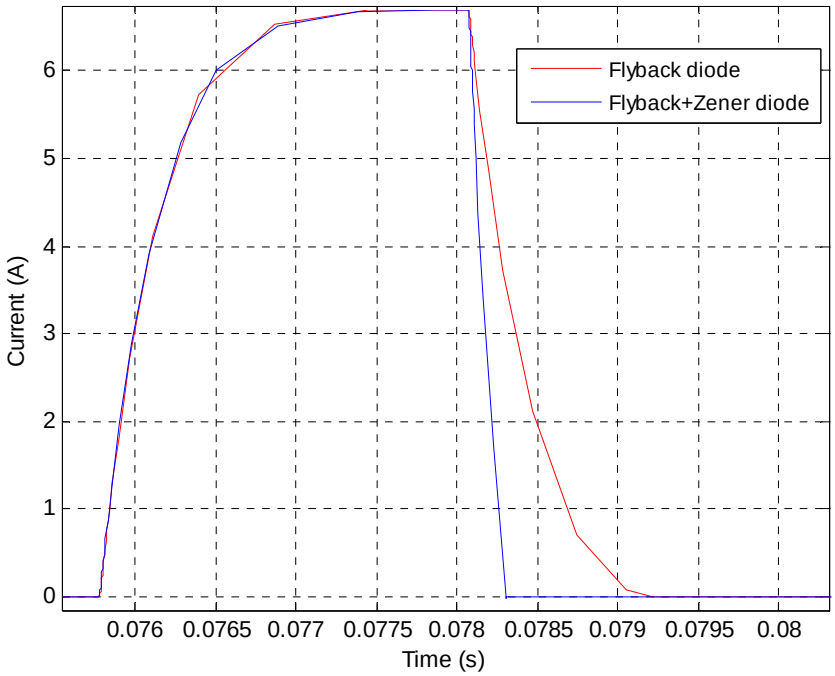

Figure 4.36. Current fall time comparison between design 1 and 2.

4.5.2 Testing of the proposed weapon detection.

Experimental tests were developed on an UMFG (3 m x 0.60 m) placing metallic objects at 30 cm over the centre of the UMFG plane and reading the measurement of sensors placed over the plane and below the targets. The tests were performed in an environment under EM interference (electronic equipments) and noise (nearby metallic objects in the illumination area) to resemble the worst working scenario of the proposed CWD system.

- **Metallic target response in search coils.**

The following tests were performed using a search coil device as showed in Figure 4.37. This search coil device allows choosing three loops arrangements. Previews test with each individual loop showed different sensitivity. The best response was obtained with 11.79 Ω, 2.525mH loop.

Figure 4.37. Search coil device.

Table 4.3. Coil parameters.

	Diameter (mm)	Inductance (mH)	Resistance (Ohms)
Large coil	150	4.414	17.833
Medium coil	120	2.525	11.796
Small coil	70	1.571	48.158

First test: **sensitivity of time constant to target orientation**

In the first test the sensitivity of time constant at target orientation is analyzed. The metallic base of a solder kit is placed 30cm over the UMFG and rotated in three positions. Search coil responses are plotted in Figures 4.38 and 4.39. The signal measured from the search coil in absence of target (red) is also included for reference.

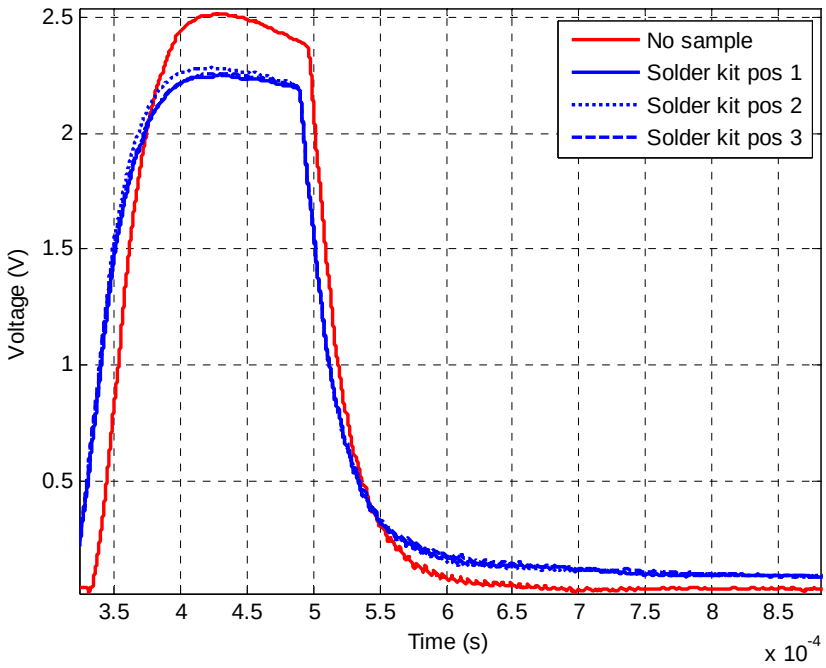

Figure 4.38. Solder kit responses at different orientation.

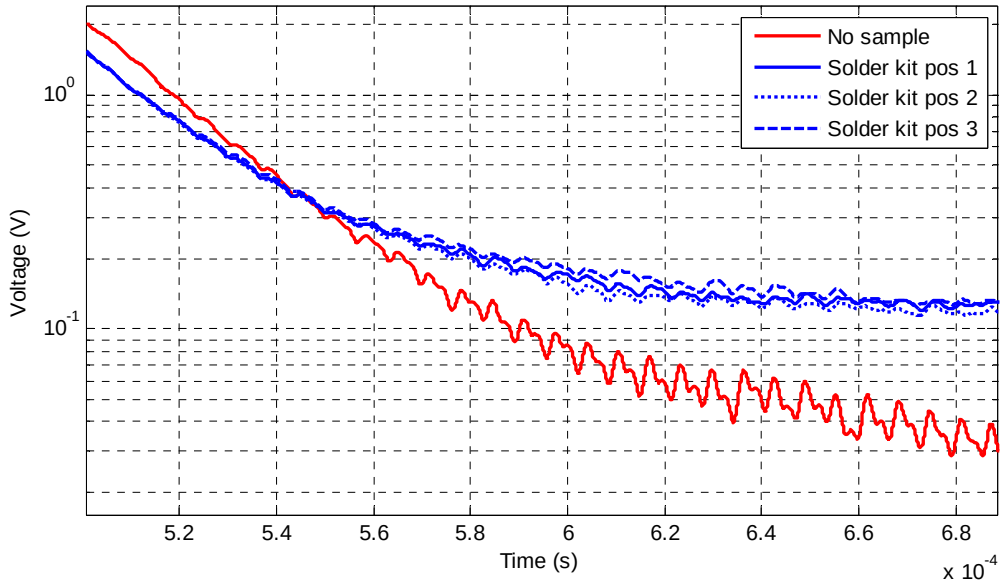

Figure 4.39. Zoomed views of solder kit responses in logarithm scale.

.

From Figure 4.38 it can be seen that target response for each position (blue curves) has similar transient profile. A zoomed view of curves (Figure 4.39), plotted in logarithmic scale, shows a first part of the transient (500-560 μs) dominated by target signals with linear profile. The second part of the transient (after 560 μs) shows coupled EM interference which is dominant because the target has already released most of the stored energy. Gradient of the curves in first part of the transient correspond to time constant which is similar for the threes positions. It probes the insensitivity of time constant to target orientation.

Second test: sensitivity of time constant to target shape

In this test, the response of samples with differentiated geometry characteristics (a base of solder kit, a mobile, and three pliers) is analysed. Measurements were taken at 30cm over the UMFG. Search coil responses are plotted in Figure 4.40(top). The signal measured from the search coil in absence of target (red) is also included for reference.

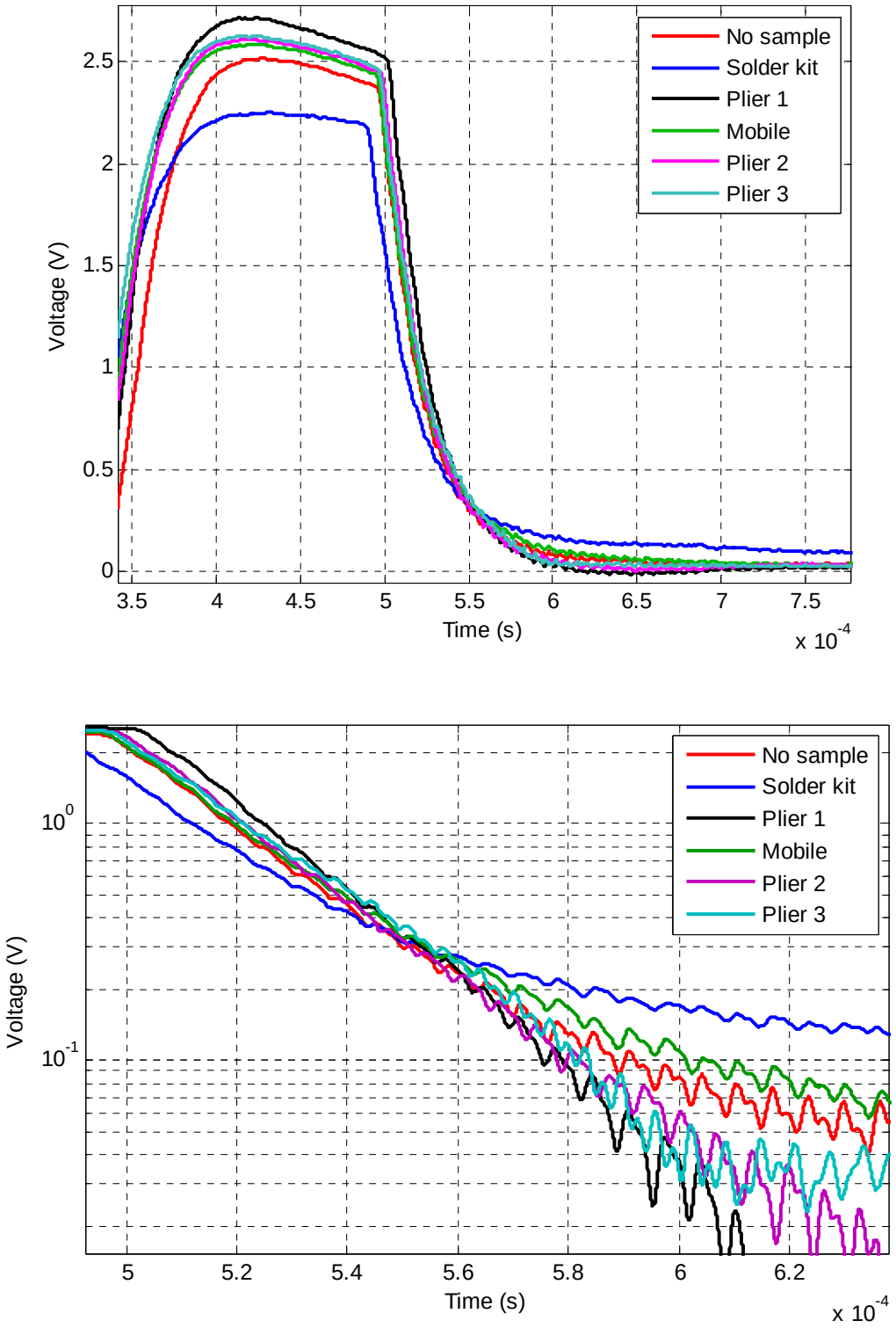

Figure 4.40. Target response signals from search coil (top). Zoomed view in logarithm scale (bottom).

Figure 4.40 (top) shows that each sample response has different transient profile. Like first test the zoomed view of curves (Figure 4.40(bottom)), plotted in logarithmic scale, shows a first part of the transient (500-550 μs) dominated by target signals with linear profile and a dominant EM interference in the rest of the transient. Now gradients of the curves in first part of the transient are remarkably different, which allow classifying samples. Thus this test probes the sensitivity of time constant to target shapes.

- **Metallic target response in magnetoresistive sensors**

Anisotropic Magnetoresistive (AMR) sensors convert magnetic fields to a differential output voltage, capable of sensing magnetic fields as low as 30 μ gauss. Most low field magnetic sensors are affected by large magnetic disturbing fields (>4~20 gauss) that may lead to output signals degradation. In order to reduce this effect, and maximize the signal output, a magnetic switching technique can be applied to the AMR bridge that eliminates the effect of past magnetic history [47].

The circuit in Figure 4.41 is the implementation of the switching technique to maximize sensitivity of AMR before UMFG illuminates the target. The circuit operates sending master pulsed signal of 14.5Hz, 9.88% duty cycle (first LM555 working as astable) to drive a pulsed current of 4A through P and N Darlington into the AMR coils. This pulsed current realigns magnetic domains of the permalloy film on each set and reset increasing the sensitivity. The master pulsed signal also pass through diodes, resistor, inverters and trigger the second LM555 (working as mono stable, 10ms output time) to produce delay before switch off the UMFG and excite the target. This circuit eliminate all past magnetic history of the sensor just before start the measurements. Figure 4.42 shows the timing diagram of signals in different part of the circuit.

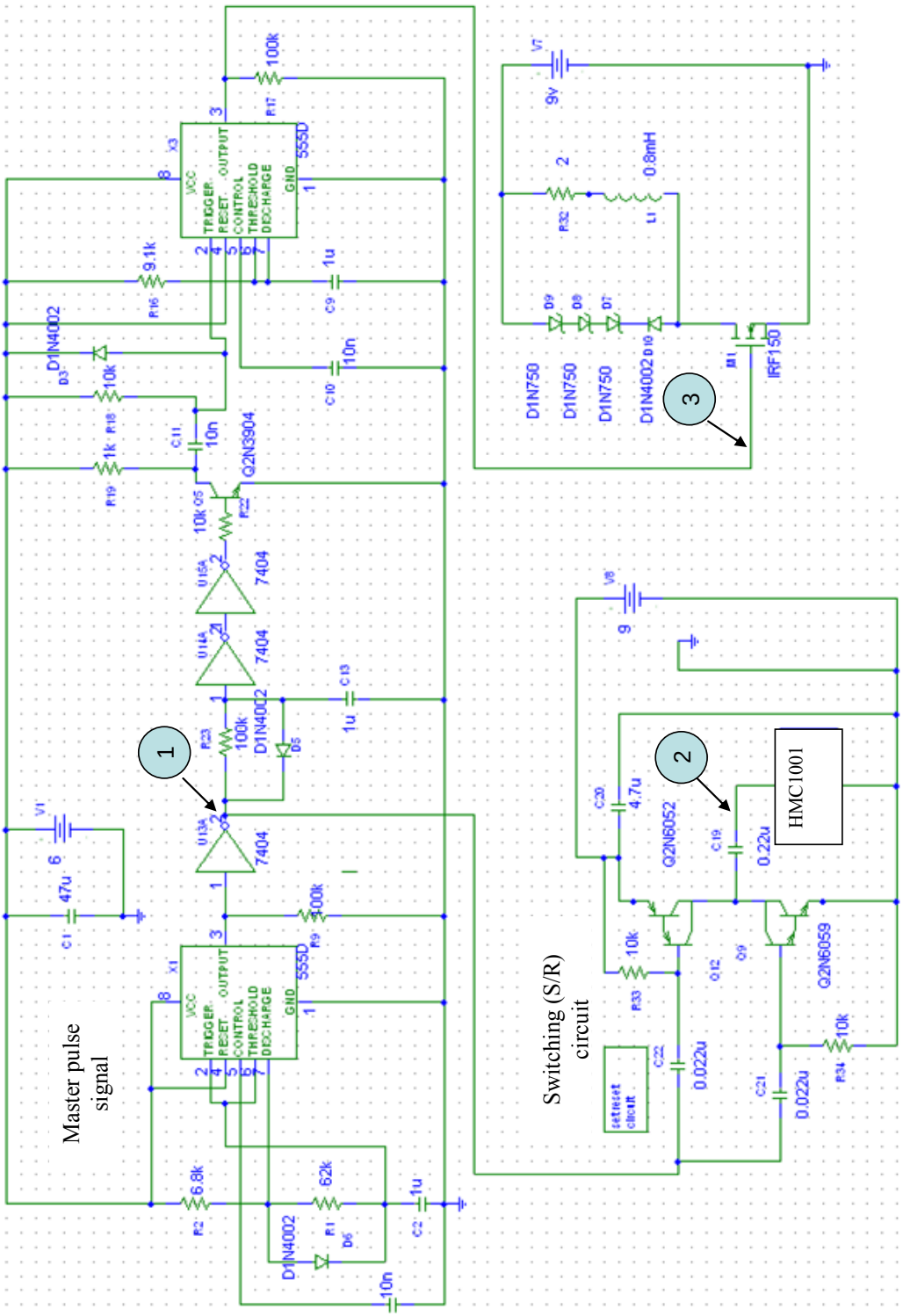

Figure 4.41. AMR sensor.

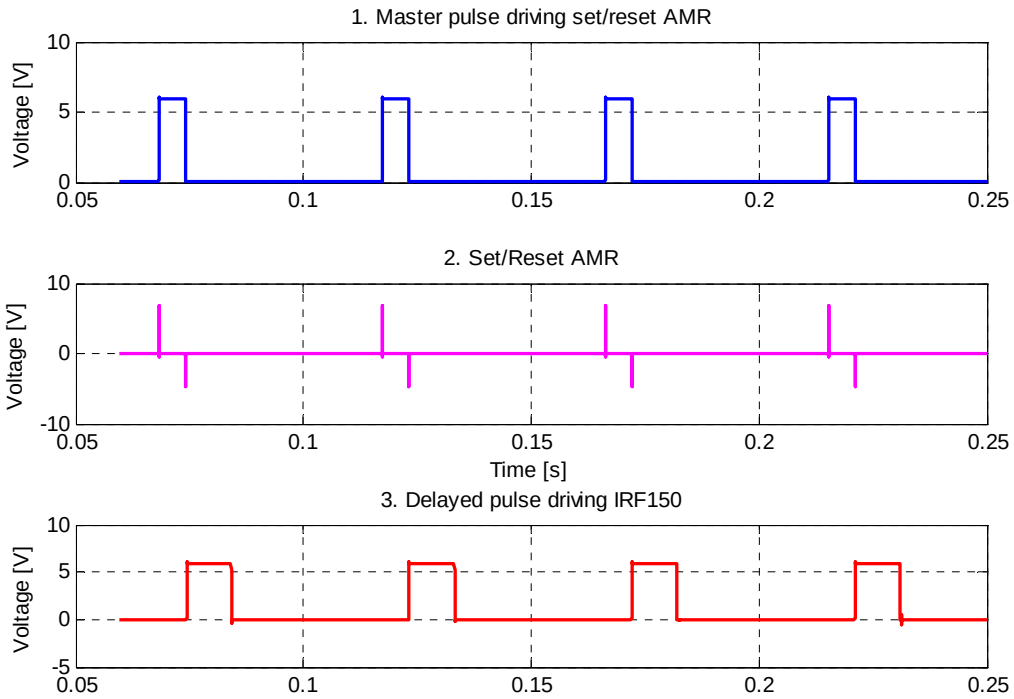

Figure 4.42. Timing diagrams.

Test: sensitivity of time constant to target shape

The sensitivity of AMR sensor to samples with differentiated shapes (a base of solder kit, a mobile, three pliers, and keys) is analysed. Measurements were taken at 30cm over the UMFG. Target responses are plotted in Figures 4.43 and 4.44. The signal measured from the AMR in absence of target (blue) is also included for reference.

The different transient profile of each sample can be observed more clearly from zoomed plot (Figure 4.44). Time constants can be extracted from first part of transient (80-100 μs) where target signals are dominant.

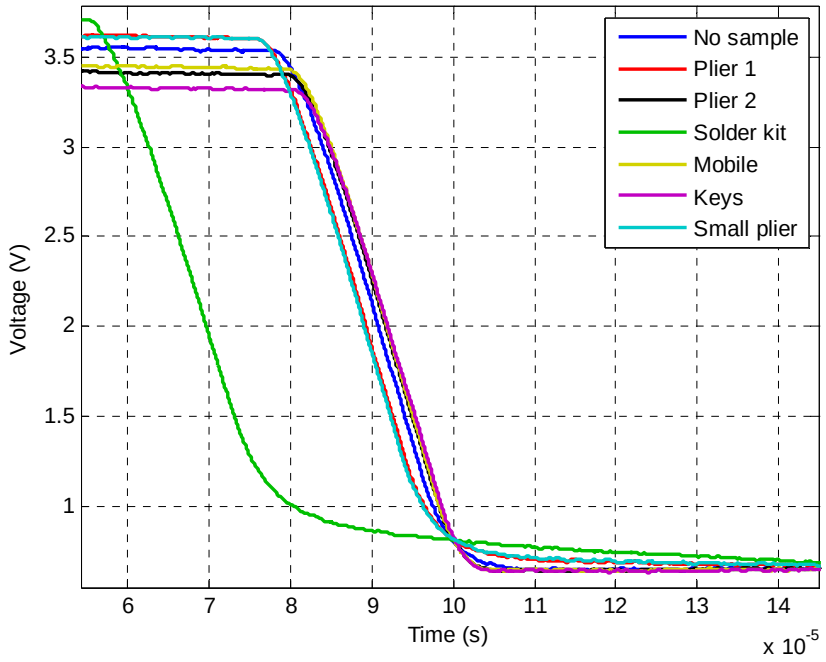

Figure 4.43. Time constant decays profile of metallic objects using AMR HMC1001.

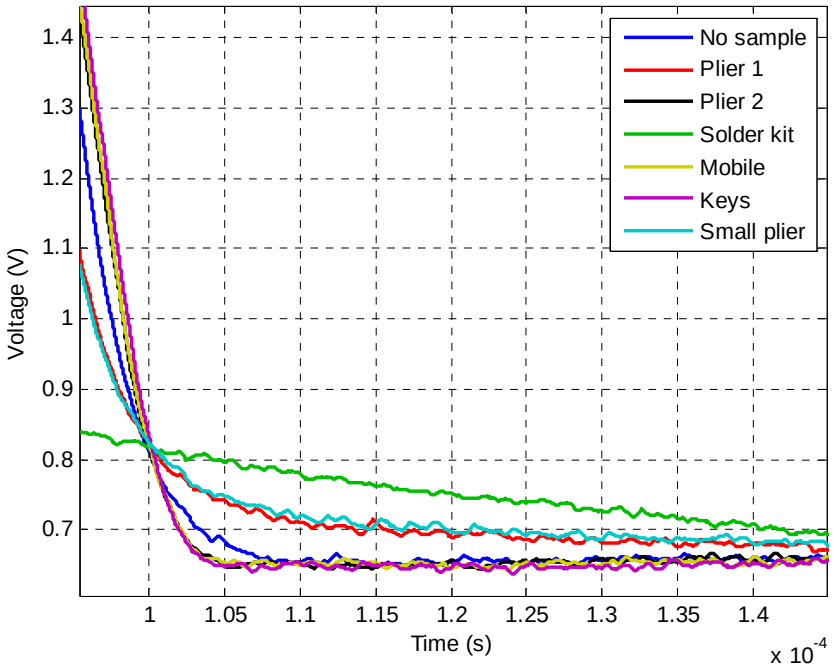

Figure 4.44. Close up of Time decay profile of metallic objects using AMR HMC1001.

4.6 Conclusions

A new proposal CWD has been proposed based on information contained in the scattered magnetic field from objects illuminated by a low frequency magnetic field. Information regarding physical characteristics, size and material composition of metallic object can be extracted from one of the parameters of the scatter signal: the time constant of the decaying magnetic field induced in the object after step excitation.
The system design discussed and proposed in the second and third part of this chapter can serve as foundation for further development of the proposed CWD.

FEA simulations have shown that time decay are sensitive to the shape, size, and material composition of the target. Furthermore, the time decay profile is independent of the strength of the illuminating magnetic field. Measurements taken in any direction also show an agreement in time decay profile. All the mentioned are requirements of a comprehensive CWD system, so the results look promising in terms of effectiveness and reduction of false alarm level.

Two sensor technologies were chosen to test the feasibility of the proposed CWD system. Signals picked up from search coil and magnetoresistive sensor (AMR) technologies showed sensitivity to shapes and insensitivity to orientation of metallic objects. Measurements were taken in an environment full of electronic equipments where noise and EM interference were present. Search coils showed less immunity to those effects comparable to those in AMR. AMR sensors could provide more space resolution detection than search coils because of the small size however it can be achieved at cost of complexity in the circuitry (i.e. switching circuit, signal conditioning, etc). More investigation is need with sensor technologies to provide high resolution and low cost solution for the proposed CWD.

Chapter 5: CONCLUSIONS

- The literature survey has identified some advantages and disadvantages of CWD systems in issues such as operating range, material composition of the weapon, penetrability and attenuation factors. Electromagnetic (EM) resonance system, which uses EM resonance as signatures to distinguish weapons and nuisance objects, shows a large sensing distance. It could detect concealed weapons at distances up to 10m. However the system shows problems with classification due to signature of an individual with a weapon is very similar to one without a weapon. CWD systems based on MMW have high penetrability (clothing mainly) but high attenuation under weather condition (water). Terahertz sensing and imaging system are currently being developed that are capable of forming images of concealed weapons suitable for weapon classification. However, the penetration of THz through the atmosphere for stand-off detection and through some types of clothing leads to poor results. Infrared imagers can be used for detecting concealed guns at nights. However infrared radiation emitted by people is absorbed by clothing. The best results for gun detection are when the clothing is tight, which is not normally the case. Ultrasound concealed weapons detector works at distances of up to 8m. However, this makes no use of the resonant cavities present in a gun to generate a unique gun signature and it is falsely triggered by non-gun items such as leather wallets. Inductive magnetic field detectors are the cheapest and common in the market but have a problem of sensitivity. When dealing with materials that are not of very high conductivity or of very small dimensions, the material is hardly to be detected. Passive CWD systems such as those based on sampling of the earth's magnetic field are very attractive because of lacking of radiation to interrogate the inspection area. However those systems need very sensitive magnetometers of high cost.

- Literature survey has identified that a comprehensive CWD needs to meet three main requirements: high sensing distance for open and outdoor environments; high penetration for detection of weapons, explosive under clothes, or even walls, and

robust weapon recognition to discriminate accurately threat/non-threat items. No a single method in the survey meets all these requirements. Most of the CWD methods described here are complementary. New CWD systems need to be an amalgamation of the techniques mentioned above permitting a reduction in the number of false alarms.

- Study of low cost complementary technologies has shown the feasibility of characterisation of guns and knives. Finite element models of Passive (Earth field distortion) and Active (EM wave illumination) weapon detection systems showed that earth magnetic field changes are sensitive to outer and inner shapes of metallic objects, however they are also sensitive to object orientation. RCS profile of metallic object illuminated by high frequency radiation (300MHz to 1GHz) showed sensitivity to outer shapes and a convenient lack of sensitivity to object orientations. This study showed that it could be possible to obtain signatures for each threatening objects to be used on identification.

- A new CWD system has been proposed to discriminate threatening metallic objects based on time constant of scattered field from pulsed magnetic field used to interrogate an area with metallic objects.

- The feasibility of the new CWD systems has been analyzed by experimental tests and FE simulation studies. Experimental tests have confirmed that the proposed CWD is sensitive to the target's shape and insensitive to target's orientation. FEA has shown that the time decay profile is independent of the strength of the magnetic flux density, so independent of the distance away from the sample; however there is a constraint on the distance because of the sensitivity limitation of the magnetic field sensors. Measurements at 45 cm from the target are in range of 10^{-5} T. There are magnetic sensors on the market able to detect these levels (search-coil magnetometer; flux-gate magnetometer; SQUID magnetometer; GMR) supporting the feasibility of the proposed CWD system.

- This thesis has provided the foundation for development of new proposals on CWD and given an input for a comprehensive multimodal weapon detector system free of false alarms.

Chapter 6: FUTURE WORK AND RECOMMENDATIONS

The present stage of this work has shown the potential of the time constant as a parameter for weapon detection and classification. The following works could be included in a further stage.

- Design specification for the hardware of the CWD. It should include sampling time and bit resolution for the acquisition card, and switching frequency for the pulse controller such that online detection and classification can be achieved.

- Even though sensing systems using search coils and AMR have shown the relatively good sensitivity and response, further studies with new low cost sensing technologies need to be included to get optimum signals and improve the detection. One of the emergent and promising technologies is the two dimensional electron gas, AlGaAs/InGaAs/GaAs (Indium Gallium Arsenide/Indium Gallium Arsenide/Gallium Arsenide) [48] 2DEG Hall device which could be included in a future work.

- Multi-axis sensor array can be included in the CWD system to have more views of the targets and improved detection.

- Implement 3D reconstruction of concealed weapons by means of UMFG modules such that resembles a walk through portal. The portal could be comprised of one UMFG lying on the floor and two UMFG attached to walls. An algorithm to reconstruct a 3D image from sensor array signals, associated with the UMFG modules, needs to be developed.

- More investigation needs to be done for multitarget detection and classification.

- The collection of signal response of different classes of guns, knives and other threatening metallic objects to develop signature database.

- Test the sensitivity of the CWD to target material composition.

- The development of robust pattern recognition system with the time constant as a main feature. Efforts need to put in Signal Processing to achieve time constant extraction and correlation algorithms with low computation time to ensure online detection and classification.

- Finally the present work needs to be complemented with other approaches at several non-overlapping wavelengths in order to produce an integrated multimodal sensing system, reducing the level of false alarms.

REFERENCES

[1] SUTTON, V., and BROMLEY, D.A., Understanding technologies of terror, *Technology in Society*, vol. 27, Issue 3, pp. 263-285, Aug 2005.

[2] PAULTER, N.G., Guide to the Technologies of Concealed Weapons and Contraband Imaging and Detection, National Institute of Justice Guide 602-00, pp. 33-50, Feb 2001

[3] ROYBAL, L.G., RICE, P.M., and MANHARDT, J.M., A new approach for detecting and classifying concealed weapons, *Proceedings of the SPIE, The International Society for Optical 54 Engineering, Conference on Surveillance and Assessment Technologies for Law Enforcement*, vol. 2935, pp. 95-107, Boston, MA, , November 1996

[4] ALLEN, G.I., CZIPOTT, P., MATTHEWS, R., and KOCH, R.H., Initial evaluation and follow on investigation of the Quantum Magnetics laboratory prototype, room temperature gradiometer for ordnance location, *Proceedings of the SPIE, The International Society for Optical Engineering, Conference on Information Systems for Navy Divers and Autonomous Vehicles Operating in Very Shallow Water and Surf Zone Regions*, vol. 3711, pp. 103-112, Orlando, FL, April 1999

[5] CZIPOTT, P.V., and IWANOWSKI, M.D., Magnetic sensor technology for detecting mines, UXO, and other concealed security threats, *Proceedings of the SPIE, The International Society for Optical Engineering, Conference on Terrorism and Counter-terrorism Methods and Technologies*, pp. 67-76, Boston, MA, November 1996

[6] KOTTER, D.K., ROYBAL, L.G., and POLK, R.E., Detection and classification of concealed weapons using a magnetometer-based portal, *Proceedings of SPIE – Vol. 4708 Sensors, and Command, Control, Communications, and Intelligence (C3I) Technologies for Homeland Defense and Law Enforcement*, pp. 145-155, August 2002

[7] IDAHO NATIONAL LABORATORY TECHNOLOGIES, *Concealed Weapon Detection using a magnetometer-based portal to detect potential threats* [online]. Available at: https://inlportal.inl.gov/portal/server.pt/gateway/PTARGS_0_200_816_259_0_43/http%3B/inlpublisher%3B7087/publishedcontent/publish/communities/inl_gov/about_inl/home_page_fact_sheets/sheets/concealed_weapons_detection_4.pdf [Accessed 20 November 2006]

[8] NELSON, C.V., Metal Detection and Classification Technologies, *Johns Hopkins APL technical Digest*, Vol. 24, Number 1, pp. 62-66, 2004

[9] TIAN, G.Y., ZHAO, Z.X., and BAINES, R.W., The research of inhomogeniety in eddy current sensors, *Sensors and Actuators* A, 58, pp. 153-156, 1998.

[10] PAULTER, N.G., Users' Guide for Hand-Held and Walk-Through Metal Detectors, NIJ Guide 600–00, NCJ 184433, Office of Science and Technology, U.S. Department of Justice, Washington, DC 20531, January 2001.

[11] NELSON, C.V., Wide-Area Metal Detection System for Crowd Screening, in *Proc. SPIE AeroSense 2003 Conf., Sensors and Command, Control,Communication, and Intelligence (C3T) Technologies for Homeland Defence and Law Enforcement II*, Orlando, FL (22–25 Apr 2003).

[12] NELSON, C.V, MENDAT, D., and HUYNH, T.B., Three-dimensional Steerable Magnetic Field Antenna for Metal Target Classification, in *Proc. SPIE AeroSense 2003 Conf., Detection and Remediation Technologies for Mines and Minelike Targets*, pp. 707–717, Orlando, FL, 22–25 Apr 2003

[13] DUCHATEAU, J.E., HINDERS, M., *Using Ultrasound in Concealed Weapons Detection*, NDE Lab, Department of Applied Science, College of William and Mary, April 2005

[14] ACHANTA, A., et al, Non-Linear Acoustic Concealed Weapons Detection, *Proceedings of the 34th Applied Imagery and Pattern Recognition Workshop***,** pp. 21-27, 2005

[15] HAMILTON, M.F., and BLACKSTOCK, D.T., *Non linear acoustics*, Boston, Academic Press, 1988

[16] KNOTT, E.F., SHAEFFER, J.F., and TULEY, M.T., *Radar cross section,* 2nd edition, SciTech Publishing, pp. 82-83, 2003

[17] U.S. Department of Justice, *Final Report – Demonstration of a Concealed Weapons Detection System Using Electromagnetic Resonances*, January 2001 [Online]. Available at: http://www.ncjrs.org/pdffiles1/nij/grants/190134.pdf [Accessed 10 Mach 2007]

[18] HUNT, A.R., HOGG, R.D., and FOREMAN, W., Concealed weapons detection using electromagnetic resonances, *Proc. of the SPIE, The International Society for Optical Engineering, Conference on Enforcement and Security Technologies*, Vol. 3575, pp. 62-67, Boston, MA, November 1998

[19] KOZAKOFF, D.J., and TRIPP, V., Antennas for Concealed Weapon Detection, *Proceedings of the 5th International Conference o Antenna Theory and Techniques*, pp. 65-69, Kyiv, Ukraine, May, 2005

[20] CHUI, C.K., *An introduction to Wavelets*, Academic Press, San Diego, CA, 1992

[21] APPLEBY, R., Passive millimetre-wave imaging and how it differs from terahertz imaging, *The Royal Society*, Vol. 362, pp. 379- 393, Number 1815, February 15 2004

[22] YUJIRI, L., SHOUCRI, M., and MOFFA, P., Passive Millimeter-Wave Imaging, *IEEE microwave magazine*, pp. 39-50, September 2003

[23] McMILLAN, R.W., CURRIE, N.C., FERRIS, D.D., WICKS, M.C., Concealed Weapon Detection using Microwave and Millimeter Wave sensors, *Microwave and Millimeter Wave Technology Proceedings, 1998. ICMMT '98. 1998 International Conference on***,** Beijing, China

[24] LUUKANEN, A., *Bolometer and Thz imaging*, Millimetre-wave Laboratory of Finland –MilliLab-Microsensing seminar 2-4-2008

[25] FEDERICI, J.F., GARYA, D., BARATB, R., ZIMDARSC, D., THz Standoff Detection and Imaging of Explosives and Weapons, *Proc. SPIE*, Vol. 5781, 75, 2005.

[26] DICKINSON, J.C., et al., Terahertz for Military and Security Applications IV. Edited by Woolard, D.L., Hwu, R.J., Rosker, M.J., Jensen, J.O., *Proceedings of the SPIE*, Volume 6212, pp. 62120Q (2006).

[27] Optics & Laser Europe, October 2008, p15, *Terahertz success relies on research investment* [online]. Available at: http://images.iop.org/objects/optics/analysis/13/9/2/pdf.pdf [Accessed 15 March 2008]

[28] McMILLAN, R.W, Terahertz imaging, milimeter-wave radar, *Conference on Surveillance and. Assessment. Technologies for Law*. Alabama**,** USA**,** 2004.

[29] THz-BRIDGE, Final report May 2004, Tera-Hertz radiation in Biological Research, Investigation on Diagnostics and study of potential Genotoxic [online]. Available at: http://www.frascati.enea.it/THz-BRIDGE/reports/THz-BRIDGE_Final_Report.pdf [Accessed 10 March 2008]

[30] KRUSE, P.W., and SKATRUD, D.D., Editors, *Uncooled Infrared Imaging Arrays and Systems in Semiconductors and Semimetals*, R.K Willardson, Eds., Academic Press, New York, 1997

[31] SLAMANI, M.A., VARSHNEY, P.K., RAO, R.M., and ALFORD, M.G., An integrated platform for the enhancement of concealed weapon detection sensors, *Proceedings of the SPIE, The 56 International Society for Optical Engineering, Conference on Enforcement and Security Technologies*, Vol. 3575, pp. 68-78, Boston, MA, November, 1998

[32] CHEN, H.M., et al., Imaging for Concealed Weapon Detection, *IEEE Signal Processing Magazine*, Vol. 22, No. 2, pp. 52-61, 2005.

[33] MAILLOUX, R.J., *Phased Array Antenna Handbook*, Second Edition, Artech House Publishers; 2nd edition , March 31, 2005

[34] PAULTER, N.G., Hand-Held Metal Detectors for Use in Weapons Detection and Contraband Detection, National Institute of Justice Guide 602-02, February 2003

[35] FELBER, F., et al., Handheld ultrasound concealed weapons detector, *Proceedings of the SPIE, The International Society for Optical Engineering, Conference on Enforcement and Security Technologies*, Vol. 3575, pp. 89-98, Boston, MA, November, 1998.

[36] YUJIRI, L., et al., Passive Millimetre-wave camera, in *Proc. SPIE Conf. on Passive Millimeter-Wave Imaging Technology*, pp. 15-22, Orlando, FL, 1997, 3064

[37] KLEIN, L.A., *Millimetre-Wave and Infrared Multisensor Design and Signal Processing* Boston, MA: Artech, 1997

[38] SHEEN, D.M., McMAKIN, D.L., HALL, T.E., Three-Dimensional Millimeter-Wave Imaging for Concealed Weapon Detection, *IEEE Transactions on Microwave Theory and Techniques,* Volume 49, Issue 9, pp. 1581 - 1592, Sep 2001

[39] NELSON, C.V., Wide-Area Metal Detection System for Crowd Screening, in *Proc. SPIE AeroSense 2003 Conf., Sensors and Command, Control, Communication, and Intelligence (C3T) Technologies for Homeland Defence and Law Enforcement II*, Orlando, FL (22–25 Apr 2003).

[40] McINTOSH, K.A., et al., Terahertz photomixing with diode lasers in low-temperature-grown GaAs, *Appl. Phys. Lett*. 67**,** 3844 (1995).

[41] DUFFY, S.M., VERGHESE, S. and McINTOSH, K.A., Photomixers for Continuous-Wave Terahertz Radiation, in *Sensing with Terahertz Radiation*, D. Mittleman ED, Springer (2002).

[42] CHAN, Y.W., JOHNSON, M., Portable Concealed Weapon Detection Using Millimeter Wave FMCW Radar Imaging, National Institute of Justice Office Science and Technology, Final Report, , pp. 1-27, August 2001

[43] BERENGER, J., A perfectly matched layer for the absorption of electromagnetic waves, *Journal of Computational Physics*, Vol. 114, No. 2, pp. 185-200, 1994

[44] KAUFFMAN, A.A., and KELLER, G.V., *Inductive Mining Prospecting*, Elsevier, Amsterdam, 1985

[45] ASTEN, M.W., On the time-domain electromagnetic response of a conductive permeable sphere, *Journal of Applied Geophysics* Volume 67, Issue 1, pp. 63-65, 1 January 2009

[46] CARUSO, M.J., and BRATLAND, T., *A New Perspective on Magnetic Field Sensing*, Honeywell, SSEC Carl H. Smith and Robert Schneider, Nonvolatile Electronics, Inc.

[47] HONEYWELL, Sensor products, application note AN213, *Set/reset function for magnetic sensors* [online]. Available at: http://www.magneticsensors.com/datasheets/an213.pdf [Accessed 10 October 2007]

[48] HANED, N., and MISSOUS, M., Nano-tesla magnetic field magnetometry using an InGaAs–AlGaAs–GaAs 2DEG Hall sensor, *Sensors and Actuators A: Physical*, Vol. 102, Number 3, pp. 216-222, 1 January 2003

APPENDICES

Appendix A: Hall Sensor Technology for CWD

Gun/Knife detection from software simulations and practical tests included in this thesis show that magnetic field detected at 50cm from the target is very low (in the order of microtesla). So it is necessary a sensor device able to measure low magnetic fields. Hall sensor technology is very cheap and spread in the market. Looking in the market of hall sensor device, the P15A from AHS technologies [http://www.ahsltd.com] is the most sensitive. The next is the design of sensor device using DC technique able to measure magnetic fields as low as 1uT with resolution in the low 100nT.

A.1 Offset cancellation

Hall elements exhibit piezoelectric effect, a change in electrical resistance proportional to strain. It is desirable to minimize this effect. This is accomplished by oriented the Hall elements on the IC to minimize the effect of the stress and by using multiple Hall elements. Figure 1 show two Hall elements located in close proximity on an IC. They are positioned in this manner so that both experience the same packaging stress. The first element has its excitation applied along the vertical axis and the second along the horizontal axis. Summing the two outputs eliminates the signal offset.

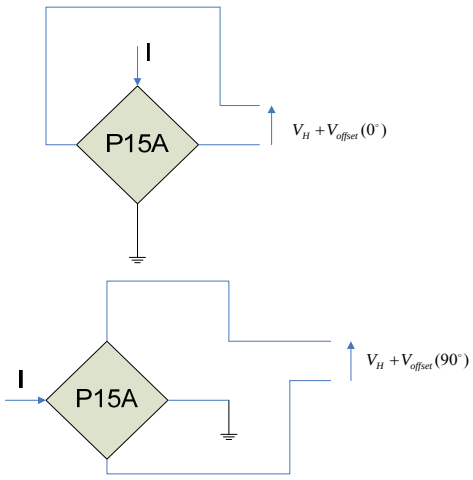

Figure A.1. Offset cancellation.

A.2 Design

The sensor system (see Figure 2) consists in a current source (LM334), which supply the P15A hall sensor via a switching circuit for automatic offset cancellation (piezoelectric effect). The commutated output from the switching circuit is connected to a low noise instrumentation amplifier (INA126) with a gain of 1000 set by one external resistor. A low pass active filter (MAX280) with a cut frequency of 0.1Hz averages the commutated output of the instrumentation amplifier. Finally the filter output voltage is fed into an amplifier with a gain of 20, which the overall gain of the circuit equal to 20000 (86dB).

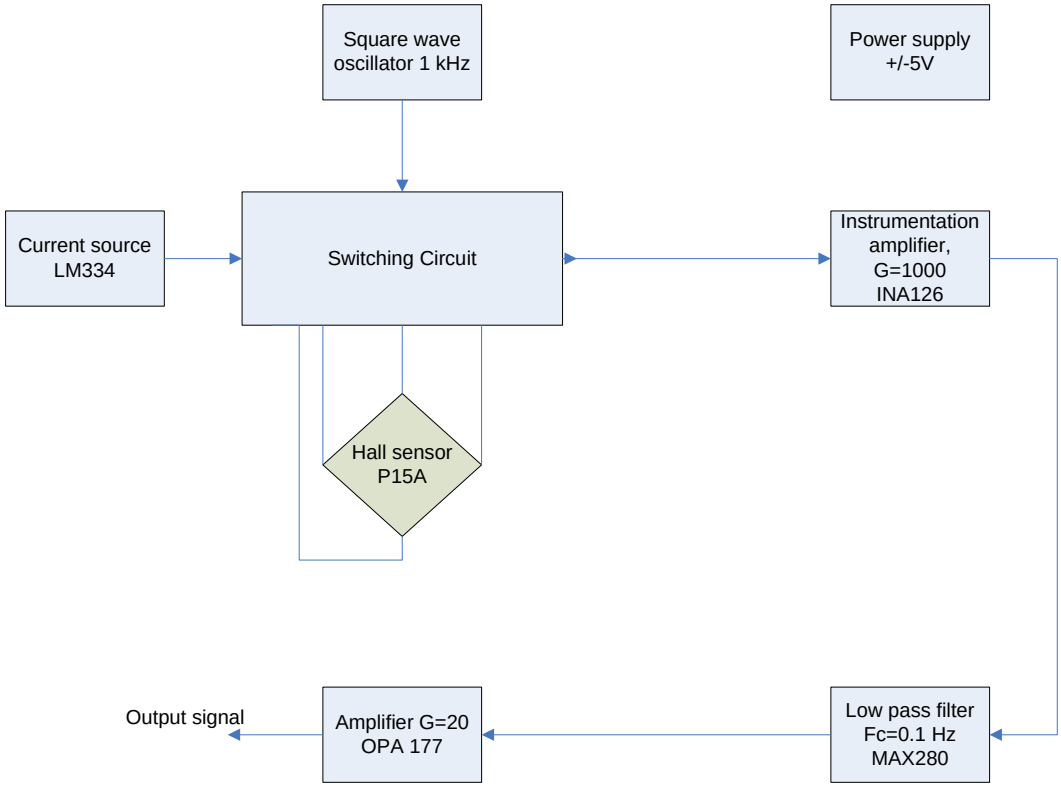

Figure A.2. Hall Magnetometer Design.

Appendix B: Cell Phone Radiation Levels

Article published by CNET staff (updated April 21, 2009)

According to the Cellular Telecommunications Industry Association (CTIA), *specific absorption rate*, or SAR, is "a way of measuring the quantity of radio frequency (RF) energy that is absorbed by the body." For a phone to pass FCC certification, that phone's maximum SAR level must be less than 1.6 watts per kilogram. In Europe, the level is capped at 2W/kg while Canada allows a maximum of 1.6W/kg. The SAR level listed in our charts represents the highest SAR level with the phone next to the ear as tested by the FCC. Keep in mind that it is possible for the SAR level to vary between different transmission bands and that different testing bodies can obtain different results. Also, it is possible for results to vary between different editions of the same phone (such as a handset that is offered by multiple carriers).

Table B.1. SAR level of cell phones.

Manufacturer and model	SAR level(digital)
Motorola V195s	1.6
Motorola ZN5	1.59
Motorola VU204	1.55
Motorola W385	1.54
RIM BlackBerry Curve 8330 (Sprint)	1.54
RIM BlackBerry Curve 8330 (U.S. Cellular)	1.54
RIM BlackBerry Curve 8330 (Verizon Wireless)	1.54
Motorola Deluxe ic902	1.54
T-Mobile Shadow (HTC)	1.53
Motorola i335	1.53